Charge-to-Breakdown Testing of MOSFETs for Reliability Analysis in Electric Vehicles

Victoria Thraves [redacted]

September 2024

Department of Electronic and Electrical Engineering

Faculty of Science and Engineering

Swansea University

Project Dissertation submitted to Swansea University in Partial Fulfilment for the Degree of Master of Science.

Summary

With a ban on fossil-fuel vehicles coming into place in 2030, the window for developing electric vehicles (EVs) with reliable performance is rapidly closing. Investigating the reliability of emerging materials, specifically silicon carbide (SiC) metal-oxide-semiconductor field-effect-transistors (MOSFETs) and gallium nitride (GaN) cascode silicon (Si) MOSFETs, this thesis uses a charge to breakdown (QBD) technique to test the reliability in electric vehicle (EV) power electronics. While traditional Si insulated gate bipolar transistors (IGBTs) have been widely studied, SiC devices offer enhanced thermal and electrical properties, making them a more efficient alternative for EV applications. However, their long-term reliability under high-voltage and high-temperature conditions remains a critical area of study.

During this research, an accelerated age testing setup was designed to assess the breakdown behavior of SiC and Si MOSFETs through QBD testing, in which the results revealed distinct differences in oxide reliability between the two materials. The SiC MOSFETs exhibited QBD values of 0.134C and 0.174C, however, the Si MOSFETs did not exhibit breakdown, highlighting the need for further investigation into their failure mechanisms and performance limitations in EV applications. By focusing on SiC MOSFETs and Si MOSFETs, this study offers insights into the importance of gate oxide reliability in maintaining MOSFET performance and therefore the reliability of EV power electronics, as well as the potential of QBD testing for future innovations of EV technology.

Declarations and Statements

This work has not previously been accepted in substance for any degree and is not being concurrently submitted in candidature for any degree.

Signed: 

Date: 09/04/2025

This thesis is the result of my own investigations, except where otherwise stated. Other sources are acknowledged by footnotes giving explicit references. A bibliography is appended.

Signed: 

Date: 09/04/2025

I hereby give consent for my thesis, if accepted, to be available for electronic sharing.

Signed: 

Date: 09/04/2025

The University's ethical procedures have been followed and, where appropriate, that ethical approval has been granted.

Signed: 

Date: 09/04/2025

Contents

List of Figures

List of Tables

Acknowledgements

I would like to express my deepest gratitude to those who have supported and guided me throughout the course of this research. First, I would like to thank Professor Mike Jennings, one of my mentors, for the design of the circuit diagrams for the charge to breakdown instrumentation. I am also profoundly grateful to Professor Karol Kalna, my second mentor, for his support, encouragement and helpful advice throughout the back end of this project. I would also like to extend my sincere thanks to Steven Batcup, a research officer who not only designed the final charge-to-breakdown PCB, but also provided tremendous assistance in the laboratory, helping me navigate challenges and ensuring the success of this research. This thesis would not have been possible without their contributions, and I am truly thankful for their support.

Abbreviations

EV	Electric Vehicles
HEV	Hybrid Electric Vehicles
BEV	Battery Electric Vehicles
SHEV	Series Hybrid Electric Vehicles
PHEV	Parallel Hybrid Electric Vehicles
FCEV	Fuel Cell Electric Vehicles
IC	Integrated Circuits
BJT	Bipolar Junction Transistors
FET	Field Effect Transistors
JFET	Junction Field Effect Transistors
MOSFET	Metal Oxide Semiconductor Field Effect Transistors
IGBT	Insulated Gate Bipolar Transistors
HBT	Heterojunction Bipolar Transistors
TFT	Thin Film Transistors
BMS	Battery Management System
ECU	Electronic Control Unit
Si	Silicon
SiC	Silicon Carbide
GaN	Gallium Nitride
GaAs	Gallium Arsenide
HCI	Hot Carrier Injection
BTI	Bias Temperature Instability
GIDL	Gate Induced Drain Leakage
QBD	Charge to Breakdown
TDDB	Time Dependent Dielectric Breakdown
HTGB	High Temperature Gate Bias
HTRB	High Temperature Reverse Bias
DUT	Device Under Testing
PCB	Printed Circuit Board

1 Introduction

The evolution of electric vehicles (EVs) has been one of the most prominent advancements in the automotive industry. With a ban on selling internal combustion engine (ICE) vehicles coming into place in 2035, as well as concerns surrounding climate change and sustainability also increasing, significant technological advancements must be made to not only create dependable electric vehicles but to also reduce greenhouse gas emissions and dependency on fossil fuels [1]. Fundamental components behind the manufacturing of EVs are the power electronics systems, made of semiconductors, which control the conductivity and manage the flow of electricity within EVs. Semiconductors hold a key part in the control of EVs. However, their reliability under the demanding operation environment of EVs remains a key concern, especially the reliability of the gate oxide, which is crucial for their long-term performance [2].

The motivation for this research is the increasing demand for more reliable, long lasting components in EVs, where power electronics are fundamental to the vehicle's performance. MOSFETs are integral to various subsystems, such as battery management systems, traction inverters, and DC-DC converters, which are essential in controlling power distribution within the vehicle [3]. As EVs continue to evolve, these devices are exposed to extreme conditions, such as high operating temperatures, elevated voltages, and frequent power cycling, which accelerates the degradation of critical components like the gate oxide [4].

One of the key challenges in the implementation of wide-bandgap (WBG) MOSFETs in EV applications is their susceptibility to degradation, particularly the breakdown of the gate oxide, which occurs due to the intense electric fields and elevated junction temperatures encountered in automotive environments [5]. Despite improvements in semiconductor materials such as silicon carbide (SiC) and gallium nitride (GaN), which offer higher efficiency compared to traditional silicon-based devices, the long-term reliability of these materials, particularly under the stress conditions typical of EV operations, remains underexplored [6]. This research seeks to address the gap in understanding the QBD of gate oxides in WBG MOSFETs, aiming to predict the operational lifetime and reliability of these devices in EV applications.

The research will use an accelerated aging stress technique to measure the charge-to-breakdown of the gate oxide layer in WBG MOSFETs. Stress tests will be performed using constant current stress to simulate the operational conditions of EVs. The MOSFETs will be subjected to increasing voltage and temperature, with leakage current being monitored to identify the breakdown point. It is anticipated that the QBD tests will prove the reliability of the gate oxide layer in WBG MOSFETs under EV-like conditions, to provide insights into the stress endurance of the gate oxide dielectric, contributing to the optimisation of MOSFET design for improved reliability in electric vehicle applications.

2 Literature Review

2.1 Introduction to Electric Vehicles (EVs)

With electric vehicles (EVs) emerging in the automobile industry, a growing awareness of environmental issues surrounding climate change and sustainable energy has led to an increase in environmentally friendly transportation solutions, especially since governments worldwide are implementing stricter emissions regulations. Due to advances in battery technology, the range of EVs is expanding whilst reducing the cost, making them more accessible to a wider range of people. Additionally, the expansion of charging infrastructure is further allowing the transition to EVs, addressing one of the primary concerns of potential EV owners, therefore making these vehicles an increasingly viable option for consumers, contributing to a more sustainable future.

EVs operate by using electrical energy stored in a battery pack to power an electric motor. The battery pack is typically composed of numerous lithium-ion cells, serving as the primary energy source for the vehicle. When the driver turns on the vehicle, the battery pack sends electricity to the motor through a power electronics controller, which regulates the amount of electrical energy supplied to the motor based on the driver's input from the accelerator pedal. The electric motor, which is usually an AC motor, converts this electrical energy into mechanical energy, therefore generating the necessary torque to turn the wheels, which propels the vehicle forward [2]. One of the significant advantages of electric motors is their ability to provide instant torque, which allows for rapid and smooth acceleration from a stopped position. This conversion is highly efficient, as it results in minimal energy loss compared to traditionally used internal combustion engines [3].

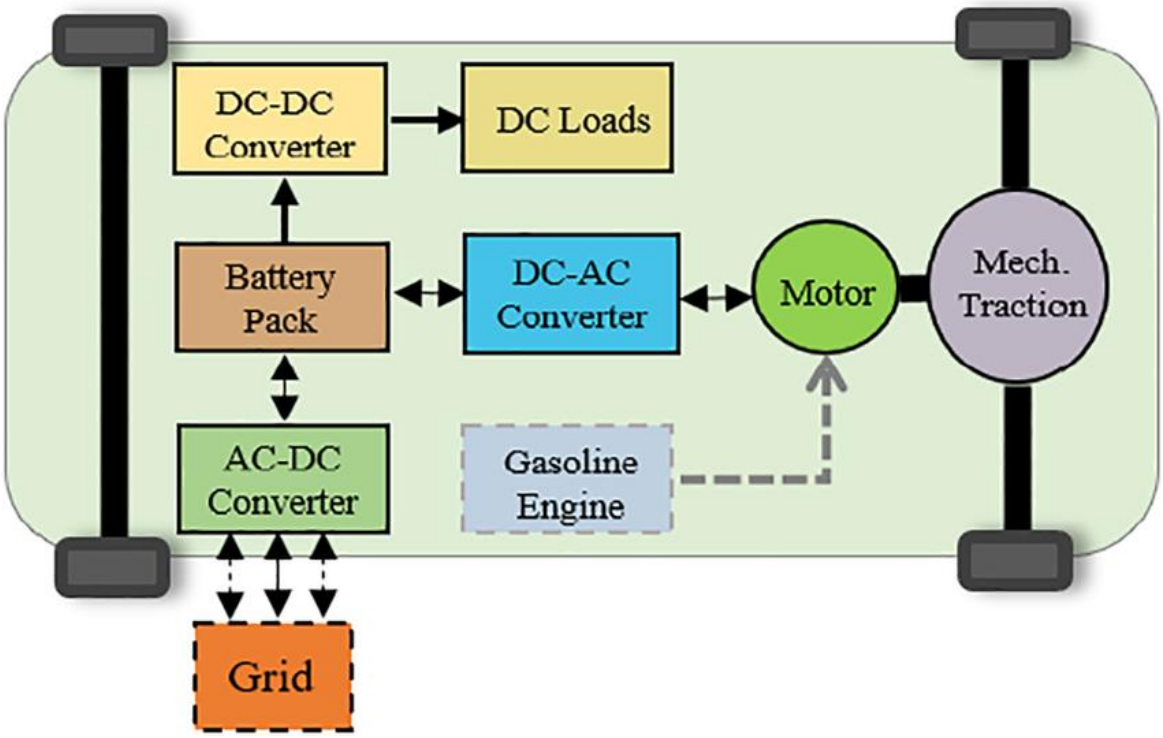

Figure 1 - Block Diagram of EV Components [9]

In addition to powering the vehicle, EVs also feature a regenerative braking system, where the electric motor operates in reverse when the driver applies the brakes, acting as a generator to convert some of the kinetic energy back into electrical energy, which is then stored in the battery pack [3]. This process not only enhances overall energy efficiency but also increases the driving range, by partially recharging the battery as the vehicle brakes.

2.1.1 Key Components of EVs

Electric vehicles are made up of various key components that work together to propel the vehicle using electric power. Although specific components of EVs and hybrid electric vehicles (HEVs) can vary, there are set components that are necessary in EVs.

Battery Pack

As one of the most important features of EVs, the battery stores the electrical energy used to power the electric motor of the vehicle. Battery packs are usually made from lithium-ion, due to their ability to hold high voltage and charge, making it a desirable choice for efficient energy storage in EVs [5]. With each battery packed densely with up to thousands of lithium-ion electrochemical cells, each of which consisting of an electrolyte sandwiched between an alloy cathode and graphite-based anode, the cell works by circulating electrons and ions [4].

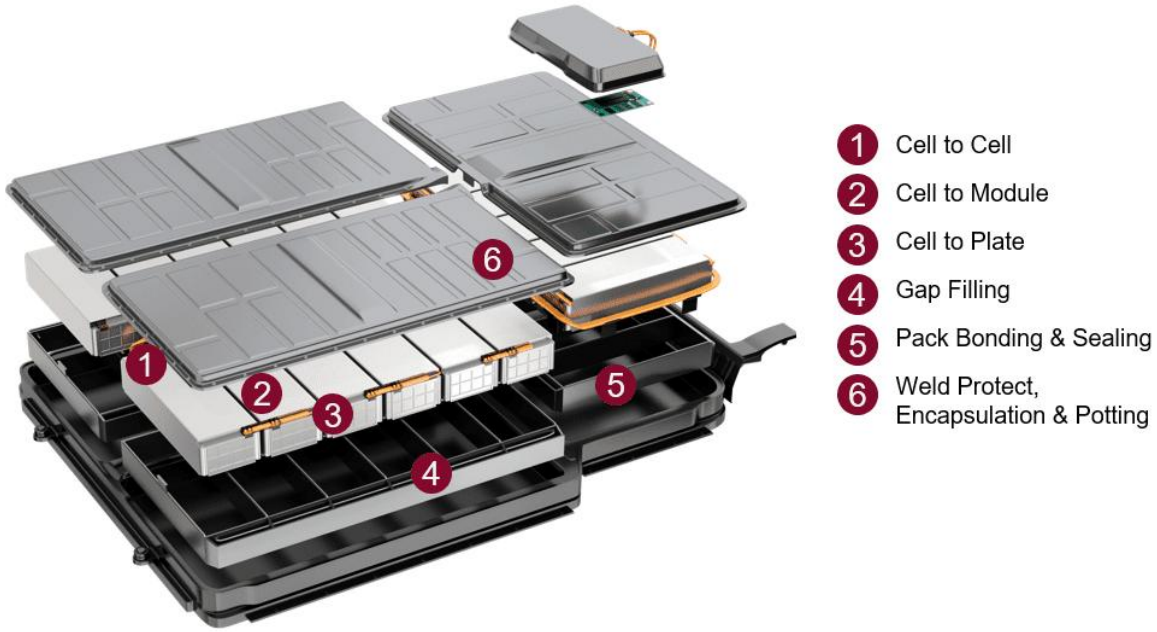

Figure 2 - Battery Pack of EVs [172]

During the charging cycles of the battery, an electric current separates the electrons from the lithium atoms in the cathode, so electrons can flow to the anode, while the now positively charged lithium atoms flow through the electrolyte to the anode, where they reunite with the electrons. During the battery's discharging cycle, the process operates in reverse, splitting atoms and electrons while directing ions back through the electrolyte and electrons through the external circuit to supply power to the motor. [5].

Power Inverter

In EVs, a power inverter is a crucial component used to convert the direct current (DC) stored in the battery of the vehicle into alternating current (AC) to drive the electric motor [8]. The inversion process is carried out as DC current is not suitable for propelling the electric motor directly, due to its limited torque control. The power inversion process is a fundamental part of EVs, as the electric motor requires AC to efficiently function, especially to control the speed and

torque; DC provides a constant flow of electricity, which limits the motor's ability to dynamically vary speed and torque. To overcome this limitation, the inverter uses IGBTs to control not only the speed at which the motor rotates by adjusting the speed of the AC output, therefore the torque of the motor by adjusting the amplitude of the signal. [6]

Electric Motor

As another component with a dominating role in EVs, the electric motor is composed of a drive motor and an associated motor controller, in which the drive motor is used to drive the wheels directly across the rear axle. The motor controller is employed to control the torque, speed and rotation direction of the drive motor according to the vehicle driving demand [7]. The drive motor of EVs comprises a shell, stator, rotor, bearing and position sensor. Once electric power is applied to the stator a magnetic field is generated.

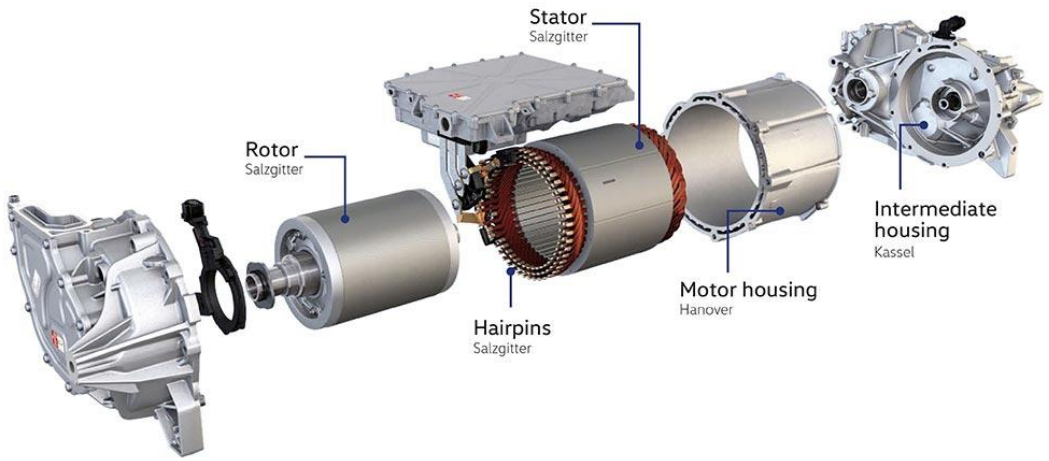

Figure 3 - Electric Motor in EVs [173]

As the current in the windings of the stator is AC, the magnetic field also alternates direction, which induces an electric current in the rotor. This induced current then creates its own magnetic field, causing the interaction between the rotor and stator to generate torque, which rotates the rotor. As this happens, the rotor follows the magnetic field produced by the stator due to their interaction, which generates mechanical power, therefore driving the wheels of the vehicle [8].

DC-DC Converter

In EVs, the DC-DC converter has an imperative role in managing the electrical power distribution between different voltage systems within the vehicle. Given the complexity of EVs, as they integrate a variety of systems and components that operate at different voltage levels, the DC-DC converter is required to either step down or boost the voltage as needed to various power components and systems [12]. The main function of this part is to convert the high DC power from the main battery to lower DC power for auxiliary systems, such as lights and air conditioning, as well as power steering. To achieve the voltage conversion for this, a high frequency switching techniques are most commonly used, in which the converter stores energy for an extended period of time and provides the output at different levels. This technique uses high speed FETs, ensuring there are minimal switching losses to promote efficiency and reliability [9].

Onboard Charger

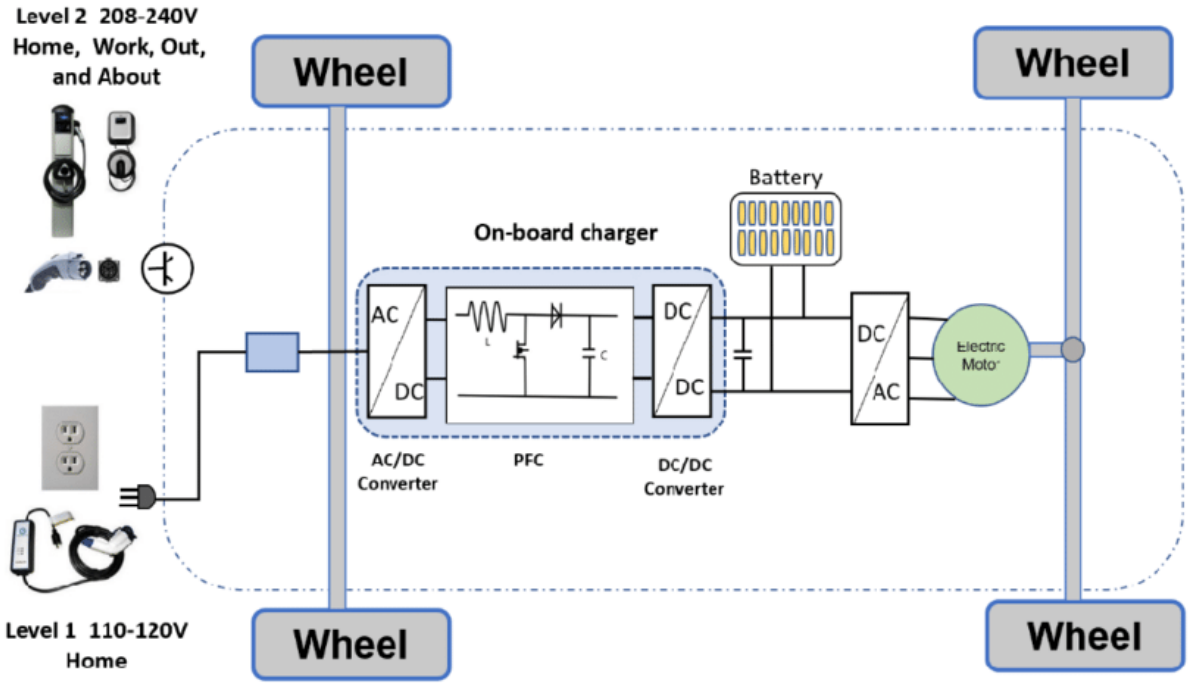

Figure 4 - Diagram of Onboard Charger in EVs [92]

Responsible for converting the AC from an external power source (such as a charging station) into DC power to charge the battery pack, the onboard charger is a key component in EVs. The AC charging system is commonly an on-board charger mounted inside the vehicle, and it is connected to the grid when the vehicle is plugged in, in which a rectifier inside of the onboard charger is used to convert the AC power to DC. This conversion is essential for the operation of the onboard charger, because EV batteries store energy in the DC form, whereas electricity supplied from the grid is in AC form. [10]

Thermal Management System

In EVs, the thermal management system is vital for maintaining optimal operating temperatures for key components, particularly the battery and electric motor. This is key for the performance, efficiency, and safety of EVs. The thermal management system consists of cooling systems and temperature sensors, as well as battery thermal management. In many EVs, a liquid cooling system is used, in which a coolant of water and anti-freeze is circulated through a network of pipes in direct contact with the key components, absorbing heat generated during operation. If not a liquid cooling system, an air-cooling system is introduced, in which fans or vents help dissipate the heat into surrounding air. Whilst this is simpler, it is less efficient for high-performance batteries [11].

One of the most important parts of thermal management is the temperature sensors, in which they are placed strategically throughout the vehicle, especially near critical components, where the temperature is constantly monitored. This relates directly to battery thermal management, as the temperature of the battery pack must be kept at an optimal range – between 15°C and 45°C [12]. In cooler conditions, the system might warm up the battery by using a heating element and in warmer conditions, it might activate the cooling systems to dissipate the excess heat [12].

Electronic Control Unit (ECU)

Acting as the brain of EVs, the ECU serves as a central control system that manages and coordinates the operation of most key components to ensure safe and efficient operation. Orchestrating the functions of all electric powertrain components, the ECU is a sophisticated system that continuously analyses data from sensors throughout the vehicle and can make real-time adjustments to optimise the vehicle's performance [18].

The ECU is also accountable for motor control, regulating the power supplied to the component to control the speed of the vehicle and the torque by coordinating with the power electronics to convert and control the flow of electrical energy between the battery and the motor, therefore managing the motors performance for optimal efficiency. [13] The ECU also controls the thermal management system, as well as the charging system, regulating not only the cooling and heating mechanisms, but also the voltage and current levels through different charging phases.

2.2 Transistors

Semiconductors play a fundamental role in modern electronics, with the evolution of their architecture enabling significant advancements in various engineering fields such as computing, communications and especially EVs [20].

2.2.1 History of Transistors

To fully understand different transistors and their purposes, significant milestones must be considered. From their creation to the present day, key technological advancements and their impact on engineering, their advancements and achievements can be considered.

The first transistor was invented by John Bardeen, Walter Brattain and William Shockley at Bell Laboratories in 1947. Their studies involved the creation of the point-contact transistor, which demonstrated the potential to replace vacuum tubes in electronic circuits [15]. Vacuum tubes were used extensively in early electronic devices; however, they were not only large, but consumed too much power, which resulted in the generation of heat, making these devices prone to frequent failures. Bardeen and Brattain had the original design and idea, which was followed by William Shockley's invention of the point contact transistor in 1947, offering an improvement in performance and reliability, marking the beginning of a revolution in electronic design and miniaturisation [22].

Introducing bipolar junction transistors (BJTs) into the electronics industry began to replace vacuum tubes in applications such as radios, televisions and early computers. This led to the development of smaller, more efficient and reliable electronic systems, setting the standard for the development of integrated circuits (ICs). During the 1950s, the development of alloy junction transistors and diffusion techniques began, enhancing the performance and manufacturing processes of BJTs. This meant that transistors were used in consumer electronics and industrial applications more quickly as a result of the rapid developments, making it easier to produce them in larger quantities and at cheaper prices [16].

The miniaturisation of devices enabled by transistors also contributed to the evolution of portable electronic devices, such as early transistor radios, which were compact, portable and had a longer battery life compared to the vacuum tube devices that came before. The trend towards these devices led to more efficient fabrication, which drove innovation in the semiconductor industry, leading to the development of microprocessors and the digital revolution [24].

Moore's Law is associated with the decreasing size and increasing power of computational devices, arising from the observation that the processing power of a chip doubles every two years, due to the scaling down of transistors, allowing them to more densely populate the chip [17]. Gordon Moore predicted this exponential growth in transistor density, which fuelled the digital revolution of the late 20th Century, driving key technological advancements and allowing the development of increasingly powerful and affordable electronic devices. From this, the cost per transistor has reduced too, making advanced technology accessible to a wider range of people, contributing to economic growth [26].

With Moore's Law playing a key role in the development of PCs, the increased transistor density allowed manufacturers to produce more powerful and more cost-effective microprocessors. This also made it possible to design and manufacture affordable PCs for the mass market, which drove the evolution of the mobile phone in the same way [26].

2.2.2 Types of Transistors

With unique characteristics and applications, there are a wide range of devices of transistors. Each type of transistor contributes to the advancement of electronic devices significantly, enabling a variety of innovation and the evolution of the electronics industry.

Bipolar Junction Transistors (BJTs)

Bipolar junction transistors (BJTs) are one of the first transistors to be developed in the electronics industry. These devices consist of three layers of semiconductor material, forming two p-n junctions, in which BJTs can be classified as either NPN or PNP types, depending on the arrangement of the layers. BJTs operate by using a small current at the base terminal to control a larger current between the collector and emitter terminals. Known for their high current gain, these components are widely used in amplification and switching applications [18].

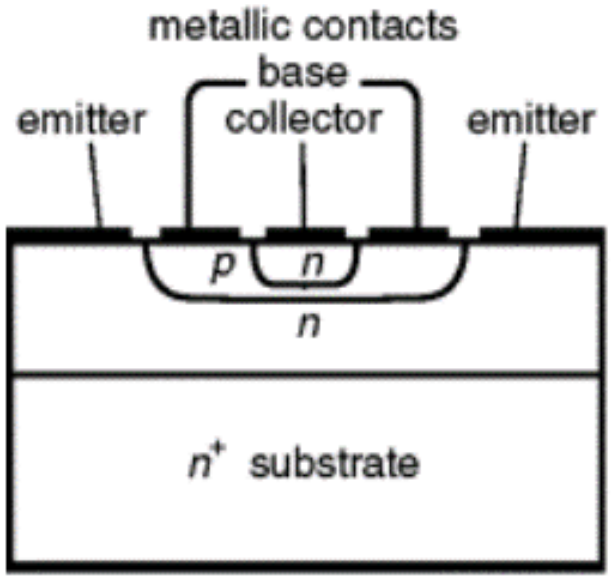

Figure 5 - Cross Sectional Diagram of a Bipolar Junction Transistor (BJT) [113]

Field Effect Transistors (FETs)

Field effect transistors (FETs) have become increasingly prevalent in the electronics industry, due to their high input impedance and low power consumption. FETs control the flow of current by applying an electric field to a semiconductor channel. FETs are configured with three terminals for their fundamental operation: the source, the drain and the gate [28]. The source is the terminal through which electrons or holes (known as carriers) enter the channel, while the drain is the exit for these carriers. The gate terminal, insulated from the channel by a thin dielectric layer, controls the conductivity of the channel. When a voltage is applied to the gate, it creates an electric field that influences the conductivity between the source and drain. The most common FETs are metal-oxide semiconductor field effect transistors (MOSFETs) and junction field effect transistors (JFETs) [19].

The high impedance and low power consumption of FETs make them suitable for a wide range of applications, especially in microprocessors and memory devices [30]. In power electronics, FETs are used in power supply units, motor controllers, and inverters due to their efficiency in handling high currents and voltages. Combining these advantages with FET's ability to control current flow with an electric field, these devices are indispensable in modern electronics.

Junction Field Effect Transistors (JFETs)

In junction field effect transistors (JFETs), the gate of the device is formed by a p-n junction, where the channel is either n-type or p-type semiconductor material. The structure of JFETs consists of a long channel semiconductor material with ohmic contacts on each end, known as the source and the drain [31]. Surrounding the channel is the gate, made from a semiconductor material of opposite doping type to the channel to form the p-n junction. In an n-channel JFET, the channel is n-type, and the gate is p-type, whereas in a p-channel JFET, the channel is p-type, and the gate is n-type. When no voltage is applied to the gate of the JFET, the channel remains fully open, allowing current to flow freely between the source and drain when voltage is flowing between the two [20].

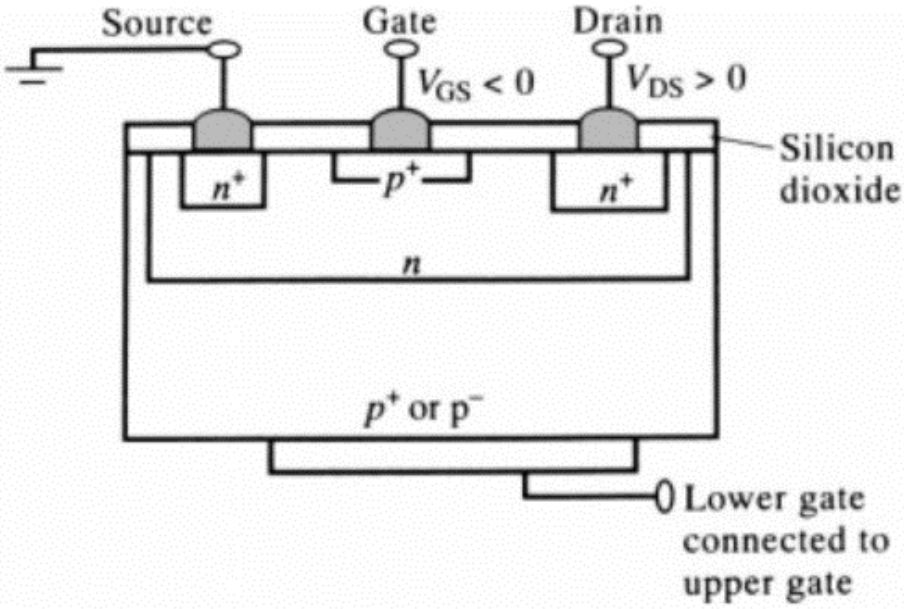

Figure 6 - Cross Sectional Diagram of a Junction Field Effect Transistor (JFET) [114]

This device is suitable for analogue signal processing, buffer amplifiers and sensor interfaces, in which minimal circuit loading is required. JFETs also hold low noise qualities, due to the lack of significant current from the gate, which introduces less thermal noise compared to BJTs, making them ideal for audio equipment and precision measurement.

Metal-Oxide Semiconductor Field-Effect Transistors (MOSFETs)

Metal-oxide semiconductor field-effect transistors (MOSFETs) are the most commonly used transistors in both digital and analogue circuits. This is due to their unique structure and operational characteristics, which make them more efficient and versatile. MOSFETs are made up of four terminals, the gate, source, drain and substrate, where the gate is separated from the semiconductor channel by a thin layer of insulating material, typically silicon dioxide (SiO_2) [33]. This insulating layer is crucial for the gate to control the conductivity of the channel without direct electrical contact, resulting in extremely high input impedance. When a voltage is applied to the gate of the device, an electric field is implemented across the insulation layer, which influences the charge carriers in the semiconductor channel, which Is located between the source and drain terminals. For n-channel MOSFETs, a positive voltage across the gate terminal attracts electrons

to the channel, increasing its conductivity. However, for p-channel MOSFETs, negative gate voltage attracts holes to the channel, increasing the conductivity of the device [21].

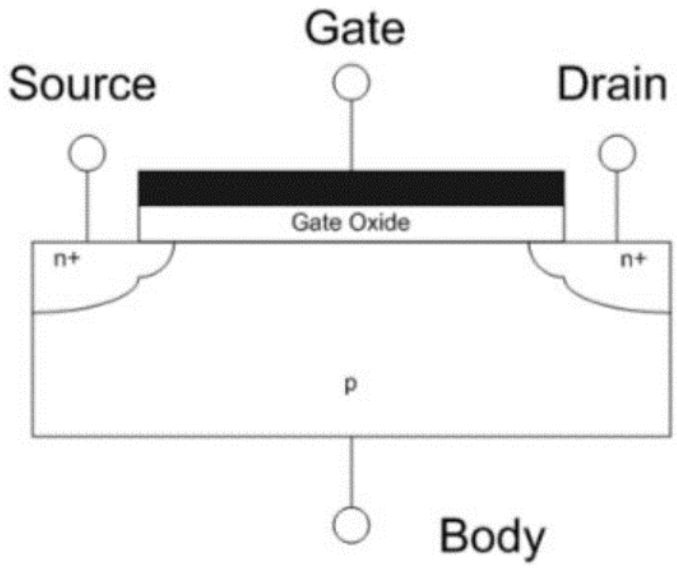

Figure 7 - Cross Sectional Diagram of Metal Oxide Semiconductor Field Effect Transistor (MOSFET) [115]

MOSFETs can also be categorised into two main operating types: enhancement mode and depletion mode MOSFETs. Enhancement mode MOSFETs are more common, where the channel is non-conductive when there is no voltage applied across the gate of the device [35]. For n-channel enhancement mode MOSFETs, a positive gate voltage is required to induce a conductive channel, but for p-type enhancement mode MOSFETs, a negative gate voltage is necessary. This operation is useful in digital logic circuits, as the MOSFET acts as a switch that can turn on and off with the gate voltage. In depletion mode MOSFETs, the channel of the device is conductive when no voltage is applied across the gate. By applying a negative voltage across a n-channel depletion mode MOSFET or a positive voltage across a p-type depletion mode MOSFET, the channel of carriers decreases, reducing or preventing the current flow. These devices are not as common as enhancement mode MOSFETs. However, they are used in more complex and specific applications, especially where normally-on characteristics are required [22].

Insulated-Gate Bipolar Transistors (IGBTs)

Insulated-gate bipolar transistors (IGBTs) combine the characteristics of BJTs and MOSFETs, offering high input impedances and high current handling capabilities, making them ideal for high power applications such as power inverters and motor drives, in which they exhibit high efficiency [37]. IGBTs consist of a complex architecture of four layers: an n+ substrate, a p- layer, an n- layer and a p+ layer, forming a p-n-p-n structure. The gate terminal of the device is insulated from the p- layer by a thin oxide, similar to MOSFETs, in which this creates the high impedance, meaning that the gate requires a small current to control the flow of charge between the collector and the emitter terminals [23].

By applying a positive charge to the gate, an inversion layer is formed in the p- region below the gate. This forms a conductive channel, which allows electrons to flow from the n+ emitter into the p- layer, where holes from the p+ substrate are injected into the n- layer, turning the device on. The electron and holes flowing through the device results in a low on-state voltage drop and high current handling capabilities, ensuring the efficient power handling of IGBTs, as a result of lower conduction losses.

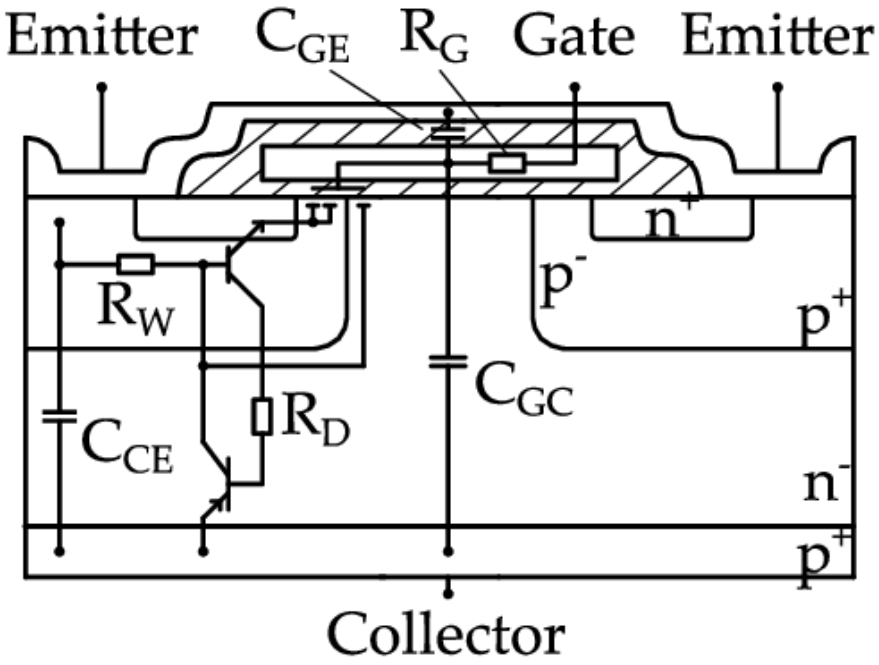

Figure 8 - Cross Sectional Diagram of Insulated Gate Bipolar Transistor (IGBT) [116]

Heterojunction Bipolar Transistors (HBTs)

Heterojunction bipolar transistors (HBTs) use two or more different semiconductor materials for the emitter and base regions, creating a heterojunction to improve the performance characteristics of the device. This allows HBTs to operate more efficiently compared to homojunction BJTs for uses in high-frequency and microwave applications, such as satellite communications.

In traditional BJTs, the emitter and base regions are made from the same semiconductor material, which is typically silicon. However, for HBTs, different materials are used to form a heterojunction, such as gallium arsenide (GaAs) for the base and aluminium gallium arsenide (AlGaAs) for the emitter. This introduces several advantages, such as bandgap engineering, where the emitter material has a wider bandgap than the base material, creating a potential barrier that improves carrier injection efficiency, reduces base recombination and increases current gain [24].

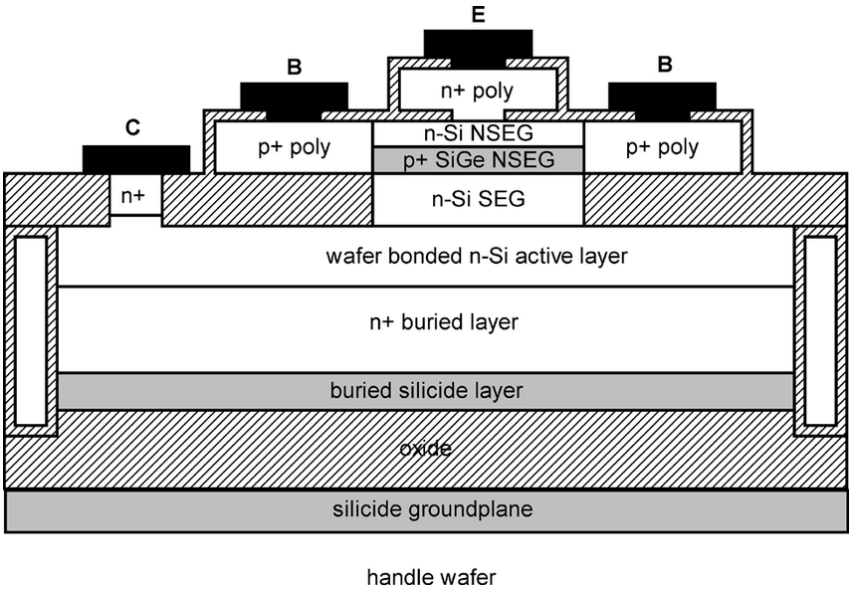

Figure 9 – Cross Sectional Diagram of a Silicon Germanium Heterojunction Bipolar Transistor (HBT) [171]

Thin Film Transistors (TFTs)

Thin film transistors (TFTs) are a type of FET in which the semiconductor layer acts as a thin film on the substrate of the device, typically made from glass or plastic. TFTs are usually utilised in liquid crystal displays (LCDs) and organic light-emitting diode (OLED) screens, to control the pixels and image quality of the display technologies. TFTs are composed of 4 integral layers, each with a specific function: the substrate, the semiconductor layer, gate insulator and the gate, source and drain electrodes. Made from either glass or from a flexible plastic material, the substrate supports the entire structure of the TFT, in which this material affects not only the flexibility and durability of the device, but the transparency of the screen. The semiconductor layer is made from materials such as amorphous silicon (a-Si) and polycrystalline silicon (p-Si), deposited as a thin layer on the substrate, where the channel of the device forms and controls the flow of current between the source and drain [25].

An insulating layer separates the gate electrode from the semiconductor layer, known as the gate insulator. This prevents the current flow between the two, whilst allowing the gate voltage to control the channel conductivity. The gate, source and drain terminals of the TFT are patterned on the substrate, in which the gate electrode controls the channel formation, while the source and drain electrodes allow current to flow from the semiconductor layer when the device is on. Applying a voltage to the gate electrode, an electric field is formed to control the conductivity in the semiconductor layer. This allows current to flow between the source and drain terminals, enabling precise control of the electrical current [26].

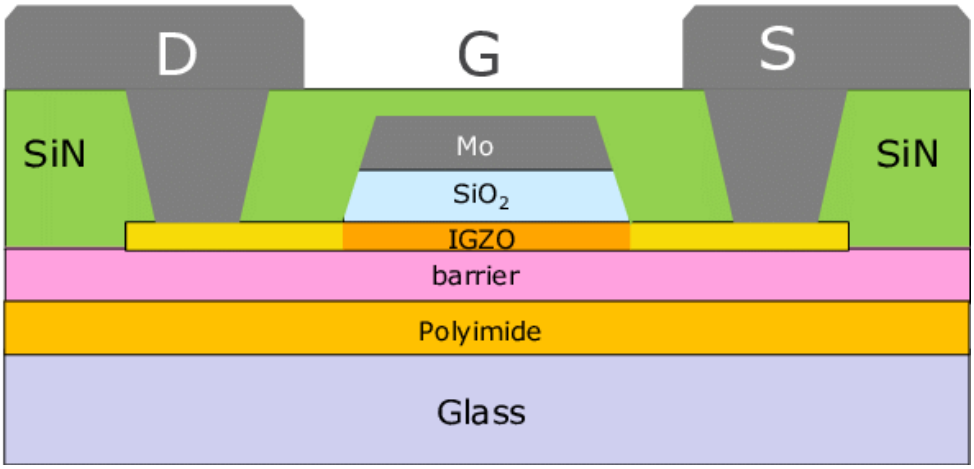

Figure 10 - Cross Sectional Diagram of a Thin Film Transistor (TFT) [170]

2.2.3 Importance of Transistors in EVs

Transistors, as fundamental components of modern electronic systems, play an indispensable role in the operating systems of EVs. Semiconductor devices, renowned for their ability to amplify and switch electronic signals, are pivotal in managing the electrical and electronic operations within EVs. From the intricate control of power conversion and distribution to the precise regulation of motor functions and battery management, transistors are a key component of the advancements driving the evolution of EVs.

Battery Management Systems (BMS)

Semiconductors are used in several parts of the BMS, not only to control charging processes, but act as protection against overcharging and over-discharging. Acting as switches, charge/discharge control FETs can control the overall current flow in and out of the battery pack, so when the voltage limit is reached during the charging process, the system automatically disconnects the battery from the charging source and prevents overcharging, which can damage the battery capacity and lifespan, thereby effecting the efficiency of the vehicle and overall reliability.

Transistors are also utilised in the BMS for cell balancing in the battery packs. Due to differences in operating conditions, individual cells may have slight variations in voltage, which causes cells to have varying capacities and discharge and charge at different rates. This leads to an imbalance in the state of charge among cells, reducing the capacity of the battery pack and therefore affecting the driving range of the vehicle. Transistors are applied to this system to redistribute the charge among cells, ensuring that all cells in the pack maintain similar states of charge. This maximises the battery capacity, thereby the vehicles efficiency and reliability and therefore the lifespan of the vehicle. [27]

The control of the flow of current is also necessary in the BMS, so cut off FETs are employed to act as current regulators, managing the rate at which energy is drawn from the battery during charging and discharging processes, to prevent excessive currents from flowing to and from the battery. This prevents overheating in the BMS, which prevents permanent damage, helps maintain the optimal performance of the battery and therefore promotes the efficiency of the vehicle as a whole [42].

Traction Inverters

A traction inverter is the electric drivetrain of EVs, in which direct current is converted from the vehicle's battery into an alternating current output, used to power the electric motor that drives

the vehicle. Transistors play a crucial role in regulating this flow of electrical energy. In the AC motor, the current in each phase must alternate the direction of flow between the positive and negative at accurate timings in accordance with the motor shaft rotation to achieve the desired torque and speed. Transistors are in charge of quickly turning on and off current, and because of this, they can quickly change the desired AC waveform, which in turn controls the vehicle's torque and speed. By modulating the switching of the transistors, the inverter can precisely control the electrical power sent to the motor, enabling smooth acceleration, deceleration, and overall motor performance [28].

Transistors in the traction inverter are used for a pulse width modulation (PWM) technique, in which the PWM regulator operates by alternating between fully 'ON' and fully 'OFF', where the 'ON' period of the transistor is varied to achieve the desired output. PWM control of the inverter offers several advantages in terms of efficiency, precision, and flexibility in managing the electric motor, and therefore the speed and torque of the vehicle. A PWM approach is also taken to control the frequency of the AC waveform generated more accurately. This allows the rotational speed of the motor can be quickly adjusted by the traction inverter. This also offers more efficient power delivery, as faster switching of transistors reduces the power dissipated in the component, improving the efficiency of the power sent to the motor in a more controlled manner [43].

2.2.4 Potential MOSFET Applications in EVs

Potential applications of MOSFETs in EV can be introduced and integrated as alternatives to IGBTs and FETs. The shift from IGBTs to MOSFETs is driven by several key advantages, including faster switching speeds, higher efficiency, and improved thermal performance. These characteristics make MOSFETs particularly attractive for various critical components within EVs, such as the traction inverter, onboard charger, and DC-DC converters [2].

Battery Management System (BMS)

In the BMS, MOSFETs could play a key role in controlling the charging and discharging processes, due to their rapid switching technologies, and ability to work with high voltages. The fast reaction time of MOSFETs and their small size make them a preferred choice for this application, as short circuit protection in a major concern for BMS design and implementing their fast-switching technologies minimises switching losses. This reduces the power dissipated and excess heat generated, decreasing the chance of breakdown, and making MOSFETs a great potential choice for this application [44].

In addition to their role in the control process, MOSFETs can also be used as a balancing resistance, when driving the MOSFET in linear mode, in which the excess energy between the battery cells can be dissipated on the MOSFET as heat [29]. This can guarantee that all of the cells receive the same amount of charge, which will help balance the cells in the battery pack, offer more stable charging, and extend the battery's lifespan—all of which will increase its dependability and efficiency [46].

Electric Motor

In this component, MOSFETs can take over the IGBTs operation more efficiently. Using MOSFETs that have a material with a wider band gap (such as silicon carbide), the device can switch at much higher frequencies, making them 10x faster than IGBTs. This means that with a higher switching speed, there are reduced power losses, meaning there is a reduction in the heat generated and so less likely to breakdown, making the component more reliable.

MOSFETs are also often used in conjunction with pulse with modulation (PWM) techniques, as PWM controls the average power delivered to the motor by varying the duty cycle of the switching

signal. Regulating the amount of time the switch is on, MOSFETs could effectively modulate the power supplied to the motor, thereby regulating the speed and torque of the motor. This makes for a more efficient system, reducing switching losses and therefore power dissipation, reducing the probability of overheating and therefore making a more efficient system [47].

Power Inverter

By employing SiC MOSFET inverters instead of Si-IGBT inverters, the efficiency and power density of the electric drive system can be increased, due to MOSFETs rapid switching technologies, they minimise switching losses, therefore there is less power dissipated, thereby the system is more efficient, and reliability is improved [30]. Although IGBTs have better short-circuit withstand time in EVs, they have higher switching losses compared to MOSFETs. MOSFETs, which have a shorter withstand time, have much lower losses that do not increase with the breakdown voltage.

MOSFETs also offer more advantages than IGBTs due to their higher saturated electron drift velocity, as well as larger bandgap, which allow for faster switching speeds and higher switching frequencies, further reducing switching losses. This also reduces conduction losses of MOSFETs, which leads to higher power density of over 70kW/L and improved efficiency of up to 98%. These parameters have been shown to extend the life of inverters by more than 80%, particularly in high voltage applications [30].

DC-DC Converters

DC-DC converters are crucial elements that must be able to provide stable DC voltages. Using MOSFETs offers several advantages to EV efficiency such as lower switching and conduction losses promotes efficiency and higher dielectric strength for operating at higher voltages and also wider temperature range applications [30].

Wide temperature range advantages are demonstrated by SiC MOSFETs, which retain fast switching abilities and lower switching energy over a wider temperature range (−183°C to 220°C) than conventional Si IGBTs. Higher switching frequencies displayed by SiC MOSFETs also improve the dynamic and steady state performance of the on-board DC-DC converters by allowing them to react to changes in load much more quickly and to reduce voltage ripple [30].

Onboard Chargers

The limited space in cars and the limited output power from outlets or charging stations mean that the primary development objectives for OBCs are to increase power density, charging efficiency, and heat dissipation capacity, making MOSFETs the perfect device to achieve these goals [49].

Original equipment manufacturers (OEMs) have gradually upgraded their on-board chargers from 3.3 kW to 6.6 kW, combined with a 7-kW AC charging station instead of the household socket for larger charging power, to meet the demand for faster charging of battery electric vehicles (BEVs). An inductor-inductor-capacitor (LLC) on-board charger with a proposed 6.6-kW output demonstrates a peak efficiency exceeding 96% and a power density of 3.42 kW/L. Additionally, the most efficient on-board charger achieves 98.9% with less than 2% total harmonic distortion (THD). Compared to Si-based on-board chargers, using SiC MOSFETs in on-board chargers can significantly reduce volume and weight by 24% and 28%, respectively, and increase power density by more than 72% when the power demand is the same [30].

Off Board Charging Applications

On-board chargers cannot keep up with the growing popularity of EVs and user demands for faster charging times because of power constraints. As a result, there is an increase in demand for off-board charging, which qualifies for higher grid charging power. Similar to on-board chargers, off-board charging applications have similar requirements for charging efficiency.

A typical DC fast-charging station consists of an isolated DC/DC converter at the back end and a front-end rectifier with Power Factor Correction (PFC) [30]. By utilising SiC MOSFETs, charging stations can enhance their efficiency to 98.2%, decrease overall losses by 24%, boost dynamic performance, minimise size, lower the cost of the cooling and magnetic systems, and accelerate charging. Because SiC MOSFETs have a higher breakdown voltage than Si-IGBTs when the vehicle voltage platform is upgraded to 800 V, they have even more potential for use in charging stations [30].

2.2.5 Failure Mechanisms of MOSFETs

MOSFETS are integral to modern electronic devices, however, their performance and longevity can be compromised by various failure mechanisms. These include issues like gate oxide breakdown, electromigration, and thermal degradation, which can lead to reduced efficiency, increased power loss, and eventual device failure. Understanding these failure mechanisms is crucial for enhancing the reliability and durability of MOSFETs in critical applications [50].

Gate Oxide Breakdown

In MOSFETs, the gate oxide is a thin insulating layer that separates the gate electrode from the semiconductor material. A MOSFET's optimal performance depends on the gate oxide's characteristics. However, the gate dielectric can only withstand a certain electric field before the insulator's qualities are irreversibly lost, allowing current to pass through the oxide, from a path formation in the dielectric material known as dielectric breakdown, ultimately leading to the breakdown of the entire device. Gate oxide breakdown is typically explained as a two-step process: first, the oxide experiences gradual damage buildup, which causes the breakdown path to suddenly form. Numerous models may be responsible for the deterioration process.

Anode-Hole Injection

Anode-hole injection is a phenomenon where positive charge carriers (holes) are injected into the gate oxide from the anode terminal of the device, when the MOSFET is subjected to high electric fields or voltage stresses. This model suggests excess energy can be transferred to an electron in the gate electrode's valence band by electrons tunnelling through the gate oxide, leaving a hole when the electron is promoted to the conduction band. Therefore, the hole can tunnel back to the oxide, generating oxide traps until a critical quantity is reached, inducing breakdown [31].

Under high electric fields or voltage stresses, the energy landscape within the MOSFET changes significantly, in which the increased electric field strength across the gate oxide leads to higher energy electrons, which tunnel through the oxide layer from the gate of the device. When tunnelling occurs, the electrons at the gate electrode transfer energy to other electrons in the valence band, promoting them to the conduction band, which leaves holes behind. These holes formed in the valence band can tunnel back into the gate oxide, which causes the ionisation of the oxide material, generating defects or traps within the oxide. As this number of traps increases, the local electric field within the oxide becomes uneven, resulting in regions of high field intensity, facilitating further tunnelling and hole injection, accelerating the degradation process [52].

Once the trap density reaches its critical level, a conductive path is formed through the oxide of the MOSFET, allowing a significant increase in current flow, leading to thermal runaway and therefore the sudden failure of the gate oxide [53].

Electron Trap Generation

This breakdown model refers to breakdown of the gate oxide via the formation of a conducting path of oxide traps. This is triggered by an increase in electrical stress, resulting in the generation

of a critical electron trap density [31]. As electrons become trapped in the gate oxide of the device, they create localised electric fields, shifting the threshold voltage of the MOSFET, altering the switching behaviour of the device, reducing the drain current and therefore inducing breakdown of the device.

Under prolonged electrical stress, electrons are injected into the gate oxide and become trapped at the defect sites within the oxide layer of the MOSFET, generating localised electric fields that alter the electric potential landscape within the oxide. This leads to an increase in the electric field strength, inducing further electron trapping and stress on the oxide, which also forms conductive paths at a certain threshold. The path is composed of interconnected traps that result in electron conduction across the oxide layer, rapidly increasing the leakage current and leading to the thermal runaway effect and therefore permanent breakdown of the device. The trapped charges in the gate oxide of MOSFETs also affect the device characteristics, especially the threshold voltage of the device [54].

Percolation Model

According to the percolation model, localised channels or pathways that allow current to flow can be produced by gate oxide imperfections or impurities. These flaws could develop over time as a result of electrical stress, environmental variables, or fabrication processes. "Percolation" describes the process by which these localised paths progressively unite or percolate, increasing the oxide layer's total conductivity noticeably. These oxide traps are generated at a specific rate and distributed at random positions across the dielectric. When two or more traps are located closely together, a conducting path is formed in which charge can flow from one trap to the other. Similar to how conducting path collections encounter a critical defect density with cumulative stress, these "clusters" will be arranged so that charge can pass through the oxide and towards the gate electrode. This is followed by either a progressive gate current increase for progressive breakdown, an instantaneous large gate current increase for hard breakdown, or a small gate current increase accompanied by a sudden gate current noise for soft breakdown [31].

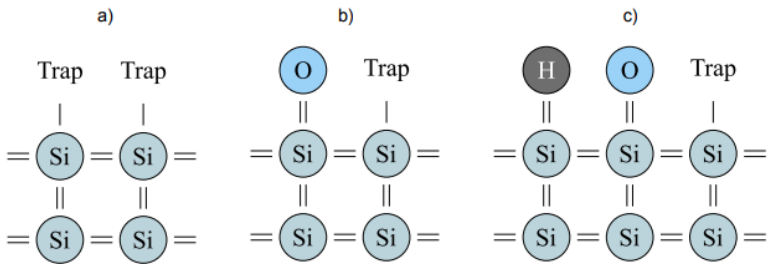

Figure 11 - a) The missing atoms generate unpaired valence electrons in the surface and generate interface traps. b) After oxidation, the majority of states are filled with oxygen atoms. c) After annealing, interface defects are reduced by the Hydrogen bonding with the remaining states. [31]

At random locations throughout the gate dielectric, oxide traps are formed due to electrical stress, high temperatures or the presence of impurities. The rate of trap generation depends not only on the intensity of the stress parameters, but on the quality of the oxide of the MOSFET. Over significant time, the accumulation of traps increases the likelihood of trap interactions, which decreases the distance between traps, forming localised conductive pathways from electron tunnelling. The percolation threshold is reached when the density of traps and their connectivity reaches a critical level, at which point the clusters of conductive paths are formed, allowing charge to flow through the oxide more freely, creating a continuous pathway from the gate terminal to the substrate, increasing the leakage current through the oxide. Depending on the distribution of oxide traps and clusters, progressive, hard or soft breakdown inevitably occurs [55].

Hot Carrier Injection (HCI)

Hot carrier injection (HCI) is a key phenomenon of MOSFETs that can lead to degradation and failure of MOSFETs over time. During normal operation of MOSFETs, a voltage is applied to the gate resulting in the formation of an electric field in the oxide layer, which induces the movement of charge carriers (electrons or holes) from the source to the drain, allowing current flow through the transistor. However, in high-power MOSFETs, carriers can gain sufficient energy in which they become 'hot carriers', which causes them to collide with the lattice atoms in the oxide layer, causing localised damage. In high power applications, the electric field near the drain can be particularly intense, accelerating carriers to a significant energy that allows them to overcome the barrier in the oxide layer. This impact can create defects to the oxide layer, such as interface states and traps [32]. Trapped carriers play a key role in reducing the effectiveness of the gate control over time, leading to a shift in the threshold voltage and therefore degradation of the device performance. As more carriers are injected and consequently trapped, the charge buildup in the oxide layer can further deteriorate the MOSFETs architecture [57].

Negative and Positive Bias Temperature Instability (BTI)

At elevated temperatures, BTI occurs under negative or positive gate voltages within the gate oxide of MOSFETs, in which this significantly reduces the operating lifetime of the device, especially in deeply scaled down transistor dimensions with advanced materials. Under negative or positive bias conditions, interface traps are generated at the silicon/silicon dioxide interface [31]. These traps capture negative or positive charge carriers (electrons or holes) in the channel region of the MOSFET, leading to a negative or positive shift in threshold voltage over time, according to the charge. Under negative BTI conditions, the threshold voltage decreases, leading to the MOSFET becoming less efficient in switching, resulting in a reduction in the MOSFET's drive current, which reduces the speed of switching and increases power losses in the MOSFET, making them less reliable and decreasing the lifespan of the device. Similarly, under positive BTI, the buildup of holes in the gate dielectric leads to an increase in the threshold voltage of the device, resulting in a decrease in the drain current, which leads to circuit failure [58].

Gate Induced Drain Leakage (GIDL)

In the GIDL mechanism, a leakage current between the drain and bulk is generated, due to the formation of electron-hole pairs by the tunnelling of valence band electrons into the conduction band. Under the gate-to-drain overlap region, a deep-depletion region forms when a high voltage is applied to the drain while the gate is grounded. Tunnelling of valence band electrons into the conduction band creates electron-hole pairs, which are then collected separately by the substrate and the drain. The deep-depletion region develops, and the band-to-band tunnelling process can continue without producing an inversion layer because all of the minority carriers generated thermally or by band-to-band tunnelling in the drain region (holes in n-MOSFETs and electrons in p-MOSFETs) flow to the substrate due to the lateral field [33].

This is often associated with trap-assisted tunnelling, in which traps in the oxide layer capture charge carriers, increasing the electric field capacity until the trapped carriers can tunnel through the oxide, causing the leakage current to flow. Excessive GIDL on the semiconductor leads to decreased switching speeds, which means that there are increased power losses meaning there is an increased power consumption on the MOSFET, leading to an increase in thermal stresses which overheat the device and lead to failure.

2.2.6 Mitigation Strategies of Failure Mechanisms in MOSFETs

To enhance reliability and longevity of MOSFETs, mitigating failure mechanism is critical. Using advanced material engineering, optimal device designs and operational techniques, effective mitigation strategies can be employed to ensure the ideal performance and functionality of MOSFETs.

Mitigation of Gate Oxide Breakdown

As transistor devices continue to scale down to the nanometre dimensions, strategies to prevent the gate oxide breakdown in devices are constantly being developed, ensuring the longevity and reliability of MOSFETs as technologies advance.

Advanced Material Implementation

By swapping out or supplementing traditionally used silicon dioxide gate dielectric with a material with a higher dielectric constant, a more advanced gate stack might be achieved resulting in a higher reliability. Materials with a high dielectric constant, such as hafnium oxide provide better insulation properties, allowing for thicker oxide layers that reduce the short channel effects that lead to gate oxide breakdown. This is achieved without compromising the electric field efficiency, thereby reducing the likelihood of breakdown [34]. High dielectric materials like hafnium oxide address the limitations of silicon dioxide, by providing a higher permittivity, which allows for the gate oxide to become thicker whilst also maintaining the capacitance levels necessary for device operation. This reduces electric field stress across the gate oxide, also lowering the chances of breakdown [61].

Fabrication Process Optimisation Techniques

Another strategy to mitigate gate oxide breakdown failures is by optimising parts of the MOSFET fabrication process to improve the quality and reliability of the gate oxide. techniques such as thermal oxidation can produce a uniform oxide layer, which involves controlling the oxidation of silicon in a high temperature furnace. By precisely managing the temperature and environment, defects in the gate oxide are minimised, as well as impurities that can lead to weak spots in the layer [35]. Between wet oxidation, where thicker oxides are produced, and dry oxidation techniques, in which thinner oxides are produced, dry oxidation is more suitable for mitigating gate oxide breakdown, as it produces higher quality oxide layers for MOSFETs. These layers have fewer defects making them suitable for more advanced tasks.

Rapid thermal annealing (RTA) is also a suitable optimisation technique, as it is used to repair defects and improve the quality of the oxide layer after deposition. By heating the wafer to a high temperature in a short period of time, defect annealing can take place, reducing the defect density and thus relieving stress in the oxide layer. This increases the lifespan of the device and ensuring reliability [36].

Mitigation of Hot Carrier Injection

To mitigate the traps and defects as a result of the hot carrier injection phenomenon, several strategies have been developed, with key focus on device design and material engineering combined with operational techniques.

Advanced Material Implementation

Using advanced material engineering, the properties of the gate oxide can be enhanced to combat the effects of hot carrier injection. Materials with a high dielectric constant, therefore a high permittivity, can be implemented instead of traditional silicon dioxide, to reduce the gate leakage of the MOSFET and improve reliability overall. Because materials with a high dielectric constant, such as hafnium oxide, can maintain a thicker dielectric layer with a higher capacitance, the electric field across the gate oxide reduces, which in turn reduces the direct tunnelling current

and therefore minimises the gate leakage [37]. A higher capacitance also provides better insulation, which reduces the impact of hot carriers on the gate oxide, increasing the lifespan of the device, improving the reliability of the MOSFET.

MOSFET Design Optimisation Techniques

By optimising the design of the MOSFET, the electric field in the device can be reduced, and the carrier energy can be distributed more effectively for a more reliable device. Implementing techniques such as lightly doped drain (LDD) structures, the electric field near the drain junction can be reduced. By using an LDD approach, lightly doped regions can be placed in the heavily doped source-drain and the channel, smoothing the potential gradient which reduces the probability of hot carriers generating [38].

Mitigation of Positive and Negative BTI

Since carriers in the channel of the MOSFET lead to shifts in the threshold voltage of the device which affects the switching power of the device, mitigation strategies are in place during the fabrication of the devices to ensure reliability.

Fabrication Process Optimisation Techniques

By enhancing the quality of the gate oxide during the fabrication process, the effects of negative and positive BTI can be avoided. For NBTI, advanced fabrication techniques, that allows the grow of high-quality gate oxides, such as chemical vapour deposition (CVD) and molecular beam epitaxy (MBE) can be employed, to produce fewer intrinsic defects. With fewer defects, the susceptibility of MOSFETs to NBTI is significantly reduced, thereby increasing the long-term performance of the MOSFET [39]. For PBTI, deposition techniques, like atomic layer deposition (ALD), are employed to ensure that gate oxide layers are deposited uniformly and with a higher quality. ALD allows for precise control over the thickness of the dielectric layers, resulting in fewer defects and impurities that increase the likelihood of PBTI, increasing the reliability of the performance of the device [40].

Another way to ensure that the risks of NBTI are reduced is by using post fabrication annealing processes. Utilising the forming gas annealing process, dangling bonds at the silicon/dielectric interface can be passivated, which reduces the number of defect sites that contribute to NBTI. Forming gas is a mixture of hydrogen and nitrogen, in which the hydrogen atoms bond with the dangling silicon atoms, neutralising the defects, therefore enhancing the reliability and lifespan of the MOSFETs [41]. For PBTI, surface passivation techniques are employed to minimise the trap density in the channel of the device. By engineering the interface between the gate oxide and silicon substrate by using a high-κ dielectric, a smoother and more stable interface is formed, reducing the defects that lead to PBTI, therefore improving the overall reliability of the MOSFETs [42].

MOSFET Design Optimisation Techniques

The design of the MOSFET can also play a role in mitigating PBTI and NBTI. By implementing adaptive body biasing (ABB) techniques, the body voltage of the transistor is modified, to adjust the threshold voltage of the MOSFET, preventing threshold shifting by carriers. Acting as a dynamic adjustment, the performance of the device is constantly maintained, even as the threshold voltage is affected by BTI [43].

Mitigation of Gate Induced Drain Leakage

As device dimensions decrease and operational voltages increase, gate induced drain leakage becomes a significant failure mechanism, requiring effective mitigation techniques to overcome this phenomenon.

MOSFET Design Optimisation Techniques

By designing optimal doping profiles in the gate and drain of MOSFETs, the electric fields that result in GIDL can be reduced. An effective method for this is using a LDD structure, in which a gradual change in doping concentration occurs, from the highly doped drain region to the lightly doped area near the gate. This gradual change aids in the distribution of the electric field more evenly across the gate-drain overlap of the device, reducing the peak electric field and thus minimising the traps and increasing the performance of the device [44].

Fabrication Process Optimisation Techniques

Post fabrication techniques such as rapid thermal annealing can be used as a mitigation strategy, in which the wafer is heated to a high temperature in a short period of time, allowing dopants to diffuse to the desired location, before they become electrically active [36]. This repairs defects made in the oxide layer of the MOSFET, optimising the doping profile and improving the interface quality between the silicon and oxide, leading to enhancements in the performance and reliability of the MOSFET [72].

2.3 Reliability

In engineering, reliability is described as the likelihood that a product, system, or service will perform its intended function without failure [76].

2.3.1 Reliability Challenges in EVs

Reliability is a critical factor for any automotive technology, and it holds even greater significance for EVs. Consumers and manufacturers alike depend on the consistent and dependable performance of these vehicles. Reliable EVs can reduce maintenance costs, enhance user experience, and build consumer trust, which is essential for market growth. However, reliability issues can hinder the adoption rate and potentially slow down the transition to more sustainable transportation [73].

Battery Degradation

With the battery being the most prominent component of EVs, it is prone to the most degradation and reliability issues. Over time, lithium-ion batteries begin to degrade, leading to a gradual loss of energy storage capacity, resulting in a decrease in the vehicle's overall performance. This is caused by several factors, especially the extreme operating temperatures and deterioration due to the constant charge-discharge cycles occurring inside of the battery pack [45].

The battery degradation leads to reliability issues surrounding the driving range of EVs. As the battery degrades the capacity of the component diminishes, which reduces the driving range of EVs, meaning charging will need to be completed more regularly, making the vehicle less efficient and unreliable [75]. This can also increase the charging time of the battery, due to the capacity decreasing, the battery may not be able to accept charge as efficiently, or at all. Overall, the aging of the vehicle is significantly influenced by battery degradation. The solution to extend the lifespan is through replacement or refurbishment, which not only compromises the reliability of EVs but also introduces financial issues [76].

Temperature Sensitivity

Reliability challenges also occur due to the extremely high operating temperatures and rapid temperature variations involved in the charging process and inverters in EVs, but particularly the battery system. With the performance of lithium-ion batteries being highly sensitive to temperature, electrothermal challenges occur between the battery and the interconnector [77]. During the charging and discharging of a cell, module or pack, the existence of a connection resistance results in a loss of electrical energy across the interface, as well as heat generation in the contact region. This means that the input energy will be partially dissipated, due to the increased resistance generated from the heat generated, reducing the available battery module capacity. Consequently, more energy is dissipated, leading to heat in the contact region of the battery cell, causing accelerated degradation or thermal runway, and ultimately breakdown of the vehicle [46].

Extreme temperature variations in EV operations can also cause material deterioration. This is the thermal expansion and contraction of materials in the system, which causes wear and tear on various components such as the battery casing, connectors, and key structural elements. If materials with different thermal expansion are joined and heat is generated at the contact interface, inhomogeneous thermal expansion could introduce shear loading or plastic deformation in the contact region, which can breakdown the contact resistance. This does not only cause inefficiency and a decreased lifespan on EVs, but also causes many safety threats from overheating [46].

Motor Reliabilities

As the motor is comprised of two components, the drive motor and motor driver, there is more room for reliability issues. The drive motor of the system is the main area for mechanical faults, especially in the bearing, rotor, and stator, whereas the failure of the motor controller is primarily caused by faults in the busbar capacitor, control module, driver module, discharging module and IGBT [7].

The control module is the most vulnerable part of the entire motor system, due to the large number of components and their different applications within the system. Failures in this system lead to a loss in the mechanical energy converted to electrical energy to drive the motor, resulting in a loss of propulsion, decreased acceleration rate and therefore less speed and torque, creating unreliability. The lack of motor reliability can also lead to unsafe driving conditions, especially during operation in high temperatures. During extreme temperature conditions, the drive motor can also be seriously impacted. With the resistance in the motor windings increasing significantly, the speed of the motor decreases and therefore the speed and torque of vehicle plummets, resulting in reduced efficiency [79].

Vehicle-to-Grid Challenges (V2G)

Vehicle-to-grid (V2G) technology allows EVs to not only consume energy from the grid but also return excess energy, creating a wider range of distributed energy storage devices instantly available. Additionally, it allows vehicles to connect directly to the grid [47]. However, it can pose challenges that affect the reliability of EVs charging cycles. Frequent charging and discharging cycles associated with vehicle-to-grid operations can contribute to increased battery degradation, causing the battery capacity to decline, meaning that the lifespan of the battery and therefore the vehicle will decrease, leading to inefficiencies and unreliability [47]. The more cycle associated with the battery also accelerates the deterioration of other components in EVs such as power electronics systems, due to the extreme temperature variations occurring in the charging and discharging processes, further leading to a shorter lifespan on the vehicle [81].

V2G technology also promotes phase imbalance and voltage instabilities, which can cause significant system disruptions. As the technology operates close to its stability limits at high load requirements, a voltage instability is caused, affecting the charging characteristics of EVs and decreasing the lifespan of the battery pack due to degradation from overcharging and over-discharging. Additionally, single-phase electric vehicle chargers lead to phase imbalances in the distribution network, due to the fast EV charging overwhelming the grid systems, leading to potential issues such as voltage fluctuations and increased losses [47].

2.3.2 Reliability Challenges of MOSFETs

Although using MOSFETs seems like a next step for the future manufacturing of EVs, there are many challenges surrounding the reliability of the devices that could pose threats to the efficiency of EVs.

Thermal Stress

With EVs often operating in demanding environments with high temperatures, especially in the power electronics and motor drive systems, the deterioration of MOSFETs can occur at an accelerated rate. Due to the elevated temperatures, the stress on the gate oxide of MOSFETs increases, leading to breakdown and therefore permanent degradation of the MOSFET and the EV. Thermal stress on EVs can also result in hot carrier injection, a phenomenon where charger carriers gain sufficient energy to create defects in the gate oxide. This accelerates the breakdown of the gate oxide, leading to failure of MOSFET and therefore causing reliability issues in EVs [53].

MOSFETs are also more susceptible to breakdown than traditionally used IGBTs as they can conduct electricity better, leading to a higher junction temperature, increasing the probability of energetic electrons through the gate oxide due to the Fowler-Nordheim tunnelling effect. This tunnelling will trap electrons in the gate layer of the MOSFET, breaking down the device from overheating [48].

Another key impact of thermal stress in MOSFETs is electromigration. Electromigration occurs at elevated temperatures, where the movement of metal atoms in the conductive path of MOSFETs can increase. This causes vacancies and deposits in the power electronic circuits. As vacancies increase, they will eventually break circuit connections resulting in open circuits, whereas as deposits increase, they will eventually close circuit connections, leading to short circuits [49].

Switching Stresses

Switching stresses in MOSFETs in EVs can pose several reliability challenges, especially in power electronics, whereby their switching behaviour is critical for overall system performance. Frequent switching in MOSFETs leads to high switching stresses, which can cause dynamic stress and therefore power dissipation, in which MOSFETs are constantly experiencing switching losses during transitions between the ON and OFF states. These losses shorten the lifespan of these devices and thereby encourage unreliability because they generate heat and can cause temperature cycling, which deteriorates the MOSFET.

During the OFF state of MOSFETs, there is a brief period during which the voltage across the device spikes. If the switching speeds of the device are increased, the voltage during this period increases and can exceed the critical avalanche breakdown voltage, which can cause avalanche breakdown. This phenomenon can lead to localised heating and therefore device degradation. The avalanche breakdown characteristics are a vital parameter to MOSFET reliability, as it can limit the voltage applicable to the device [50].

Electromigration

As devices begin to shrink due to miniaturisation, electromigration (EM) in MOSFETs is a severe reliability issue in advanced ICs, where densely packed interconnects are under high currents. This issue occurs when electrons moving under the influence of an electric field collide with atoms in the interconnects, transferring momentum to the metal atoms, causing them to drift in the direction of electron flow [51]. In the interconnects within MOSFETs, electrons move rapidly due to the electric field applied. During this movement, frequent collisions occur between the high energy electrons and the metal atoms of the interconnect material, which result in the transfer of momentum from the electrons to the metal atoms, initiating the gradual displacement of atoms in the direction of the current flow. This causes gaps and defects to occur in the interconnect material, increasing the resistance of the interconnect, leading to open circuits and therefore circuit failure [52].

EM can occur due to several factors, such as higher current densities, which cause the rate of electron collisions to increase, accelerating the EM process. Elevated temperatures also enhance this effect, as it causes the metal atoms to easily move and form defects.

2.4 Promising MOSFET Technologies

2.4.1 Wide Bandgap Materials

In terms of addressing key requirements such as efficiency, power density and thermal performance, wide bandgap MOSFETs are rapidly gaining popularity in improving these parameters. Materials such as silicon carbide and gallium nitride are being implemented more into the production of EVs due to their better ability to handle higher voltages, operate at higher temperatures and therefore provide better efficiency to EVs [87].

Silicon Carbide (SiC)

Silicon carbide MOSFETs are regarded as one of the most important milestones in the development of power semiconductors. Compared with traditionally used silicon MOSFETs, SiC MOSFETs can withstand higher breakdown voltages, making them more suitable for high-voltage applications such as power inverters for EVs, renewable energy systems and high-power industrial applications. These devices also exhibit much lower switching losses than Si MOSFETs, which is beneficial in applications that require high frequency switching, such as motor drives and power supplies [30]. Reduced switching losses lowers the amount of power dissipation, therefore decreasing the thermal stress on the device, contributing to a higher overall system efficiency and longer lifespan [88].

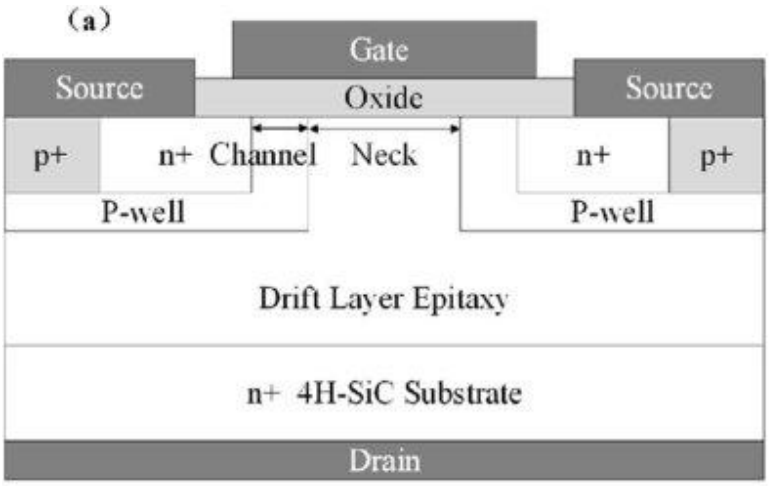

Figure 12 - Cross Sectional Diagram of SiC MOSFET [110]

Whilst there are significant advantages, challenges arise such as higher manufacturing costs and the need for more advanced and specialised packaging. Major challenges in the application of SiC MOSFETs include electromagnetic interference (EMI) and heat dissipation issues, which arise from the higher peak voltages and currents, seriously affecting the performance of the control loop and the stability of the power system, resulting in issues with reliability [30].

Gallium Nitride (GaN)

As GaN is a wide bandgap device, it can operate at higher temperatures than Si MOSFETs, as well as able to handle higher voltage levels, making GaN MOSFETs more reliable with its improved power density and efficiency. GaN MOSFETs also exhibit a high electron mobility, which means that charge carriers can move more quickly through the semiconductor material, resulting in faster switching speeds, reducing switching losses and decreasing the amount of power dissipated, making them adequate in high-frequency applications [53].

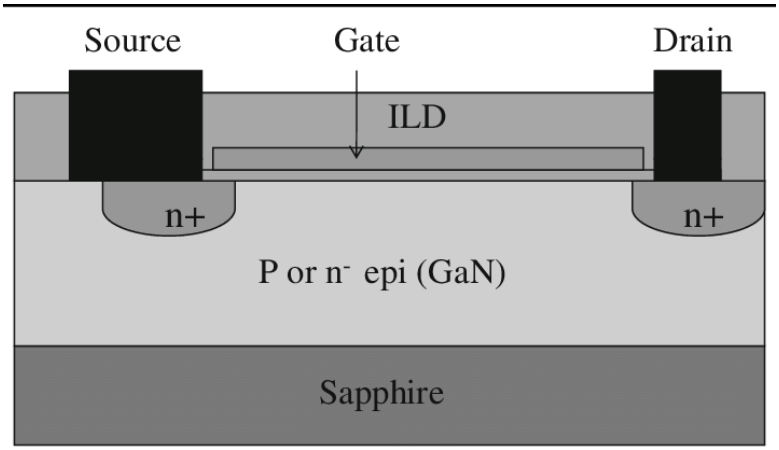

Figure 13 - Cross Sectional Diagram of GaN MOSFET [111]

There is constantly on-going research and technology to make GaN devices more accessible. However, they are very expensive to manufacture and therefore purchase. Despite the optimal operational properties of GaN, this material has no oxide dielectric in the gate structure to be used in MOS devices. Thus, there is less current control over the source and drain terminals of the device [53].

Gallium Arsenide (GaAs)

As a compound semiconductor, GaAs MOSFETs have unique properties that differ from other semiconductors, making them very attractive for high frequency operations. GaAs MOSFETs have an extremely high electron mobility, allowing for faster charge carriers, making them ideal for high-speed electronic devices [54]. Due to this, they are mostly used in RF and microwave applications such as amplifiers, mixers, and other communication systems. GaAs also has a direct bandgap, which allows for efficient emission and absorption of light, making these devices exceptional for LED and laser diode applications.

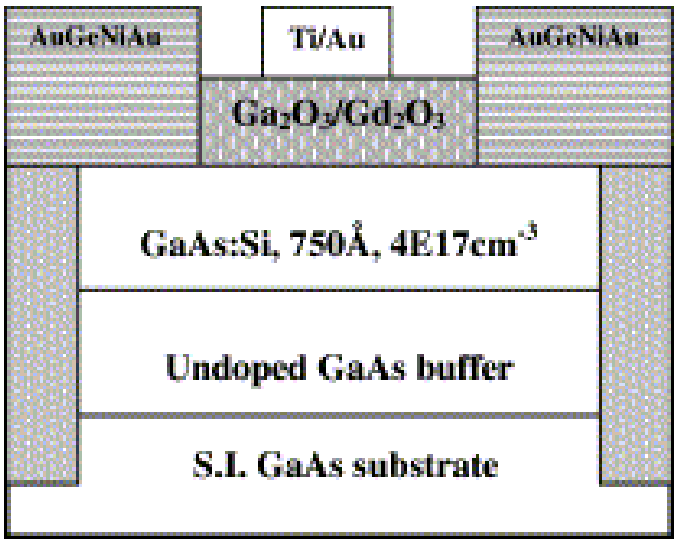

Figure 14 - Cross Sectional Diagram of GaAs MOSFET [112]

Although there are many benefits to these devices, GaAs MOSFETs pose particular manufacturing challenges compared to silicon devices, as GaAs is brittle and expensive. The most serious challenge is the development of a suitable gate dielectric with a low density of the states at the dielectric-semiconductor interface needed to maintain a high electron mobility in the channel of a GaAs MOSFET [91].

2.4.3 High-Frequency Switching

Because of their efficiency and high-speed switching capabilities, MOSFETs are widely used in electronic devices. Given how quickly technology is developing, it's critical to highlight significant research findings.

Miniaturisation and Scaling

For the last 50 years the advancements of the electronics industry have relied on Moore's Law, representing the doubling of the number of transistors every two years, along with the speed and capability of the devices. By incorporating scaling down technologies, a greater number of transistors can be manufactured on a single wafer, reducing the costs of the circuitry while increasing the performance and speed of the devices, but also increasing power dissipation. By reducing the device dimensions, the processing speed and radiofrequency (RF) performance are improved, along with the cut off frequency and maximum oscillation frequency, which are crucial parameters for RF systems [59]. Because the devices can operate at higher frequencies without signal degradation, device scaling increases switching speeds.

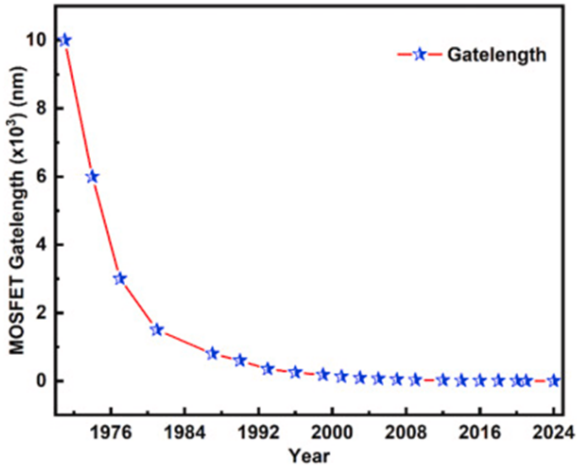

Figure 15 - Gate Length Reduction of MOSFETs Over 50 Years [59]

However, with the scaling of MOSFETs, limitations arise surrounding reliability of the devices during key operations. As the electron thermal voltage, kT/q, is constant at room temperature, the ratio between the operational voltage and the thermal voltage decreases, resulting in increased leakage currents caused by the thermal diffusion of electrons. The thermal diffusion of electrons results in quantum mechanical tunnelling from the gate to the channel through the dielectric layer. This process causes a gate leakage current, which grows exponentially as the oxide thickness decreases in thin dielectric films. This phenomenon decreases the lifespan of MOSFETs at an accelerated rate and, therefore, reliability of the devices [60].

The device scaling to nanoscale dimensions increases also variability of device structures leading to variability in device characteristics. Consequently, the supply voltage cannot be decreased proportionally to the length of the channel. The device scaling will thus increase the electric field strength in the channel and across the gate oxide. The increased electric field leads to barrier failure and increased leakage currents that permanently damage the device, leading to accelerated breakdown and device unreliability [60].

FinFETs and Nanosheet Technologies

Fin field-impact transistors (FinFETs) are three-dimensional transistor, the devices which evolved from MOSFETs, but with the addition of a fine Si 'fin' inversion channel above the substrate, expanding the gate to the left side and to the right side of the device channel [59]. Therefore, the FinFETs architecture, with its vertical fin design, allows for better control of the channel through which the current flows, helping to mitigate short-channel effects and other scaling limitations such as reduced leakage current. This enhances power efficiency and reduces heat generation, making FinFETs more reliable devices than standard MOSFETs [94].

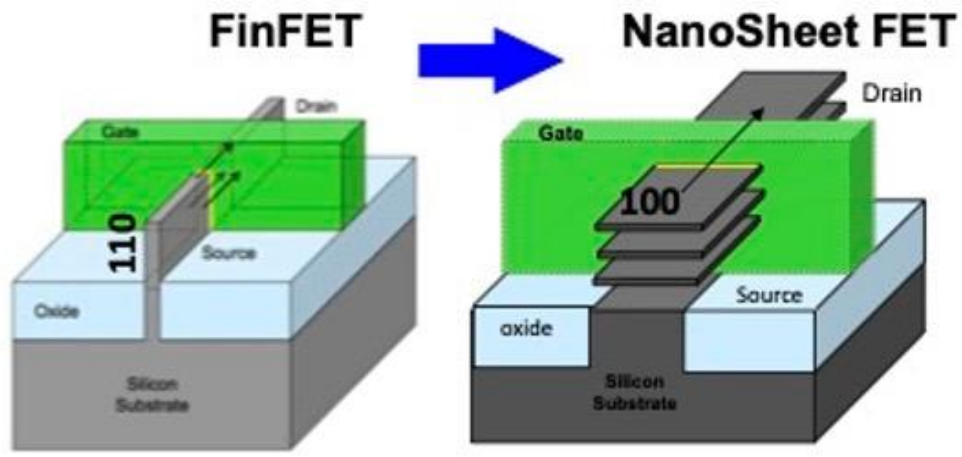

Figure 16 - FinFET and NanoSheet FET [94]

Compared to FinFETs, nanosheet transistors have a horizontal sheet structure, in which the conducting channel consists of thin horizontal sheets of semiconductor material, allowing for better control of the current flow, maintaining electrostatic integrity. These transistors typically feature a Gate-All-Around design, where the gate material surrounds the conducting channel on all sides. This configuration enables a higher drive current compared to FinFETs when scaled down, while maintaining superior electrostatic integrity – especially very low leakage current. This provides enhanced electrostatic control over the channel, helping to mitigate short-channel effects, reduce the power dissipated in the device, lower the thermal stress, and increase switching speeds [61].

2.5 Reliability Testing Methods

There are several techniques for evaluating the reliability of MOSFETs and other semiconductor devices. One of the commonly used techniques is accelerated breakdown testing, which involves intentionally raising voltage or current stress conditions above standard operating levels to induce breakdown and gather breakdown data. An alternative approach involves employing modelling and simulation techniques, which use computational methods to digitally comprehend the fundamental physics of breakdown mechanisms and predict device reliability under different operating conditions [96].

2.5.1 Charge-to-Breakdown (QBD) Testing

Charge to breakdown (QBD) testing of MOSFETs is a reliability testing method used to assess the susceptibility of MOSFETs to charge-related breakdown mechanisms, especially the breakdown of the gate oxide. The gate oxide inside MOSFETs acts as an insulator between the gate terminal and the channel underneath. When under operating stress and over time, the oxide layer can degrade due to charge accumulation, leading to catastrophic failure. This is because the gate leakage current under different fields of MOS capacitors follows a universal envelope. This behaviour can be used to predict the oxide lifetime, with the assumption that the breakdown of the dielectric is caused by the critical charges flowing through the oxide [62].

In QBD testing, the MOSFET under testing is subjected to high electric fields in order to obtain the charge required to induce breakdown or failure of the gate oxide at an accelerated rate. This can be done through passing a constant current through the gate-source terminals of the device under test, and monitoring the time taken for breakdown of the device to occur. As the charge accumulates in the gate dielectric of the MOSFET, the electric field across the oxide increases until the critical point is reached, and breakdown occurs. The charges that pass through the dielectric can be calculated by integrating the leakage current to the time taken to breakdown as [63]:

$$Q_{BD} = \int_0^{t_{stress}} I_G \cdot dt \tag{1}$$

2.5.2 Electrothermal Modelling

Obtaining a reliable estimate of the electrothermal behaviour of MOSFETs is crucial to improve the dependability and reliability of electronic systems. Electrothermal modelling of power MOSFETs utilises simulations to address both thermal and electrical problems. While the electrical model describes the device's behaviour, considering temperature-dependent thermal properties, the thermal model calculates the temperature distribution and evolution of the device. This calculation considers both external heat exchanges and internal heat sources [64].

The most prominent cause of degradation and reliability issues in MOSFETs under operation is from thermal stress [53]. Therefore, a model that can link both electrical and thermal aspects allows communication of power dissipation to the thermal model. This enables the determination of the junction temperature [65]. A finite element electrothermal model for MOSFETs must accompany the experiment work to collect the aging results of the device. The model requires all geometrical parameters of the tested MOSFET, along with the material, electrical, and thermal parameters, for the simulation. After conducting the simulation, it generates the temperature distribution, junction temperature, and thermal stress analysis. These results are then utilised to assess the reliability of the MOSFETs.

2.5.3 Time Dependent Dielectric Breakdown (TDDB) Testing

Time dependent dielectric breaking (TDDB) testing is typically used as a critical reliability evaluation method to assess the long-term durability of the gate oxide dielectric, based on the

field-driven mechanism. This can be accomplished by operating at high temperatures and applying either a constant voltage or current stress to the DUT's gate oxide, simulating the severe operating conditions found in real-world systems [66]. The testing parameter running through the device is set to be over the normal operating voltage to accelerate the breakdown process. The time to breakdown in the device is measured and used to estimate the reliability of the gate oxide under normal operating conditions. However, this test is completed at low electric fields (E_{ox} > 8.5 MV/cm) to achieve more accurate lifetime predictions. Therefore, it could take a long time to obtain results from the experiment [63].

A commonly used technique to analyse TDDB data and predict the reliability of the gate oxide is the Weibull analysis. This is achieved by plotting the time-to-breakdown data on a Weibull probability plot, in order to help to identify the lifetime characteristics and the shape parameter, which indicate the reliability distribution [67].

2.5.4 High Temperature Gate Bias (HTGB) and High Temperature Reverse Bias (HTRB) Testing

To identify gate-oxide degradation in MOSFETs, high temperature gate bias (HTGB) testing is implemented due to its ability to accelerate the aging of the device, especially under high switching conditions. Under HTGB test conditions, the gate or oxides of the device samples are biased during operation in a static mode at, or near, maximum rated oxide breakdown voltage. In a conventional HTGB test, a constant DC voltage is applied at the gate-source of the MOSFET to act as the stress voltage. This gate-source voltage biases the gate oxide, as well as the drain-source voltage [68].

HTGB testing is also used to monitor variations in the threshold voltage of the tested device following prolonged application of DC voltage to the gate-source of the MOSFET at high temperatures. In this process, the MOSFET under test is secured in an environmental chamber that maintains a constant temperature. It is then bias stressed by applying a constant gate-source DC voltage, with the drain shortened to the source. This process is monitored weekly for six weeks, during which the threshold voltage is reviewed and ensuring the temperature is maintained [69].

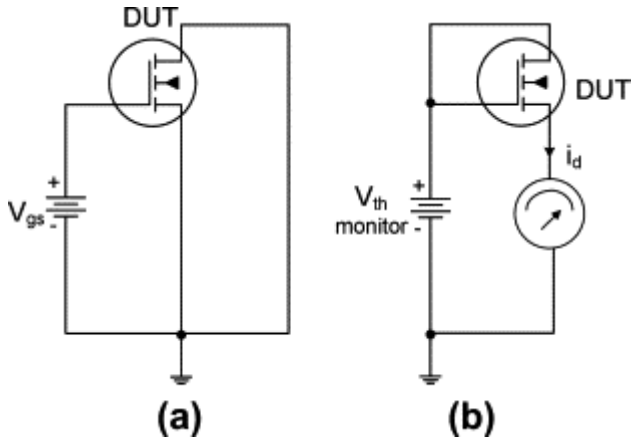

Figure 17 - Schematic of Gate Bias Circuit (a) During Stress and (b) For Threshold Voltage Measurement [87]

Alongside HTGB testing, high temperature reverse bias (HTRB) testing can be implemented to monitor the leakage current of the devices under the reverse bias conditions over a long period of time. Combining electrical and thermal stresses, HTRB testing can be used to check the junction integrity, identify crystal defects, and evaluate the level of ionic contamination. These factors will reveal degradation effects in the tested devices, to prove how reliable the devices are. To carry out this test, four MOSFETs can be tightly screw pressed onto a hot plate at a constant temperature, whilst being supplied with a constant high voltage. Eighty percent of the maximum rated reverse breakdown voltage is then applied to the gate-source of the device, with the gate being shorted to the source. This is monitored for 6 weeks at weekly intervals [69].

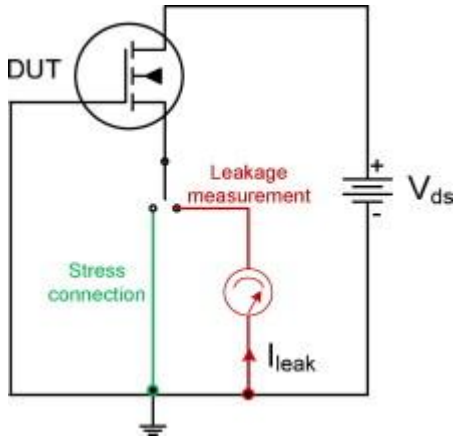

Figure 18 - Schematic circuit for HTRB test [87]

2.6 Constant Current Sources

Constant current sources are a fundamental part in electronic circuits, in which their role is to provide a stable current regardless of voltage changes or load variations. These configurations are essential in numerous applications, including LED drivers, battery charging circuits and precision analogue circuits [105].

Designed to deliver a stable current regardless of voltage changes, constant current sources must be stable and allow precise control of a predefined current. The fundamental principles behind constant current sources involve understanding how a consistent current flow is maintained, despite varying load conditions. The primary operation of constant current sources is based on Ohm's Law, which states that the voltage is directly proportional to the current based on the resistance. In order to maintain a constant current, the voltage must be dynamically adjusted across the load to maintain the desired current, despite changes in resistance. Many constant current sources use feedback mechanisms to regulate the current, typically using a transistor or an op amp, to monitor the flow of current flowing through the load and adjust the control element to compensate for any deviations from the desired current, ensuring the output current remains constant [106].

Another key principle of constant current sources is the generation of a high impedance path in parallel with the load. This ensures that the current through the load remains unaffected by

changes in the load voltage, which can be achieved using components, such as transistors, in a specific configuration to form a high impedance [107].

2.6.1 Resistor-Based Sources

The simplest and most widely used constant current source is a resistor-based design, in which a resistor is placed in series with a voltage source, with the current defined under Ohm's Law. From using a stable voltage source and resistor appropriate to the current desired, a constant current can be achieved as long as the resistance does not change [70]. This simple and cost-effective design is often used due to its minimal components. It can be easily integrated into basic circuit configurations, such as basic LED driving circuits and current limiting applications, where precise current control is not critical.

2.6.2 Transistor-Based Sources

Transistor-based current sources are a significant improvement over resistor-based designs, in terms of stability and precision. By employing transistors, such as BJTs and MOSFETs, the current sources can provide more stable and controlled current [109]. This can be done by using a transistor device to control the current flowing through the circuit, by creating a reference current that sets the desired current level, as well as using a feedback loop to ensure the output current matches this reference [110]. This is achieved by using either the emitter follower configuration, where a BJT is employed, or the source follower configuration, which utilises a MOSFET.

Emitter Follower Circuit

In the emitter follower circuit, the emitter current, which is equal to the collector current of the configuration, is set by a reference voltage applied to the base and a resistor placed in the emitter [103]. The BJT adjusts the voltage drop across the load to maintain a constant emitter current. The configuration is known as 'emitter follower', as the output voltage at the emitter follows the input voltage applied to the base, minus a small voltage drop (which is 0.7 V for Si transistors) due to the base-emitter junction. By applying a reference voltage to the base of the BJT, setting the operating point of the transistor, ensuring that the current through the device remains constant [71]. A resistor is then placed at the emitter terminal of the transistor, which determines the current flowing the circuit. According to Ohm's Law, the current at this point, I_E, is given by:

$$I_E = \frac{V_B - V_{BE}}{R_E} \tag{2}$$

where V_B is the base voltage, V_{BE} is the base-emitter voltage of 0.7 V and R_E is the emitter resistor.

The transistor then adjusts the voltage drop across the load to maintain a constant emitter current, which is almost equal to the collector current, due to the high current gain of the transistor. The BJT adjusts the emitter voltage dynamically to maintain a constant output current, and therefore a stable constant current source is formed.

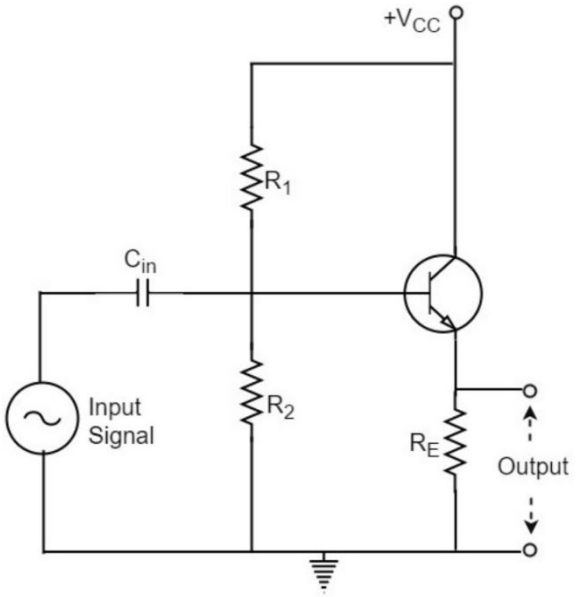

Figure 19 - Emitter Follower Current Source Configuration [99]

2.6.3 Current Mirror

A more complex configuration to produce a constant current source is known as a current mirror, a design which replicates the current flowing through one transistor into another transistor. This ensures the current in one branch of a circuit is accurately duplicated in another branch. The reference transistor sets the initial current, in which this is connected with a precision resistor or a reference current source to establish a stable current. The second transistor, known as the output transistor, is configured to mirror the current flowing through the reference transistor. The two transistors are usually identical in characteristics, and connected via their gate or base terminals, ensuring that the voltage applied to the two MOSFETs is equal [72].

The key principles of current mirrors rely on the duo of transistors, subjected to the same voltage, will conduct the same current. The drain current in a MOSFET is then given by:

$$I_D = \frac{1}{2}\mu_n C_{ox}\left(\frac{W}{L}\right)(V_{GS} - V_{th})^2 \quad (3)$$

where μ_n is the electron mobility, C_{ox} is the oxide capacitance per unit area, V_{GS} is the gate-source voltage and V_{th} is the threshold voltage and W and L represent the width and length.

In Eq. (3), the drain current is determined by the gate-source voltage, the threshold voltage and the physical dimensions and the properties of the transistor. When the gate-source voltages of two identical transistors are equal, the drain currents through those transistors will also be equal, therefore achieving current mirroring [73].

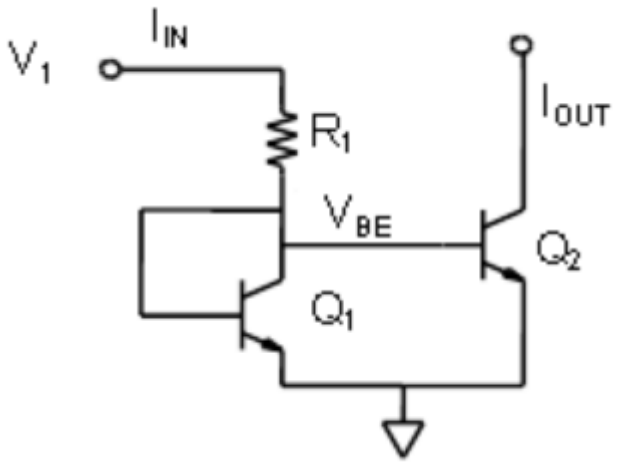

Figure 20 - Current Mirror Configuration [72]

Current mirrors offer high precision in constant current generation and replication, making them ideal for applications where two currents of the same value are required. This makes them easy to implement in ICs, as they occupy less space on the chip, therefore they can be fabricated with higher accuracy. These advantages make them ideal for current-mode signal processing, especially in operational amplifiers, active filters and analogue multipliers, where precise current control is essential [74]. In contrast, current mirrors have a complex design, in which they require the careful match of transistors so errors in the current do not occur.

2.6.4 Op-Amp Based Sources

In op amp based constant current sources, an op amp controls the current through a transistor or MOSFET. The op amp ensures that the voltage across a reference resistor remains constant, regulating the current. This method utilises the op amp high gain and precision to provide a stable and accurate current source. Configured into a feedback loop, the op amp maintains a constant voltage source across a reference resistor. This reference resistor acts as precise resistor in the circuit, where the desired constant current is set by a voltage applied across it, following Ohm's Law [75]. The op amp senses the voltage drop across the reference resistor. Its non-inverting input is connected to the reference voltage, while the inverting input is connected between the reference resistor and the source of the MOSFET. Acting as a variable resistor, the MOSFET is controlled by the op amp. The op amp adjusts the transistor gate voltage to maintain the voltage across the resistor equal to the reference voltage. This ensures the current through the resistor and load remains constant and accurate.

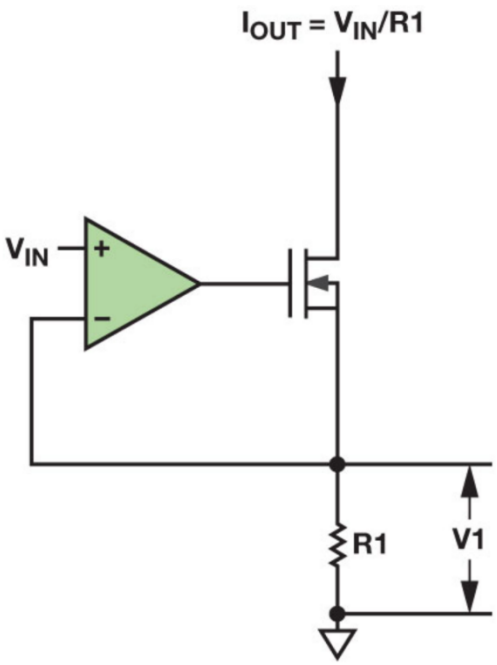

Figure 21 - Op Amp Based Current Source Configuration [98]

The feedback loop formed by the op amp, reference resistor and MOSFET ensure that any variation in load or supply voltage is fixed dynamically in order to maintain a stable output current. The high gain characteristics of the op amp offers significantly accurate control of the current, due to the feedback loop correcting errors, therefore providing stable and efficient current regulation. This current source can also drive a wide load of resistances, making it ideal for applications in analogue-to-digital converters (ADCs) and digital-to-analogue converters (DACs), due to its precise control [108]. However, this configuration also requires a stable power supply and precise reference voltage, meaning any fluctuations in the two can negatively affect the operation and, therefore, the reliability of the current [109].

2.7 Research Gap

In reviewing the current literature surrounding MOSFET reliability in the context of EVs, it is evident that significant progress has been made in understanding and mitigating various failure mechanisms. However, a critical gap remains in research on the QBD testing of gate oxides, specifically in relation to the reliability demands of EV applications. While QBD testing is a well-established method for evaluating gate oxide reliability, most studies focus on its application in standard semiconductor devices and operations. There is a lack of comprehensive studies addressing the challenges in MOSFETs caused by the harsh operating conditions in EVs, such as wide temperature ranges, high voltages, and frequent switching operations. These conditions accelerate the breakdown mechanisms of gate oxides. Therefore, it is crucial to adapt QBD testing methods to improve predictions of the long-term reliability of MOSFETs in EV applications.

Moreover, the literature studied focuses on traditional silicon-based MOSFETs, with limited exploration of how QBD testing can be adapted for emerging materials such as SiC MOSFETs, which are being increasingly integrated into EV power electronics, due to their superior electrical and thermal properties. The gate oxide reliability of these materials used in MOSFETs remains underexplored in the context of QBD testing, particularly surrounding their behaviour in high-stress environments of EVs. Whilst there is some focus on other accelerated testing methods such as TDDB for predicting oxide lifetime, the potential of QBD testing as a more accurate and efficient approach for evaluating long-term reliability in EV applications has not been entirely investigated. Whilst significant gaps remain in the understanding in the research on QBD testing for MOSFET reliability in EV applications, some studies have explored the aspects of this issue. For example, Yige Xu's research titled 'Applications and challenges of Silicon Carbide (SiC) MOSFET technology in electric vehicle propulsion systems: A review' and 'A review of silicon carbide MOSFETs in electrified vehicles: Application, challenges, and future development', written by Bufan Shi et al. However, these papers do not use a breakdown approach to assess the reliability of these devices.

Addressing the gaps in this research is essential for advancing the reliability of MOSFETs in EVs, ensuring that semiconductor devices can withstand the demands of the advancing automotive applications [123]. This work is inspired by Peter Moen's research in his paper titled 'A Charge-to-Breakdown (QBD) Approach to SiC Gate Oxide Lifetime Extraction and Modelling'. Moen's insights into the experiment and evaluation of SiC gate oxides has provided a foundation for this study, to guide with the creation of similar QBD testing apparatus.

3 Methodology

3.1 Requirement of Testing Equipment

Charge to Breakdown (QBD) testing of MOSFETs is a crucial experiment for assessing the reliability of the gate oxide layer. QBD testing involves subjecting the MOSFET gate to controlled electrical stress until the oxide layer fails, thereby providing a measure of its reliability. This testing method is invaluable for evaluating the endurance of the gate oxide under operational conditions and predicting the device's lifespan. The gate oxide layer is a vital part of the MOSFET, influencing the device's overall performance and stability. Evaluating its reliability with a charge to breakdown approach ensures that the device can operate effectively under various conditions. This testing experiment is to identify the failure mechanisms of the gate oxide, such as oxide breakdown. This experiment is also essential for assessing the endurance of MOSFETs under the operational conditions in EVs. By applying a controlled electrical stress to the MOSFET, QBD testing simulates the conditions the MOSFET will face during actual operation. By obtaining the time taken to breakdown, the results obtained can be used to predict an accurate prognosis of the MOSFETs lifespan, helping to determine potential failures and design more reliable systems.

In addition, the results from QBD testing offer valuable feedback for improving the design and materials used in MOSFETs, such as the gate oxide layers and material of the semiconductor, insulator and catalytic metal. Understanding how different materials and structures perform under stress can lead to the development of more durable devices. The aim is to determine the QBD value for different MOSFET samples and analyse the various stress conditions on the durability of gate oxides. The first step is to select the MOSFETs to be used as samples for this test procedure. Given the high-power and high efficiency demands of EV applications, selecting wide bandgap (WBG) devices is key, as they are known for their superior performance under extreme conditions. The selected MOSFETs for testing include Si and SiC devices. These materials were chosen due to their high voltage and temperature tolerances, fast switching capabilities, and overall robustness, making them ideal candidates for stress testing in the QBD experiment.

The next step is to configure the power supply for the test equipment. It must be a high voltage supply capable of delivering a controlled and stable voltage significantly higher than the normal operating voltage of the device under test (DUT). This capability ensures that the gate oxide can be subjected to the necessary electrical stress to induce breakdown. The power supply must also have precise voltage control to incrementally increase the stress applied to the gate oxide, allowing for accurate determination of the QBD value. The most crucial requirement for this experiment is a reliable current source, in which a constant current must be provided to the gate of the MOSFET, ensuring consistent electrical stress until the gate oxide breaks down. A steady current must be maintained, regardless of variations in voltage or resistance within the circuit. A precise current measurement configuration is also key, where high precision and accuracy are required to continuously monitor the gate current throughout the testing process. This monitoring is essential for identifying the exact time at which the gate fails, thereby determining the QBD value. The measurement device should have both high resolution and low noise levels to detect small fluctuations in current with high accuracy.

Voltage measurement is also key to QBD testing. Accurately measuring the voltage across the MOSFET's gate oxide is crucial for determining the point at which the gate oxide fails. This requires a precise voltage measurement circuit designed to handle the high-voltage conditions and dynamic changes that occur within this test. The voltage measurement circuit must be capable of accurately measuring a wide range of voltages, extending beyond the normal operating range of the MOSFET. This is essential for applying and monitoring the high voltage stress needed

to induce gate oxide breakdown. With these requirements, the hardware can be designed before QBD testing can begin.

3.2 Hardware Design

3.2.1 Current Source

Designing a current source for QBD operation involves several factors to ensure the current remains stable and unaffected. This configuration requires a constant current output, regardless of changes in load resistance or supply voltage.

Initial Current Source Design

Before finalising the design of the current source, I developed an initial version using the components described above, including the MAX6102 voltage reference, TLV271IS op amp, LND150 MOSFET, capacitors, resistors, and potentiometers. However, I decided not to proceed with this design due to its complexity.

Circuit Schematic

The initial constant current source was composed using three key components – a MAX6102 voltage reference, a TLV271IS CMOS rail-to-rail output op amp, and a depletion mode n-channel LND150 MOSFET. The circuit also contains one 1µF capacitor, two 0.1µF capacitors, as well as three resistors, with values of 9kΩ and 4kkΩ, and two variable resistors with values of 9kΩ and 4kΩ. The MAX6102 is utilised to provide a stable reference voltage by ensuring that the voltage applied to the non-inverting input of the op amp is constant, and the TLV271IS is chosen to amplify the difference between the input voltages and drive the MOSFET.

For this circuit, the resistor values can be defined through the following calculations of Maximum Load Voltage:

$$V_{L(max)} = I_L \times R_{L(\max)} = 0.8\ V \tag{4}$$

of Minimum Drain to Source Voltage:

$$V_{DS(min)} = I_D R_{D(on)} + 1\ V \tag{5}$$

$$V_{DS(min)} = (0.5m \times 1k) + 1V = 1.5V \tag{6}$$

$$V_{R1(max)} = V_{CC} - V_{L(max)} - V_{DS(min)} \tag{7}$$

of Maximum Voltage Through Resistor Sequence:

$$V_{R1(max)} = 5\ V - 0.8\ V - 1.5\ V = 2.7\ V \tag{8}$$

Once this is found, this can be used in the equation for Ohm's Law to find the values for the resistance:

$$R_1 = \frac{V_{R1}}{I_L} \tag{9}$$

$$R_1 = \frac{2.7V}{100\mu A} = 27k\Omega$$

$$R_{series} = R_1 + R_2 + R_3 \tag{10}$$

$$\therefore R_1 = 9k\Omega, RV_2 = 9k\Omega, R_3 = 9k\Omega$$

Using the value for drain-source voltage of the MOSFET, the Ohm's Law equation can be utilised again to find the resistance for R_4 and RV_1, in which the value can be split into two, since the resistors are both in series.

$$V_{DS} = 0.8V \text{ when } I_L = 100\mu A \tag{11}$$

$$R = \frac{0.8\,V}{100\mu A} = 8\,k\Omega$$

$$\therefore R_4 = 4k\Omega, RV_1 = 4k\Omega$$

For this circuit to operate, a ±5V and 60V supply voltage is required, which results in the values for the calculated resistance.

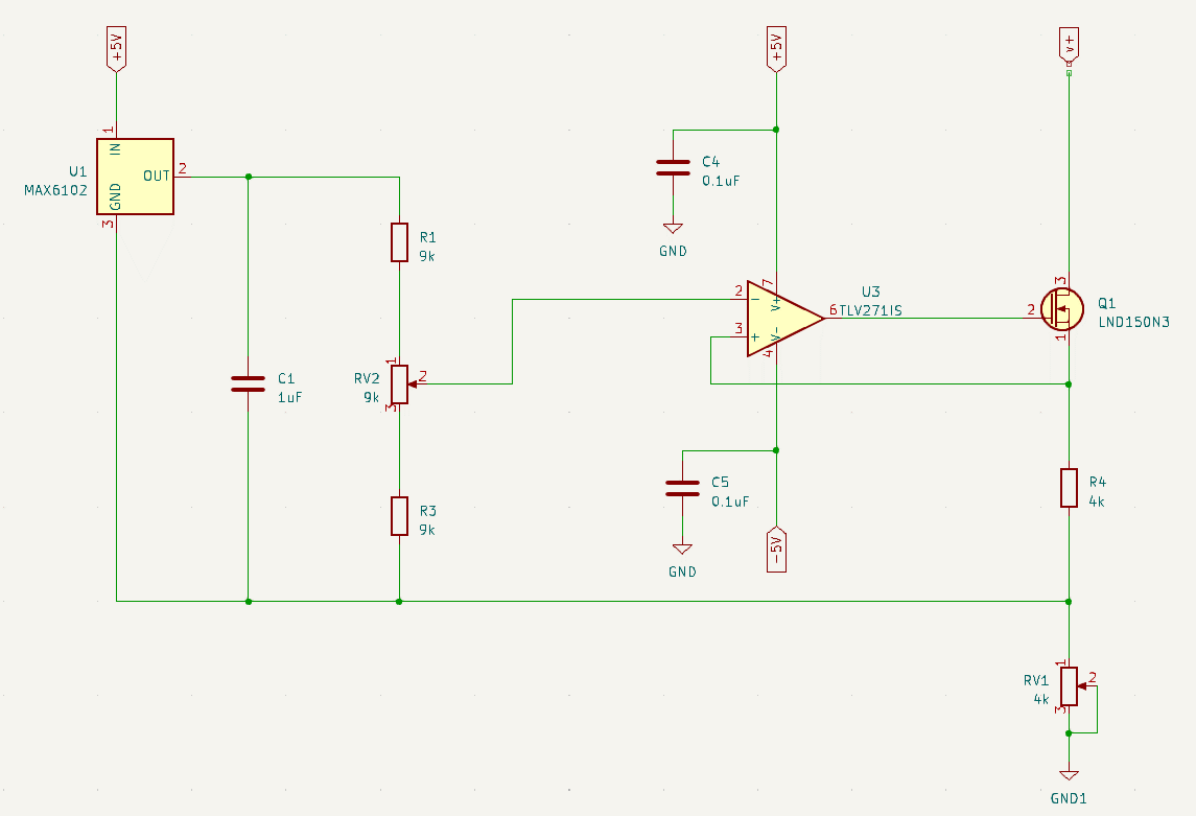

Figure 22 - Initial Schematic of Current Source in KiCAD, developed by Stephen Batcup

Operation Principle

By beginning the circuit with the MAX6102, this component provides a stable reference voltage which is applied to the non-inverting input of the TLV271IS op amp. To ensure a stable voltage, which is necessary to maintain a stable current, one of the capacitors is placed across the reference voltage and power supply, in order to filter out the high-frequency noise and stabilise the voltage. Starting from this point, the TLV271IS compares the reference voltage with the voltage across a feedback resistor. Resistor R1 is connected between the source of the MOSFET and the ground. The voltage drop across the feedback resistor is proportional to the current flowing through the MOSFET and the load, allowing for constant current regulation. When the op amp detects a difference between the reference voltage and the feedback voltage, it adjusts the gate voltage of the MOSFET. This alteration in gate voltage modifies the resistance, ensuring that

the desired current remains constant even when there are variations in load resistance or supply voltage.

The potentiometers are implemented for fine tuning the input and output signals, to allow precise control of the output current. The first variable resistor is connected to the inverting input of the TLV271IS, in which this configuration allows the reference voltage to be easily adjusted, ensuring a table and accurate input voltage. By maintaining the reference voltage, the variable resistor helps maintain the desired operating conditions for the op amp, contributing to the overall stability of the circuit. The second variable resistor is used to refine the output current produced. This works by adjusting the feedback resistance, which directly influences the output current, in which this is essential for the QBD application, as a constant and specific current is required to accurately test the durability of the gate oxide layer of the DUT.

Despite its potential for accurate current regulation, the design was too complex due to the number of components and the configuration could be simplified to achieve the same performance. This complexity not only increased the difficulty of assembly and testing but also increased the chances of reliability issues during the QBD experiment.

Final Current Source Circuit Schematic

By simplifying the original circuit designed, a constant current source for this QBD application is assembled by two key components – a dual JFET input TL082 op amp and a depletion mode n-channel LND150 MOSFET. Two 1µF capacitors are also utilised as well as a 10kΩ resistor. Below is the schematic for this circuit, which was made using KiCAD. The schematic was designed using KiCAD due to its accessibility and suitability for circuit prototyping. It allowed for easy modification and visualisation for circuit design. The TL082 and LND150 are implemented to control and stabilise the current, ensuring a precise and constant current is formed. This is done by configuring the op amp into a feedback loop, in order to monitor and adjust the control element. The 5V supply powers the TL082 operational amplifier, ensuring stable operation of the feedback loop

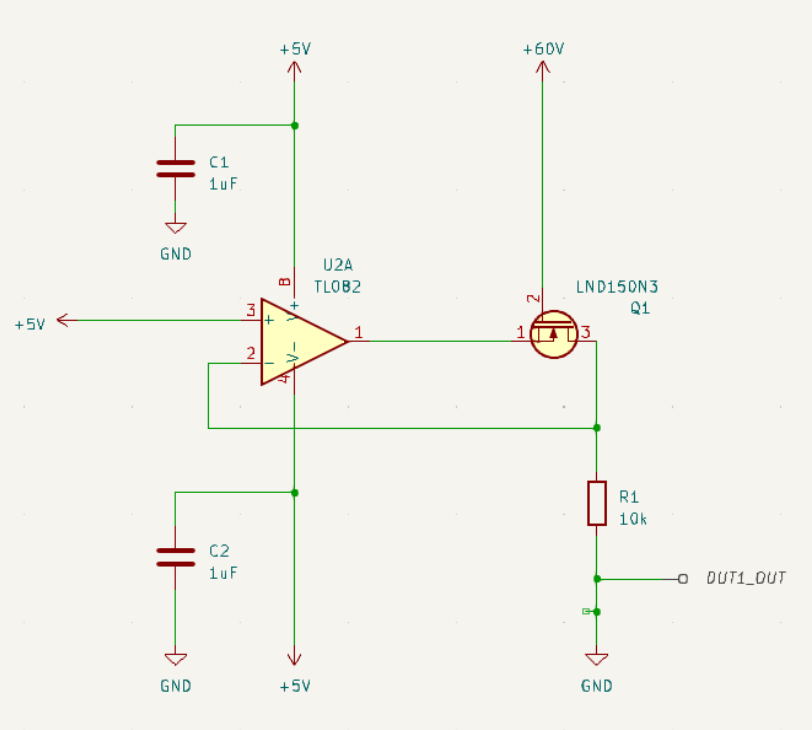

Figure 23 - Schematic for Current Source in KiCAD,, developed by Stephen Batcup

With a stable reference voltage being applied to the non-inverting input of the op amp, this can be used with the feedback resistor in between the source of the MOSFET and ground to determine the set current of the current source circuit. The relationship between the reference voltage, resistor value and output current are given by Ohm's law. A resistor value of 10kΩ has been chosen, so a set current value of 0.5mA can be achieved considering constant current source as:

$$I_{set} = \frac{V_{ref}}{R_{sense}} = \frac{5}{10000} \tag{12}$$

$$I_{Set} = 0.5\text{mA}$$

Component Selection

TL082 Dual JFET Input Op Amp – This op amp was selected for this circuit due to its low cost, high speed, and wide bandwidth. This wide bandwidth makes it ideal for this application, as it can maintain higher gains at higher frequency. This op amp also has internally trimmed offset voltage and requires a low supply current, which is ideal, as the output constant current required should be in the nanoscale. This circuit component acts as the control element in this constant current source, to prevent any unrequired noise. This is done by adding two bypass capacitors at the positive power input and negative power input of the op amp [76].

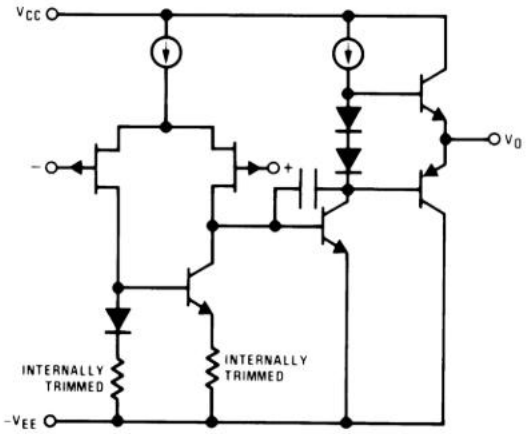

Figure 24 - TL082 Dual JFET Input Op Amp Schematic [101]

LND150 N-Channel Depletion Mode MOSFET – A depletion mode MOSFET was chosen for this configuration, due to its high voltage capabilities and lateral DMOS technology. The LND150 is also compatible with the TL082, being an ideal duo for precision constant current sources. This device also has excellent thermal stability capabilities, so it can withstand the large voltage supply going across it in the current source configuration. In this circuit, the MOSFET acts as a variable resistor, to adjust the drain current going through the gate-source voltage of the device, until the desired current is achieved [77].

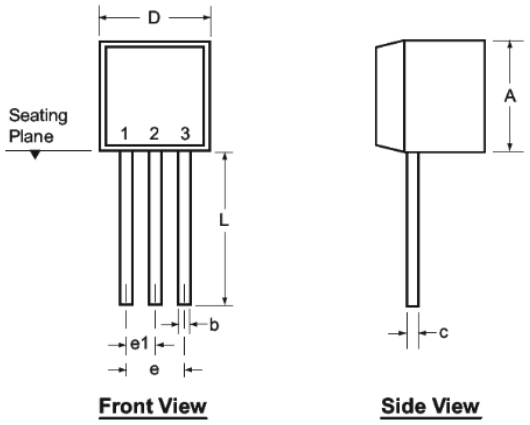

Figure 25 - LND150 N-Channel Depletion Mode MOSFET [102]

Operation Principle

The constant current source shown in Figure 23 is based on a feedback loop, in which the op amp continuously adjusts the gate voltage of the MOSFET to maintain the desired current. This is first done by connecting the inverting input of the op amp between the sense resistor R_1 and LND150 and connecting the non-inverting input to the reference voltage, $V_{Ref.}$ The desired current, I_{Set}, can then be determined through V_{Ref} and R_{Sense} as:

$$I_{Set} = {V_{Ref}}/{R_{Sense}} \tag{13}$$

With this value, the op amp adjusts the output, so voltage across R_{Sense} is equal to V_{Ref}. As the voltage across R_{Sense} is proportional to the current across R_{Sense}, maintaining V_{Ref} across R_{Sense} ensures I_{Set} is constant. The output of the op amp drives the gate of the MOSFET, and as this device is depletion mode, V_{GS} increases, which leads to a decrease in the channel resistance, adjusting the value for drain current, I_{Drain}, until it matches the value for I_{set} by $V_{Ref.}$ To ensure the current is kept constant, any load variations that change the current are rectified through the op amp adjusting V_{GS} of MOSFET.

Current Source Simulation

To verify the current source circuit is going to provide a constant output, before construction, it must be simulated to ensure it is operating correctly. By using the built-in LTSpice and PSpice simulation tools on KiCAD, the theoretical design can be verified. The circuit for this is shown below, where the circuit is built around the TL082 op amp and LND150 MOSFET, which are the primary components in the circuit that achieve the constant current output.

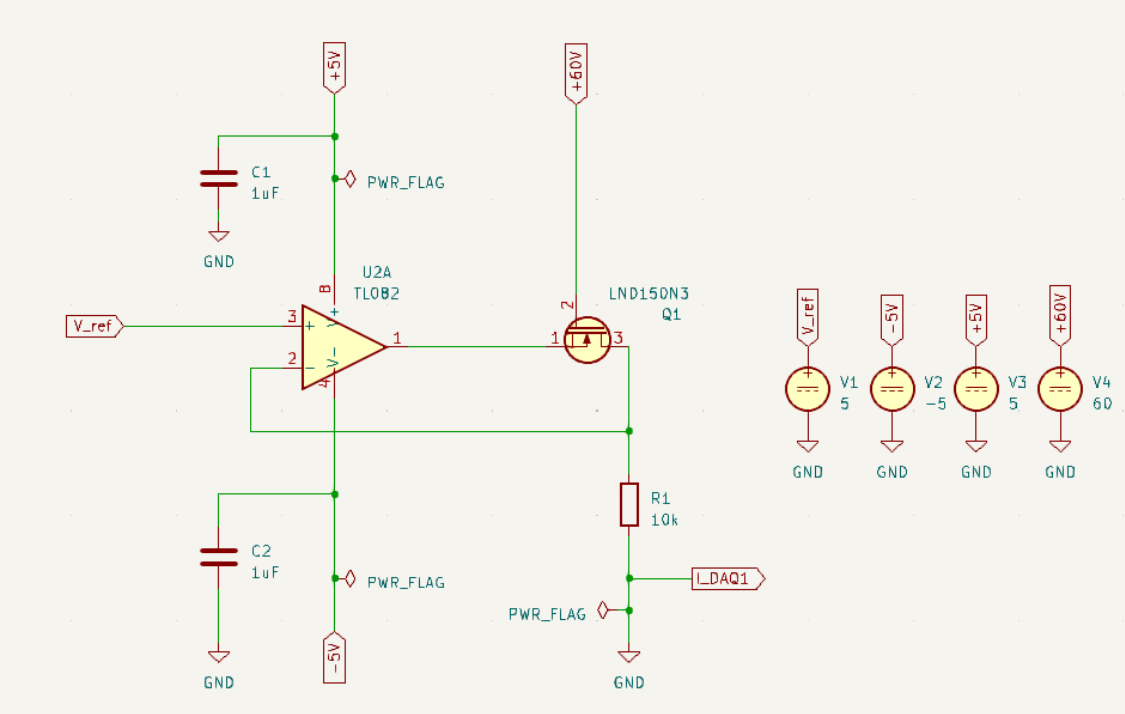

Figure 26 - Current Source Simulation Circuit

The circuit for this is shown below, where the circuit is built around the TL082 op amp and LND150 MOSFET, which are the primary components in the circuit that achieve the constant current output. By connecting a reference voltage of 5V to the non-inverting input of the TL082 op amp, as well as connecting the +5V, -5V and 60V input voltages to the circuit, the simulation can start by initiating the DC analysis. By setting the starting value of the 5V input reference voltage to zero and using a time step of one and setting the 60V input voltage passing through the gate of the MOSFET with a starting value of zero, incrementing in steps of ten, the output voltage of the TL082 and the LND150 can be plotted.

The initial transient observed in the voltage trace is due to the turn-on characteristics of the MOSFET and the charging of the circuit elements. After stabilisation, the voltage flattens at 3.2V, indicating steady-state operation. This op amp is configured to regulate the voltage and control the MOSFET, so as the circuit is powered, the output current from the TL082 begins to increase, due to the op amp responding to the initial conditions of the circuit, such as the supply voltage and reference voltage. As the TL082 continues to adjust the voltage, the circuit begins to stabilise, which can be seen as the horizontal line on the graph. This is due to the feedback mechanism of the op amp, which fine-tunes the voltage passing through the op amp, until it reaches the desired current level. Once this level has been reached, the circuit enters a steady-state operation where the current remains constant.

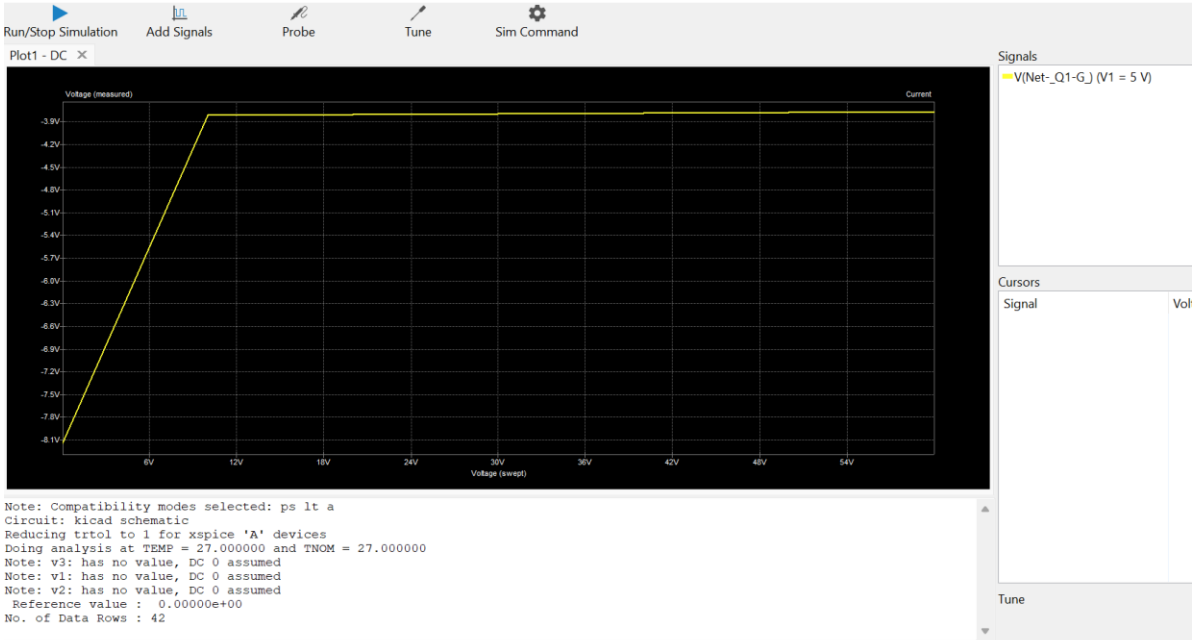

Figure 27 - Voltage Across TL082 Output

The voltage across the MOSFET output is plotted, in which the oscilloscope trace is shown in Figure 28. The voltage at this point illustrates a similar behaviour, however it flattens off at 3.2V. This is because for the QBD experiment, a very low current is required, therefore the MOSFET has lowered the constant current produced. The difference between the current levels of the two traces can be explained by the characteristics of the depletion mode MOSFET. In this circuit, the depletion-mode MOSFET dynamically adjusts the current to match the requirements of the QBD experiment by modifying the gate voltage. Since the QBD experiment requires a very low current, the MOSFET must reduce the current flowing through the circuit, which it does by adjusting the gate voltage.

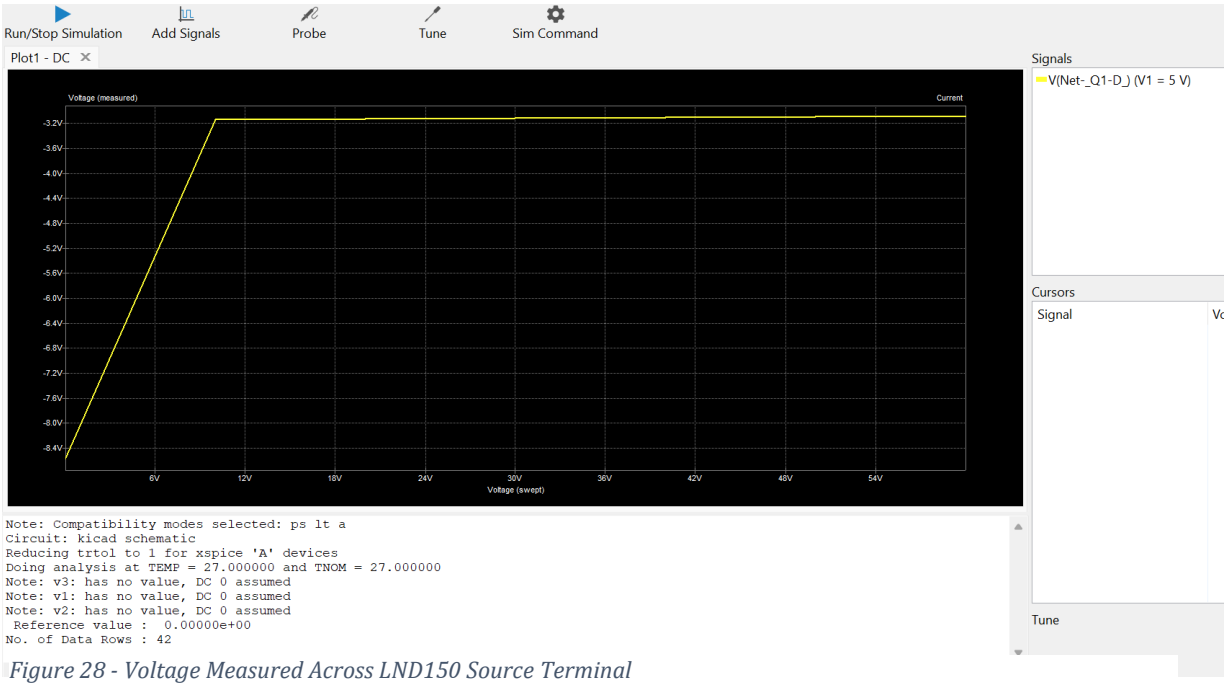

Figure 28 - Voltage Measured Across LND150 Source Terminal

The voltage and current output of the current source circuit can also be simulated. The trace for this is shown below, when the reference voltage is 5V. The simulation for this shows an initial decrease in current, where the trace reaches a steady state zone and flattens off, indicating that there is a constant current source being produced. This initial decrease is due to the current flowing through the sense resistor, to stabilise and set the current to the desired level of the experiment. Once this has been stabilised, the circuit successfully maintains a constant current, regardless of the variations in the load voltage.

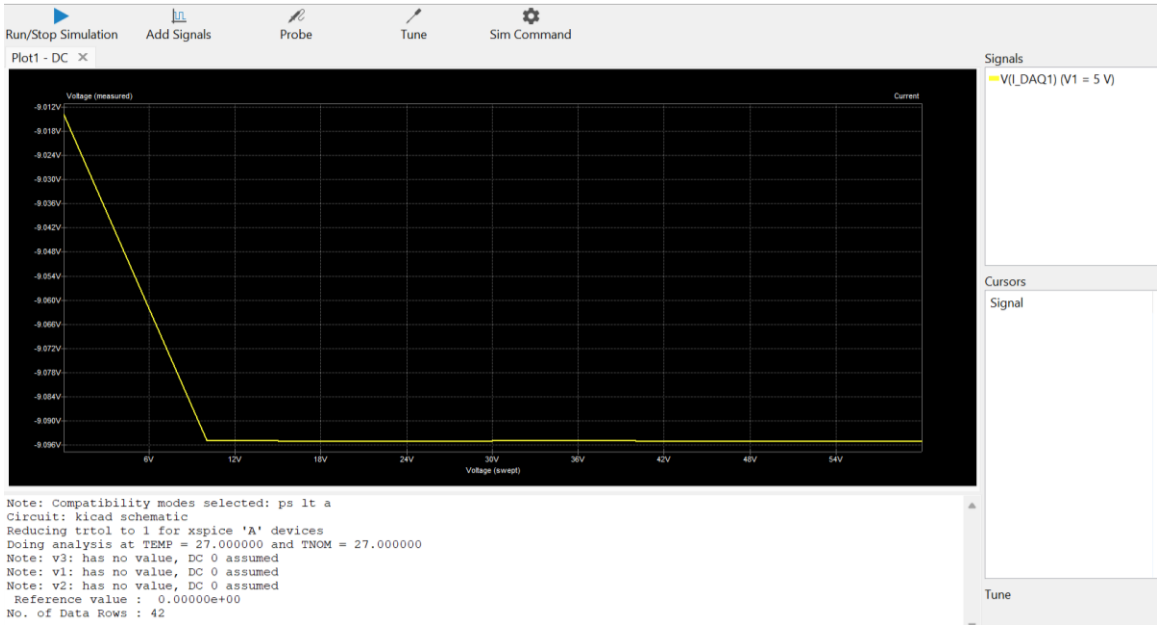

Figure 29 – Output Voltage of Current Source Circuit

3.2.2 Voltage Measurement

The voltage measurement circuit required for the QBD testing apparatus is a vital part of this experiment for monitoring not only voltage variations but also determining the precise point at which the gate oxide of the DUT fails. Therefore, a circuit that can provide precise and accurate measurement is required. This entails using high-quality, low-noise components to ensure that the readings are not affected by extraneous factors. Additionally, the circuit should have a high input impedance to prevent load and effects. and must be capable of handling high-frequency transients that may occur during the breakdown event.

Circuit Schematic

The voltage measurement circuit for the QBD configuration consists of two key components – one part of the TL082 dual JFET input op amp and a TL071 single JFET input op amp, as well as a 390kΩ resistor, 10kΩ resistor and two 0.1µF capacitors. The schematic for this circuit is illustrated below, created using KiCAD.

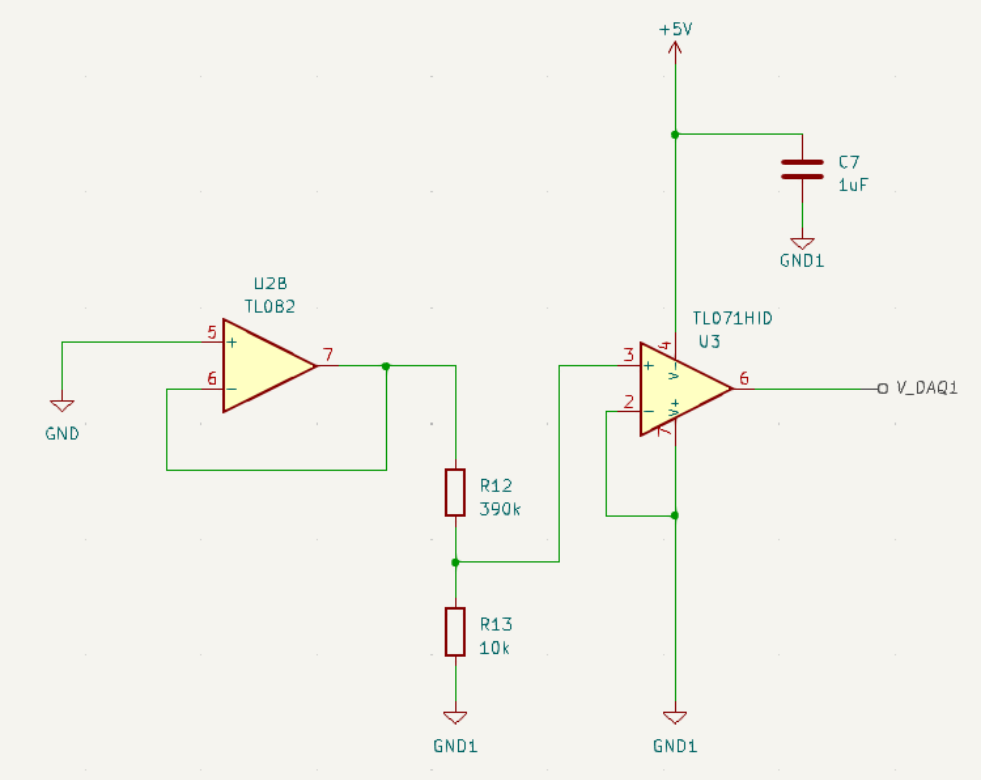

Figure 30 - Voltage Measurement Circuit Schematic in KiCAD, developed by Stephen Batcup

As the resistor are placed in series at the output of TL082 and are connected to the inverting input of TL071, the TL082 acts as an initial signal conditioner, where the connection is made to the inverting input of the TL071 through the junction of the two resistors, to achieve a voltage divider to act as a voltage measurement circuit. The resistors for this circuit were selected to be 390kΩ and 10kΩ, as the resistors form a voltage divider that scales down the output voltage of the TL082 before it is fed into the TL071.

For this circuit, the TL071 input voltage can be defined through:

$$V_{in} = V_{out} \times \frac{R_{13}}{R_{12}+R_{13}} \tag{14}$$

$$V_{in} = V_{out} \times \frac{10k}{390k + 10k} = V_{out} \times 0.025$$

This calculation shows that the input voltage to the TL071 is 2.5% of the output voltage of the TL082, which enables a voltage divider network.

Circuit Components

TL071 Single JFET Input Op Amp – This component has been selected for this circuit due to its low input bias current, enhancing its high impedance applications. With its similarities to the TL082 op amp, the TL071 op amp also has a wide bandwidth and low power consumption, making it suitable for a variety of high-frequency applications and stable operating systems, which are necessary for the nature of this precision circuit [78]. This op amp acts as a filter, due to its low noise qualities, reducing the impurities of the output signal to produce a clear measurement result of the voltage.

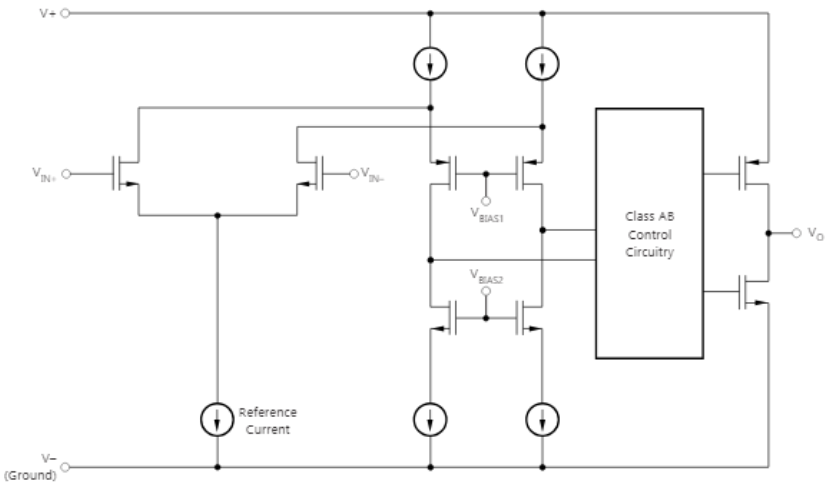

Figure 31 - TL071 Single JFET Input Op Amp Schematic [103]

Operation Principle

The voltage measurement area depicted in Figure 30 first operates through the TL082 op amp. As the TL082 receives the input voltage signal, it acts as a voltage buffer, where a high input impedance is created in the circuit, which isolates the measurement points required from the rest of the circuit, by minimising the loading effect on the voltage sources. This buffered voltage is then output, and passed through the two resistors, which form a voltage divider, where the voltage at the junction of the two resistors is a fraction of the output voltage from the TL082. This voltage then drives the inverting input of the TL071 op amp, which is configured to filter the signal, in order to produce an accurate voltage measurement. The resistor network is crucial, as it ensures that the voltage fed into the TL071 is scaled down from the TL082 output, to make it suitable for processing. It also has a feedback loop to stabilise operation of the TL071, to further ensure precise voltage measurement.

Voltage Measurement Simulation

To ensure the voltage measurement circuit is operating correctly, it is simulated in KiCAD ensuring that it is measuring the voltage flowing through the DUT correctly. The simulation circuit is shown in Figure 32, in which it is constructed around the dual TL082 op amp and the TL071 op amp. By connecting a 5V voltage to the non-inverting input of the TL082, the initial voltage can be set to zero with an increment of 1V, the simulation can begin.

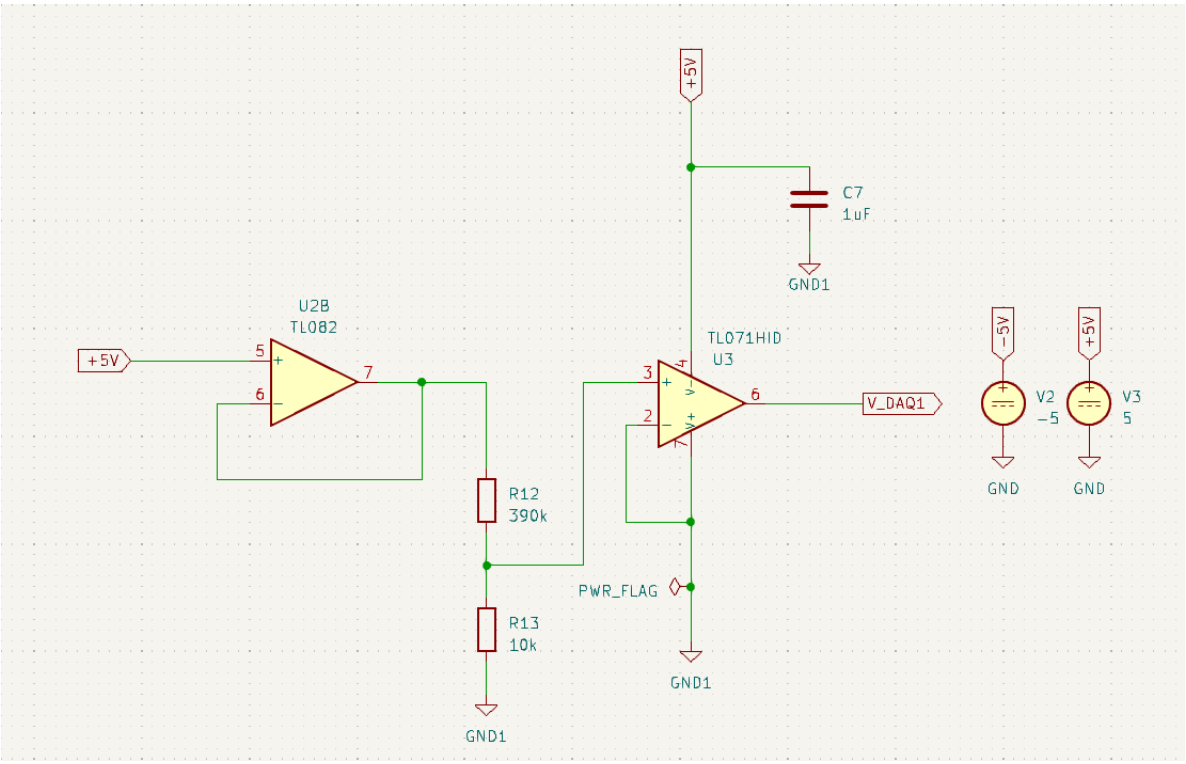

Figure 32 - Circuit Schematic for Voltage Measurement Simulation Circuit

By collecting the oscilloscope trace of the output of the second component of the TL082 op amp, it can be seen that as the voltage passes through the TL082, it results in a linear output that peaks around 2.7V. This increasing trace observed on Figure 33 confirms that the output voltage is being scaled appropriately. This also means that a consistent voltage is being applied to the rest of the circuit, as this op amp is typically used for precise measurement applications, verifying that the input signal is being correctly processed.

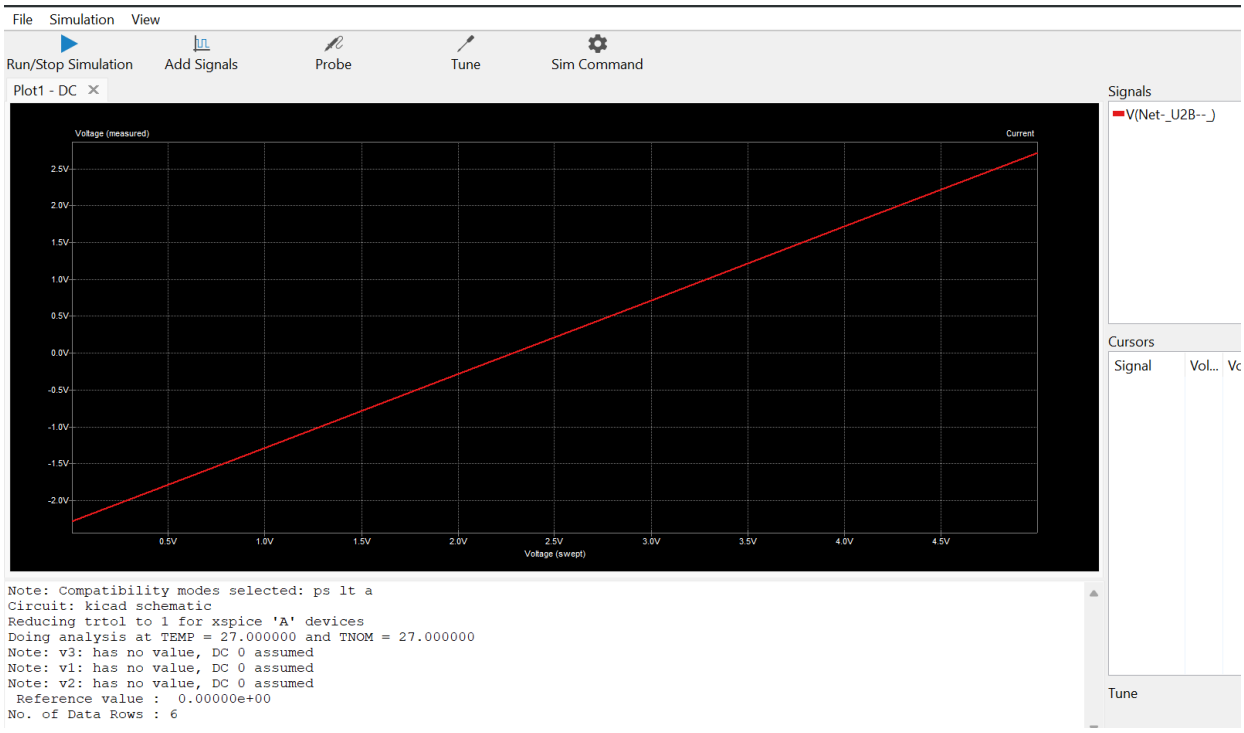

Figure 33 - TL082 Output Trace of Voltage Measurement Circuit

From this, the signal passes through the resistor junction, in order to make a voltage divider to pass into the non-inverting input of the TL071, in which the simulation results for this are shown in Figure 37. This trace depicts the voltage to overall be decreasing, but with fluctuations where the line goes up and down. This can be explained with the behaviour of the voltage divider network implemented in this part of the circuit, which reduces the voltage at the input of the TL071, compared to the original signal. The signal is also decreasing, due to the resistors in the network, which scale down the input voltage, so it is suitable for the TL071 to process, however the fluctuations illustrate that there is instability within the signal due to the noise produced, which would not provide an accurate output signal to measure the voltage.

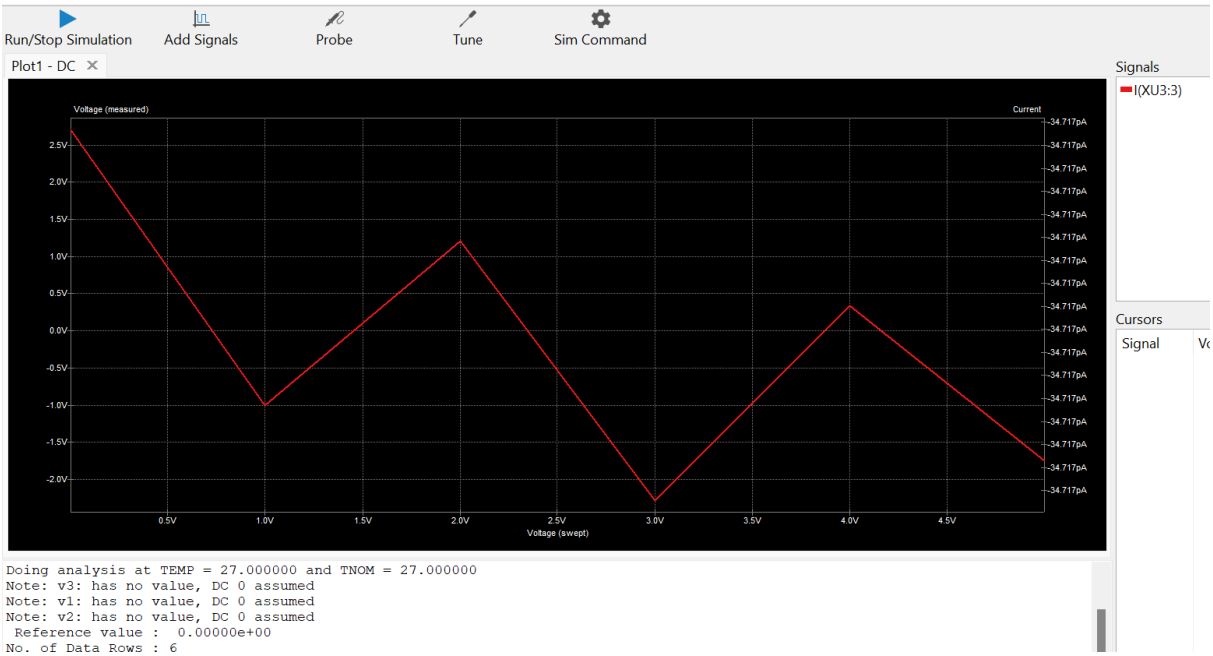

Figure 34 - TL071 Input of Voltage Measurement Circuit

After the signal has passed through the TL071 op amp, the signal continues to decrease. The oscilloscope trace for this is shown below. Since the input to the TL071 was already decreasing, it is expected that the output would follow the same trend. However, the linear nature of the output trace suggests that the op-amp is effectively buffering the input signal while also filtering noise and fluctuations introduced by the voltage divider. This indicates that the TL071 is operating in a stable linear region, producing a consistent and proportional output. The clear decline in output voltage over time suggests that the TL071 is effectively processing the signal. This outcome confirms that the circuit is well-designed and does not exhibit non-Ohmic behaviour.

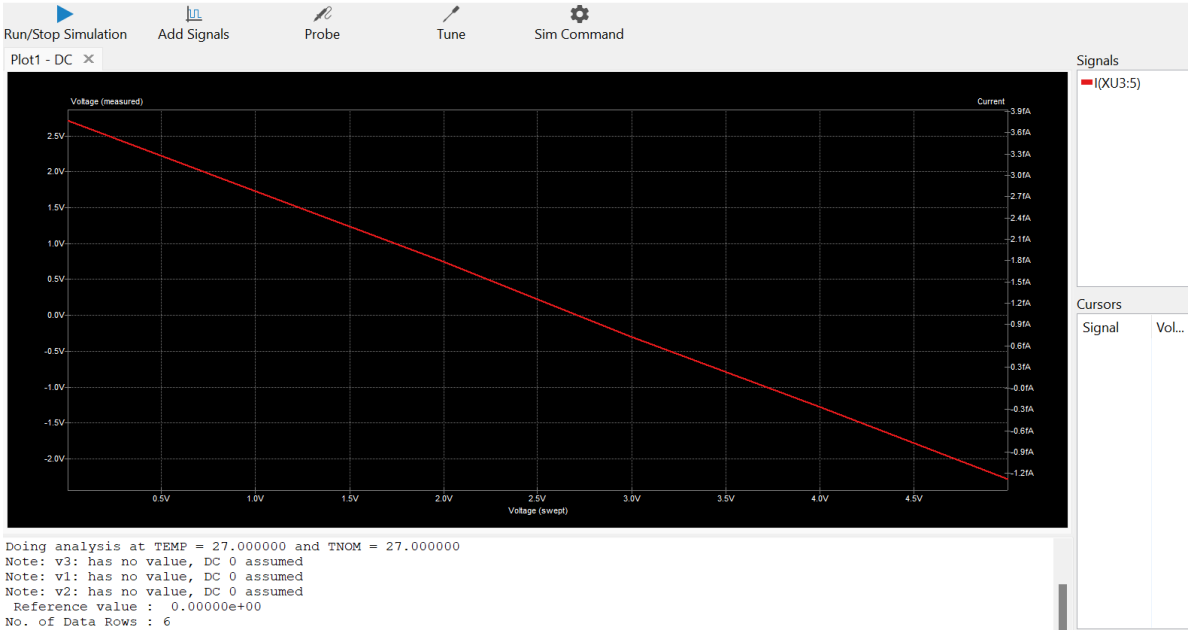

Figure 35 - Output of Voltage Measurement Circuit

3.2.3 Current Measurement Circuit

High precision and stability techniques are required for this circuit, to accurately measure the current flowing through the DUT at gate oxide breakdown. This involves using components with tight tolerance and low noise characteristics to ensure minimal measurement error and interference. Additionally, the circuit must incorporate grounding practices to prevent external electromagnetic interference from affecting the measurements. The stability of the power supply and the precision of the current sensing elements are critical to obtaining reliable and repeatable results during the breakdown testing.

Circuit Schematic

For the QBD experiment, the current measurement circuit incorporates three essential components: the TLV274CN quad rail-to-rail input op-amp, a BZT03C Zener diode, and a Bourns 3269W-1-105LF trimmer resistor. Additionally, the circuit configuration includes nine precision resistors ranging from 100Ω to 100kΩ, and two 0.1µF capacitors. This carefully selected combination of components ensures high precision, stability, and reliability in the current measurement process.

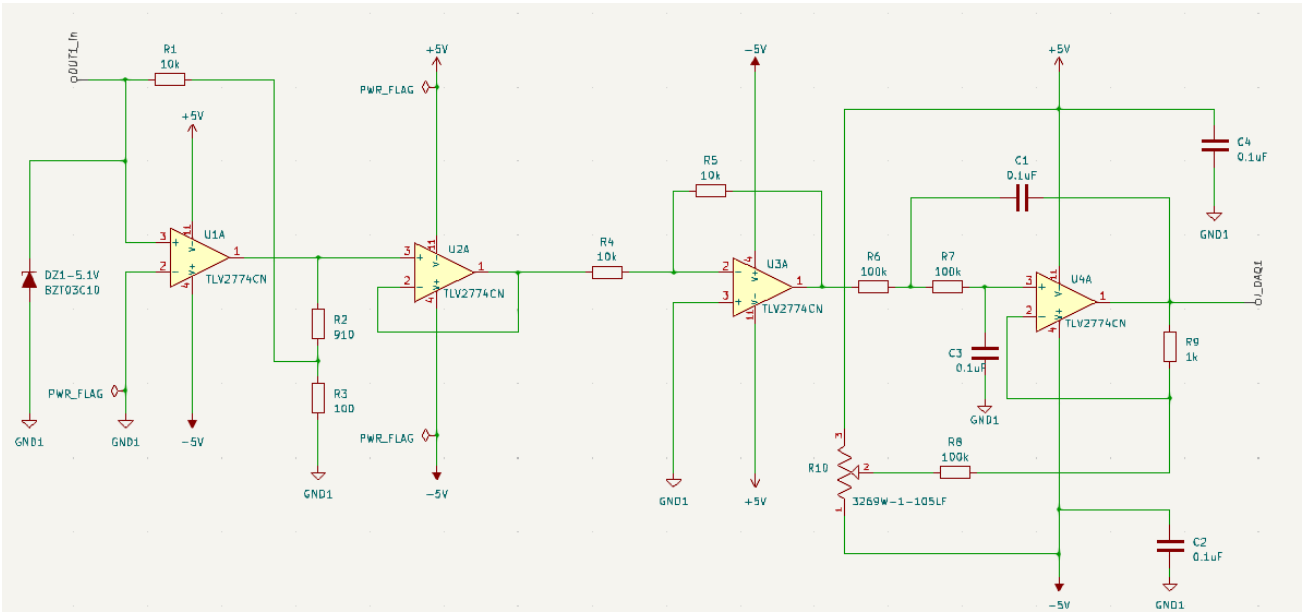

Figure 36 - Current Measurement Circuit on KiCAD, developed by Stephen Batcup

Circuit Components

TLV2774CN Quad Input Rail-to-Rail Op Amp – The TLV2774CN was selected for this circuit as it is a versatile, low power, rail to rail op amp, particularly useful in precision applications, due to its ability to swing the output close to the supply rails, making it very useful in maximising the dynamic range in low voltage applications. The low power qualities in this device also make it suitable for high impedance precision applications, because of its low input bias current and offset voltage, as well as minimal loading on the signal source, helping to maintain the accuracy in the current measurement. The TLV2774CN is also unity gain stable, so it can operate as a voltage buffer without requiring additional components, making it ideal for this application [79].

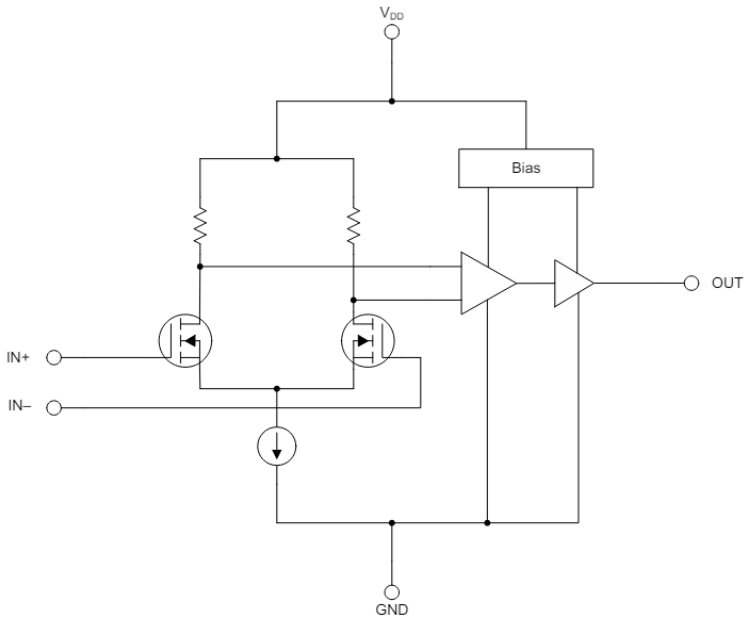

Figure 37 - Block Diagram of TLV2774CN Quad Input Rail-to-Rail Op Amp [104]

BZT03C Zener Single Diode – The BZT03C series Zener diode is a common component found in voltage regulation applications, due to their high-power dissipation capabilities and low dynamic impedance for maintaining stable voltages in electronic circuits, as well as ensuring minimal variation in output signals [80].

Bourns 3269W-1-105LF Trimmer Resistor – Considering the fine adjustment requirements of this circuit, this specific trimmer resistor is selected due to its high-precision qualities and wide resistance range that provide high reliability for fine tuning [81]. The 3269W-1-105LF allows for fine and precise adjustment of resistance, making it compatible with this circuit configuration, due to the number of resistors implemented.

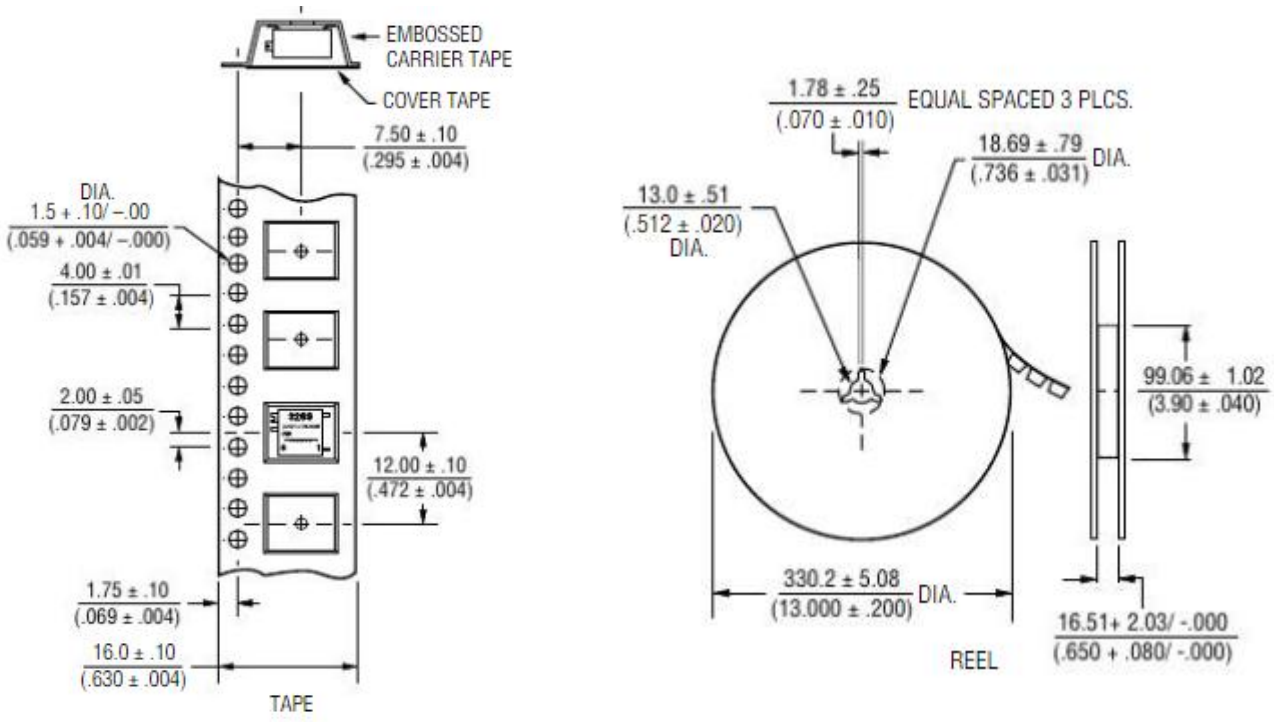

Figure 38 - Illustration and Dimensions of Bourns 3269W-1-105LF [106]

Operation Principle

The current measurement circuit can be divided into several different stages: current sensing, signal conditioning, filtering and output adjustment. With the first stage of the circuit acting as a current sensor, the current is measured however the output is found to be negative, therefore it must be converted into a voltage signal, by using resistor R1, in which the voltage drop across this resistor follows Ohm's Law. The TLV247CN op amp is used to amplify the voltage across the current sense resistor. By feeding R1 into the non-inverting input of unit B of the op amp, the component is configured with feedback to set the gain of the circuit. From this, this signal can be sent through an inverter, made from unit C of the TLV2774CN, to form the positive output. By doing this, noise interference and electromagnetism is created which negatively impacts the output signal, creating inaccuracies. In order to control this, a Sallen key filter is implemented using unit D of the quad input op amp, to filter out the impurities and produce the DC current

output measurement. The Sallen Key low pass filter is a type of active filter that uses the op amp in conjunction with resistors and capacitors to achieve the desired frequency response.

Using R1 and R2 from Figure 39 as an example, these resistors determine the cutoff frequency and the quality factor of the filter, whereas C1 and C2 work with the resistors to filter out high frequency signals, allowing only low frequency signals to pass. The op amp is configured in a non-inverting form to buffer the filter and provide gain. The combination of R1, R2, C1 and C2 form a frequency dependent voltage divider, where at low frequencies, such as the current measurement circuit, the capacitors have a high impedance which means most of the signal passes through the output, besides the noise and impurities.

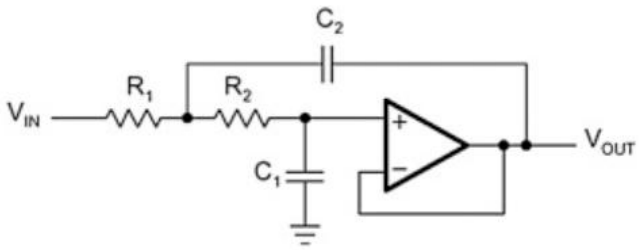

Figure 39 - Sallen Key Inverter [107]

To find the corresponding resistor values to ensure the value for output current measured is accurate, the equation is derived below. With the transfer function of the circuit of the Sallen key inverter given as:

$$A_s = \frac{A_0}{1+\omega_C[C_1(R_1+R_2)+(1-A_0)R_1C_2]s+\omega_C^2R_1R_2C_1C_2s^2} \quad (15)$$

The design of the circuit has a unity gain of 1, so the transfer function is simplified to:

$$A_s = \frac{1}{1+\omega_C C_1(R_1+R_2)s+\omega_C^2R_1R_2C_1C_2s^2} \quad (16)$$

The coefficient comparison between the two equations yields:

$$A_0 = 1 \quad (17)$$

$$a_1 = \omega_C C_1(R_1 + R_2) \quad (18)$$

$$b_1 = \omega_C^2 R_1R_2C_1C_2 \quad (19)$$

Given C1 and C2 are 0.1µF each, the resistor values R1 and R2 can be calculated through:

$$R_{1,2} = \frac{a_1C_2 \pm \sqrt{a_1^2C_2^2-4b_1C_1C_2}}{4\pi f_C C_1C_2} \quad (20)$$

To obtain the real values under the square root, C2 must satisfy the following conditions [82]:

$$C_2 \geq C_1\frac{4b_1}{a_1^2} \quad (21)$$

Throughout the circuit, the Zener diode is used to control the voltage through the op amps, to maintain consistent performance and prevent the voltage from overloading the op amps. To ensure stable operation, the bourns 3269W-1-105LF trimmer resistor is implemented to control and maintain the gain accurately through the feedback loop of the op amps.

Current Measurement Simulation

To ensure the circuit is going to provide accurate and stable constant current measurements, the designed circuit must be simulate using the built in LTSpice and PSpice simulation tools on KiCAD, to verify the circuits performance and validate the theoretical design. Comprised around the quad input TLV2774CN op amp, the primary objective is that all components are configured to achieve a stable DC current output and correct measurement capabilities. The simulated circuit schematic for this is shown below.

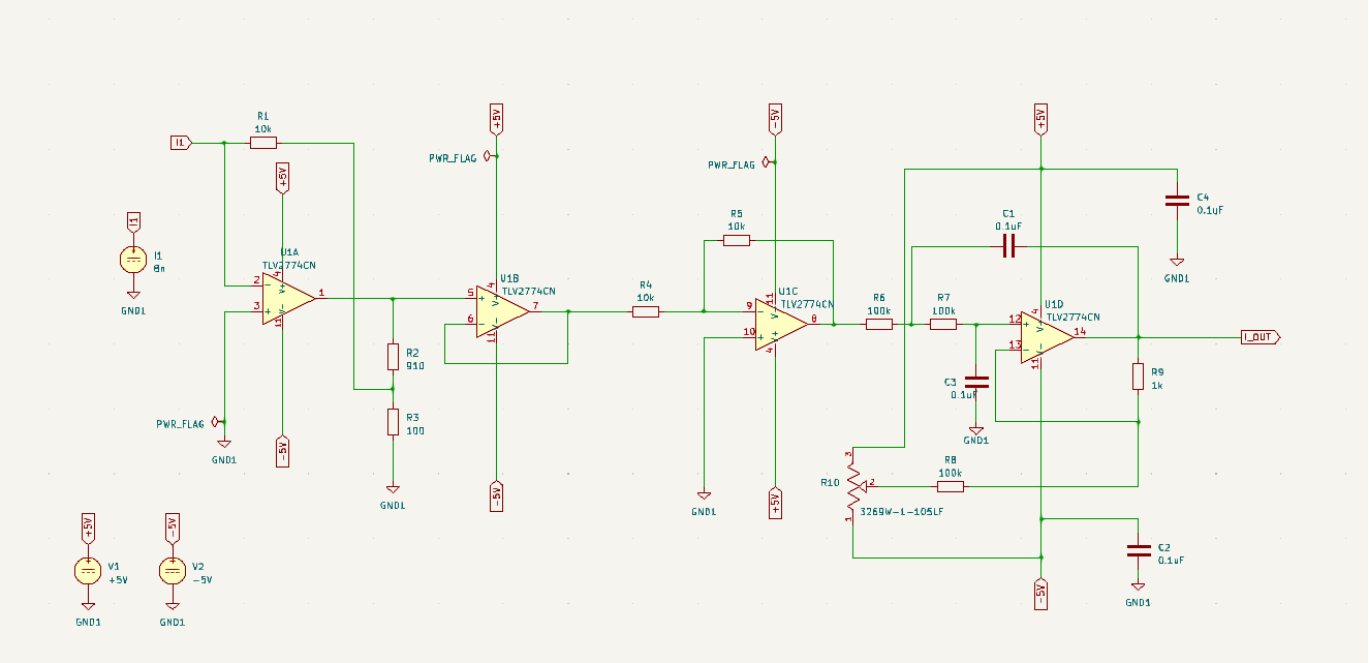

By applying an 8nA current to the input of the circuit, as well as connecting the -5V and +5V voltages throughout the circuit, the simulation can begin using DC analysis. Setting the starting value of the current input to zero and incrementing in steps of 100pA until 8nA is achieved, the voltage inputs, voltage across the output current, voltage across the inverter output at U1C, as well as the voltage across output of U1B can all be added to the simulation graph. The results for this are shown below. From the graph, it can be observed that all inputs and outputs produced are constant and in horizontal formations. For the voltage inputs V(+5V) and V(-5V), this simulation output indicates that the current is independent of the voltage over that range, and that the inputs going through the op amps are constant. For the outputs of U1B and U1C, the simulation result presents the outputs to be exhibiting current limiting behaviour, where the circuit is preventing the current from exceeding a certain current level, despite an increase in voltages. This is a protective feature from the Bourn's potentiometer, to protect the op amps from excessive current damaging the circuit. This feature means that a constant current is always maintained.

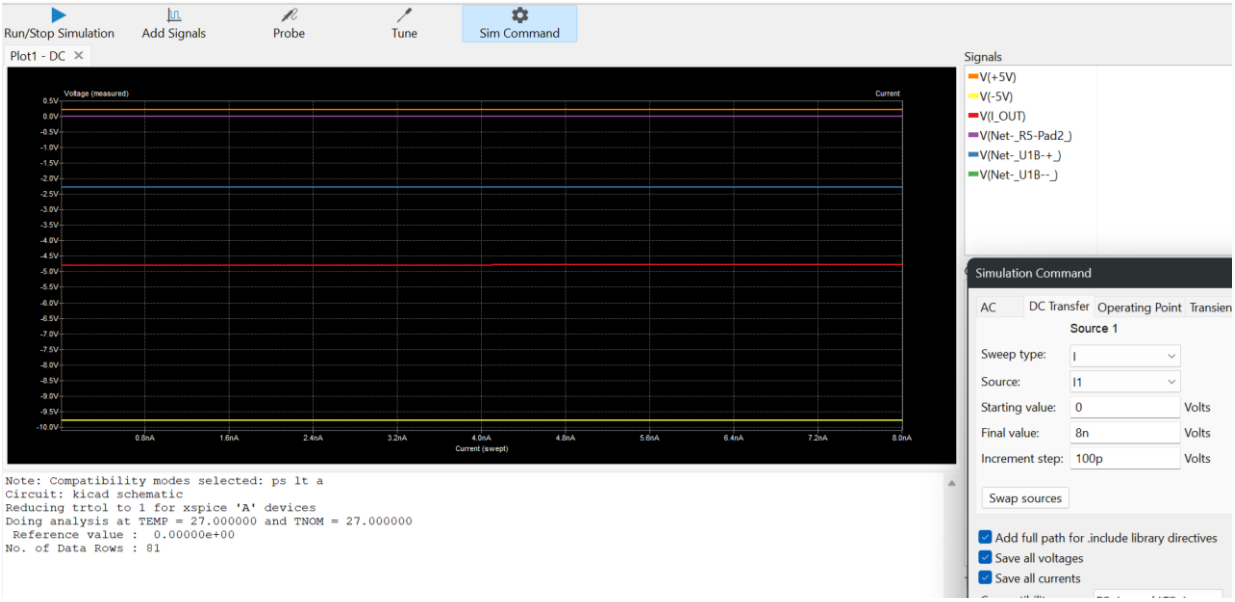

Figure 40 - Simulation Results of Voltage Inputs, U1B Output, U1C Output and Circuit Output

For V(I_{OUT}), it can be confirmed from the result that the circuit is behaving as a constant current source. This is because the current remains constant regardless of changes in voltage, in which this is achieved by the precision op amps and the potentiometer in the circuit. This result confirms that a constant and steady current is measured across the circuit, which validates the theoretical predictions and the operation principle of the current measurement circuit.

By using the same simulation parameters, the input current and the output current can be plotted on the simulation together. The input current 8nA formed by the simulation presents a linear relationship, exhibiting Ohm's Law. Since the slope of the line represents the resistance of the circuit, it is resented that the resistance is lower resistance, as the line is not steep. Comparing this with the output current, it can be observed that the current measured is also following Ohm's Law and reaches 8nA, with the same resistance as the input current. The two results are almost identical, however the output current measured has slight noise and impurities, which can be seen with the lack of linearity in the line. This means that the current going into the circuit is almost identical to the current measured, validating the purpose of the circuit.

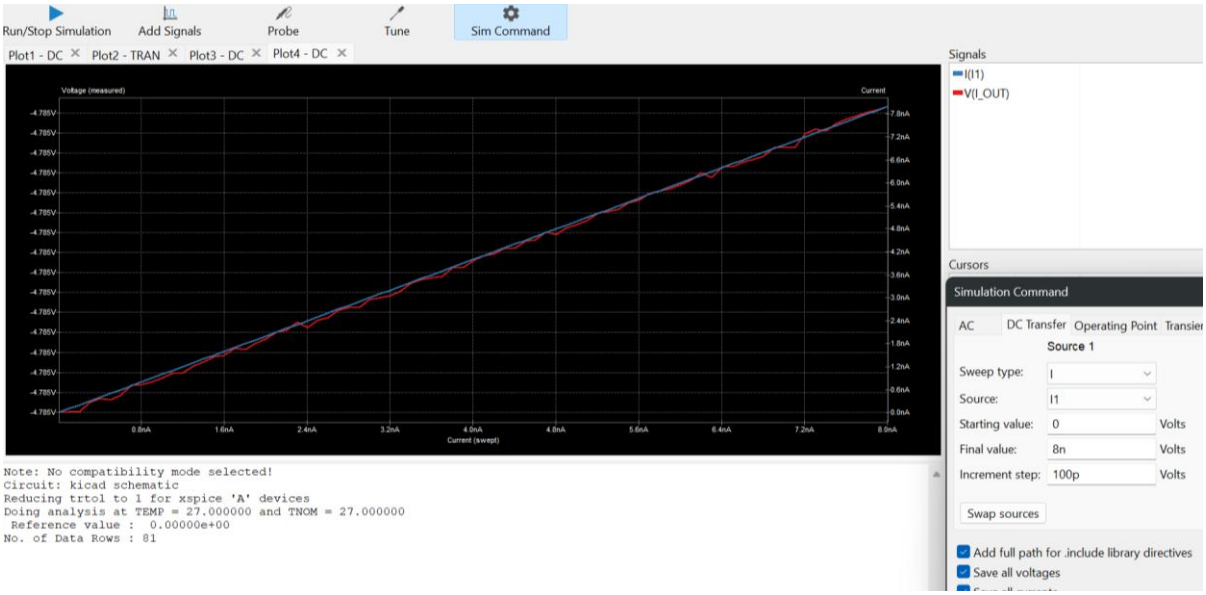

Figure 42 - Simulation Results of I1 and V(I_OUT)

By changing the increment step of the simulation to 50pA, the difference between the voltage across the input current V(I1) and the voltage across the measured output current V(I_{OUT}) can be compared with I(I1) and V(I1).

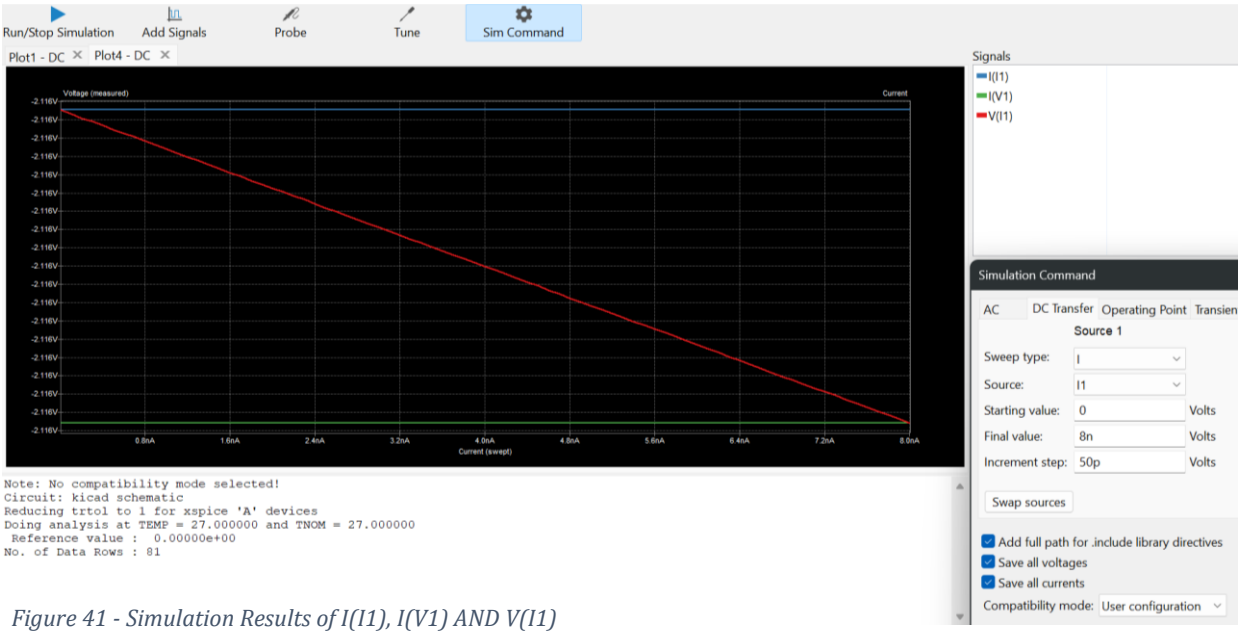

Figure 41 - Simulation Results of I(I1), I(V1) AND V(I1)

From the simulation results, it can be observed that the input current is a constant source, indicating that even though there are changes in the supply voltage, the input remains steady, which aids in the accurate current measurement of this circuit. This indicates that the Zener diode in this circuit is stabilising the voltage in combination with the current source, ensuring that both the current and voltage are maintained at the desired levels, providing reliable operation. This stability is necessary for the operation principle of this circuit, and it can be validated that it is operating correctly by the simulation results.

The simulation also depicts that the voltage across the input current is decreasing, following Ohm's Law. This is due to the change in impedance from the Zener diode to account for the changes in operating regions and maintain the constant current that is being measured by the circuit. This can also be due to a decrease in load resistance, which results in a voltage drop, which correlates with Ohm's Law in order to maintain the same constant current. By keeping the same circuit parameters but adjusting the simulation to provide the results for the voltage across the output current of the circuit, the program can be run again to produce the oscilloscope traces. The results are shown below, with I(I1) and I(V1) remaining the same.

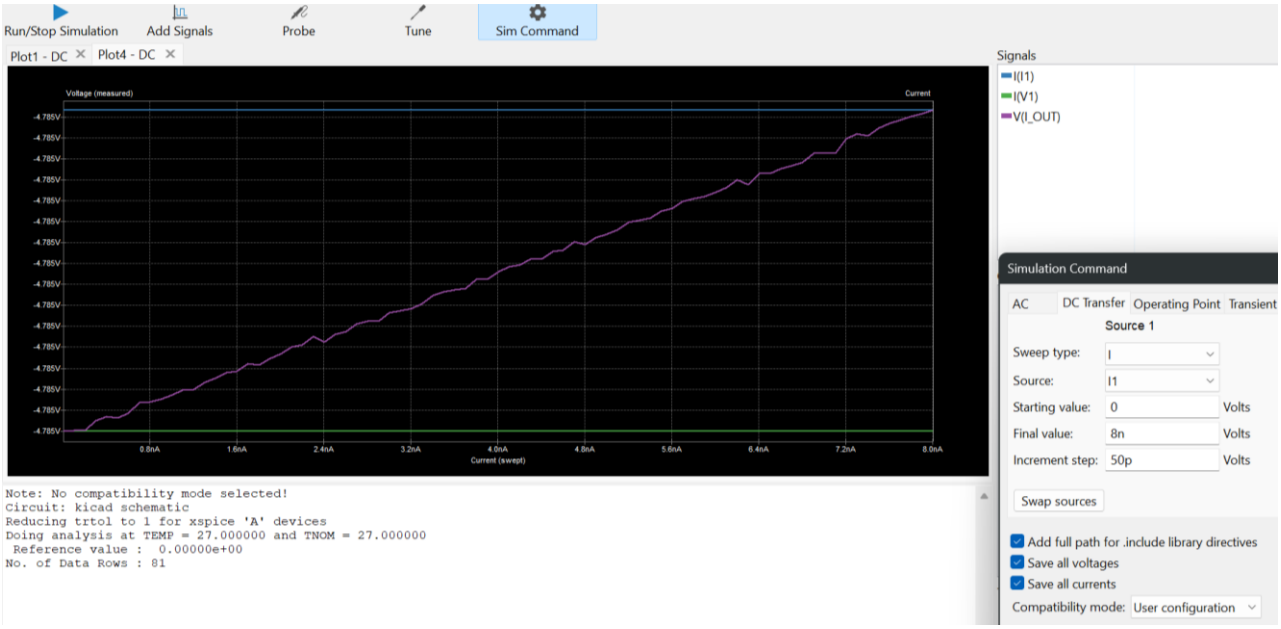

Figure 43 - Simulation Results of I(I1), I(V1) and V(I_OUT)

The voltage across the measured output current can be seen to be increasing from the simulation results, which indicates that the resistance across the circuit must also be increasing. This is supported by the circuit schematic. Additionally, the voltage across the input current can be seen to be the opposite, demonstrating the proper operation of the circuit's inversion application. The Sallen Key filter is also functioning, as evidenced by the minimal noise and impurities formed, therefore validating that the current measurement circuit is operating correctly and producing an accurate measurement.

3.2.4 Power Supply

To supply stable voltages and steady currents to the current source, voltage measurement and current measurement circuits, it is essential that a high-quality power supply is designed, to ensure that the QBD experiment delivers accurate results, in a safe manner.

Circuit Schematic

The power supply designed for the QBD apparatus consisted of a 1A0505S DC-DC converter, a Bourns RLB0914-6RBML power inductor, as well as two 1nF capacitors. The circuit for the power supply also has connectors for the voltage and current inputs for the current source, voltage measurement and current measurement circuits, so all the power inputs and outputs are controlled in one place on the PCB.

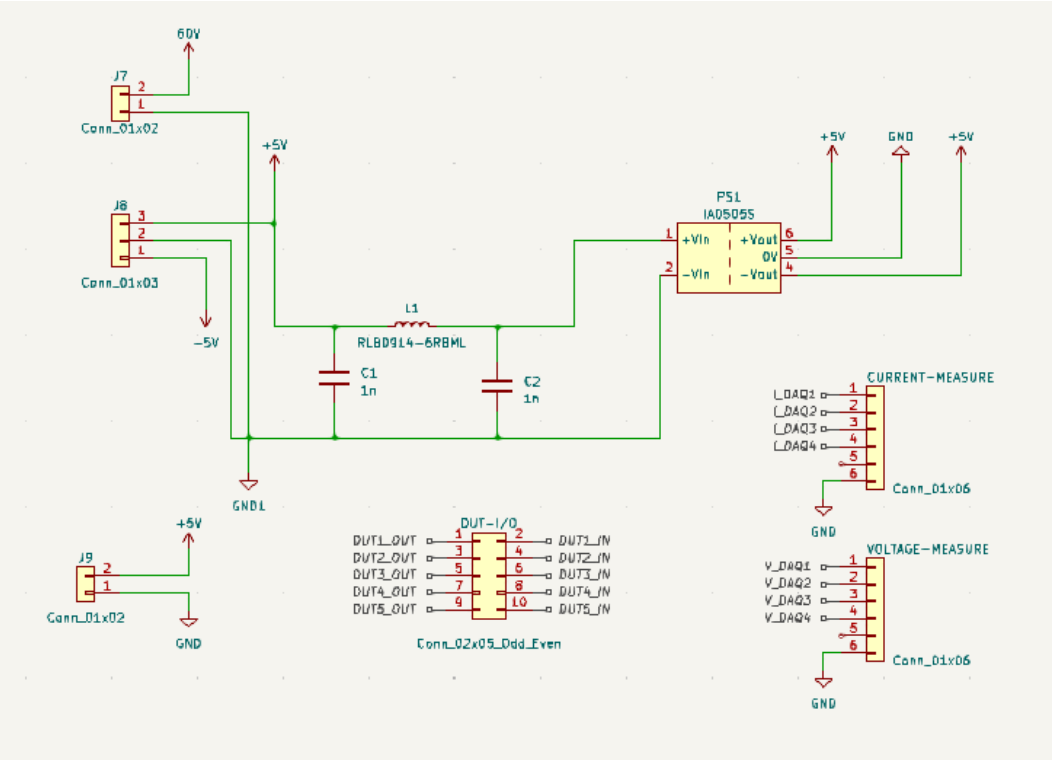

Figure 44 - Circuit Schematic of Power Supply on KiCAD, developed by Stephen Batcup

Component Selection

Bourns RLB0914-6R8ML Power Inductor - The Bourn's RLB0914-6R8ML power inductor is a versatile component used in various high-current and high-frequency applications. Its key specifications, including a 6.8µH inductance, appropriate current ratings, and low DC resistance, make it suitable for use in power supply circuits. The choice of 6.8 µH inductance is based on design requirements, including the switching frequency, ripple current, and desired transient response of the converter The low DC resistance of this device makes it suitable for this application, as it results in fewer power losses, ensuring the power going through each circuit is stable [83]. This power inductor is crucial for this DC-DC converter circuit, as it maintains the output current and ensures a steady voltage.

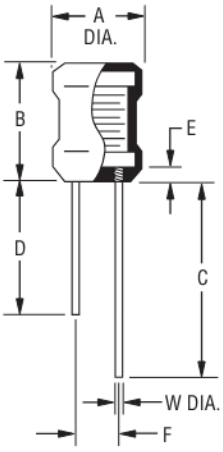

Figure 45 - RLB0914-6R8ML Bourns Power Inductor [83]

XP Power IA0505S DC-DC Converter - With substantial isolation and high efficiency, the XP Power IA0505S DC-DC Converter is a flexible and dependable component that can produce steady 5V power from a 5V DC input. This ensures consistent voltage levels, despite variations in the input voltage, making it ideal for the power supply circuit, that is handling power to three separate circuits. This component also offers 1500V DC isolation between the input and the output, which helps protect sensitive electronics from potential ground loops and electrical noise [84].

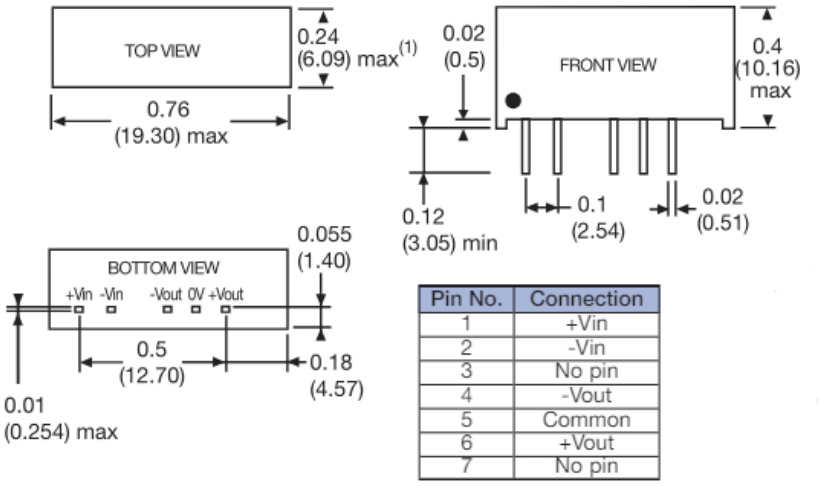

Pin No.	Connection
1	+Vin
2	-Vin
3	No pin
4	-Vout
5	Common
6	+Vout
7	No pin

Figure 46 - XP Power IA0505S DC-DC Converter [84]

With a power output of 1W and high efficiency, the IA0505S is also designed to provide sufficient power for low-power applications while minimising energy loss. The high efficiency means that less energy is wasted as heat, which is beneficial for maintaining the reliability and longevity of the converter and the overall system.

Operating Principle

The input voltage, of 5V, is first applied to the positive voltage input of the IA0505S DC-DC converter, with the negative input of the converter connected to ground. Across these inputs, the 1nF capacitors are connected, to not only filter out the high frequency noise, but also stabilise the input voltage, to ensure any transient noise from the power source does not affect the performance of the IA0505S.

The RLB0914-6R08ML power inductor is placed in series with the input voltage of the IA0505S, in which its primary function is to smooth out variations in current which can be formed from the switching actions inside the converter. By storing energy when current flows through the device and releasing energy when the current decreases, the inductor regulates the input current, so the output current has a reduced noise, ensuring a consistent power supply. This device is placed between the two capacitors, to form an LC filter that effectively reduces both voltage and current ripple, providing a clean DC input to the converter, so an accurate output can be produced. With the core function of this device being to step or step down the input voltage to provide a stable 5V DC output, high switching frequency occurs inside the IA0505S, to convert the input DC voltage to an AC signal and then back to a stable DC voltage. This process allows for precise voltage regulation, which is essential for the operation of the power supply.

3.3 PCB Construction

An essential part of electronic circuits, the printed circuit board (PCB) provides the components' electrical connections and structural support. The design, fabrication, and assembly of the power supply, current source, voltage measurement and current measurement PCBs can be designed, to assemble one overall QBD rig, used in the gate oxide breakdown experiment.

3.3.1 Current Source

The first step into constructing the PCB layout of the current source circuit is by using the wiring schematic. By using KiCAD, the circuit diagram is automatically translated onto the virtual PCB, where the positioning of components and routing of electrical connections can be formed. First, a two-layer PCB was selected for this layout, in which the top layer is the primary layer and is used for the majority of electrical routing, while the bottom layer serves as a ground plane, crucial for providing stable reference points for signals and to minimise noise throughout the circuit. The components in the PCB were placed strategically, spaced out enough to minimise signal path lengths and reduce electromagnetic interference, to ensure the circuit is operating correctly and reliably. The TL082 op amp is placed centrally, to minimise the distance to the resistors and capacitors, enhancing signal integrity, which makes the PCB more efficient. This layout means the LND150 can be placed at a suitable distance from the op amp, to maintain an organised appearance.

From this, the voltage connections can sit near the edge of the PCB, making it easier for those connections to be made. Wider traces were also employed in the PCB layout to protect the traces from damage and manage the high voltage entering the circuit. The use of wider traces also reduces resistance and improves current-carrying capacity, which is essential for performance and reliability for the high voltage going through this circuit.

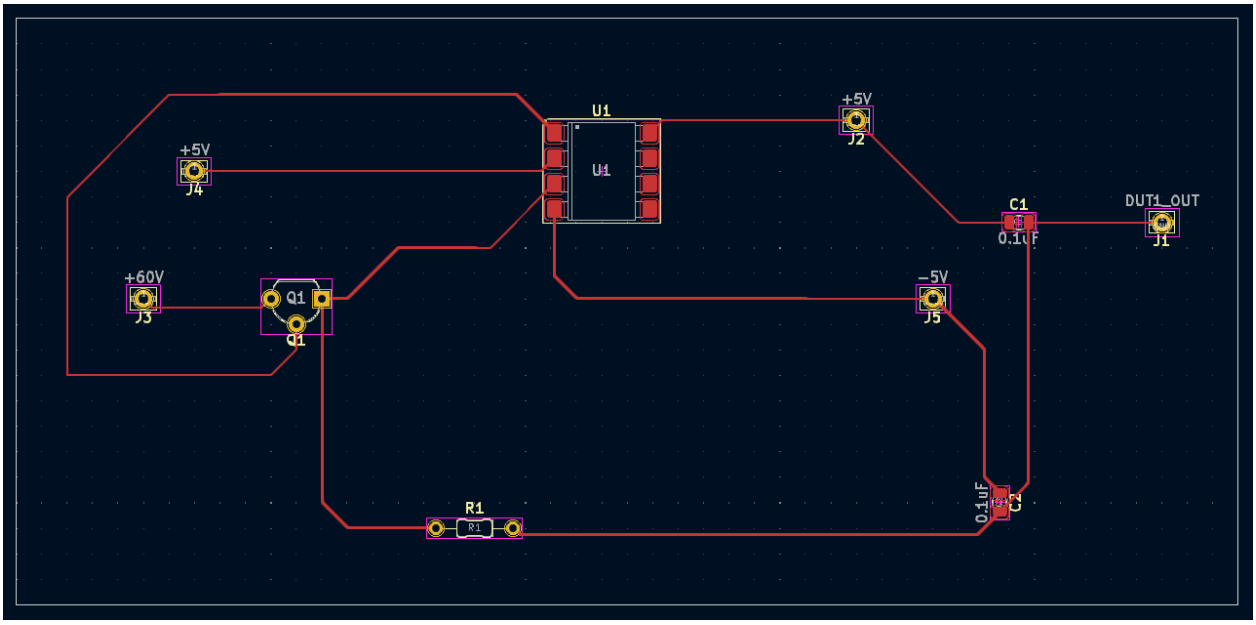

Figure 47 - PCB Layout of Current Source Circuit

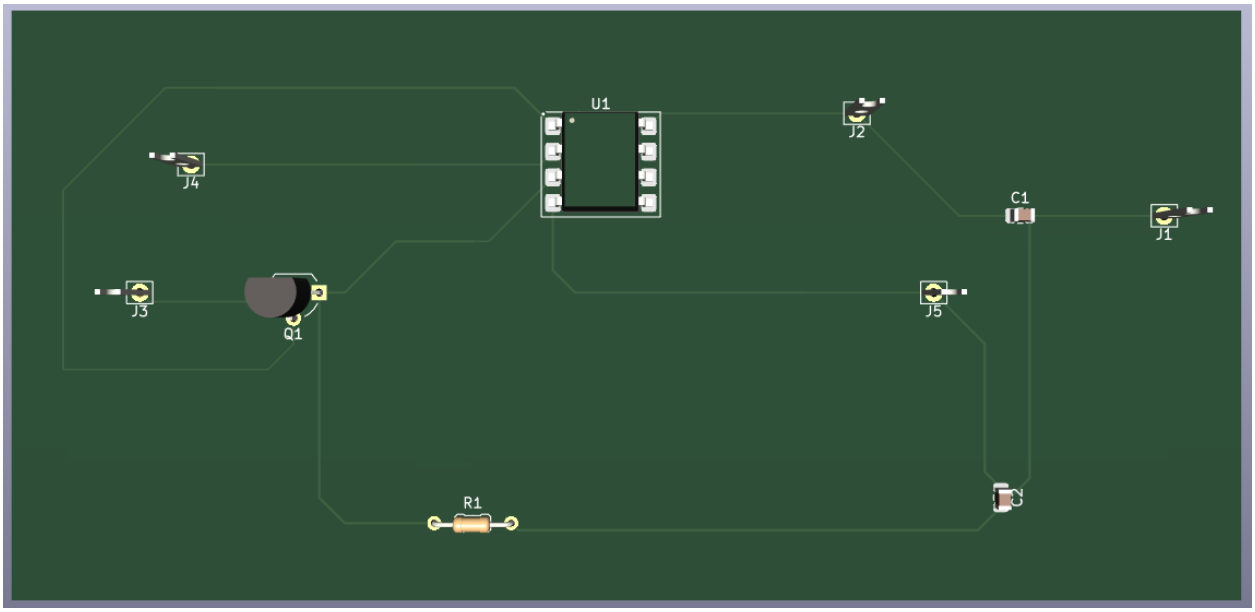

Figure 48 - 3D View of Current Source PCB

3.3.2 Voltage Measurement

Using the circuit schematic of the voltage measurement circuit, KiCAD automatically translates the components into their respective footprints on the virtual PCB layout, so the assembly process can begin. A two-layer printed circuit board (PCB) was selected for this design. The top layer serves as the primary layer and is primarily used for electrical routing, while the bottom layer serves as a ground plane, like the current source PCB. This dual layer enhances the performance of the circuit by providing stable reference points and reducing the potential for EMI.

By centring the op amps, the design simplifies the connections between the components, allowing for more efficient routing, which minimises the lengths of traces and therefore reduces the likeliness of signal degradation. The op amps sitting in the centre of the board also increases the distance between the two resistors and capacitor, which also helps prevent EMI, allowing for the creation of larger tracks that are less susceptible to physical damage. To further maintain an organised appearance of the board, the input and output pins are arranged along the outer edges of the board, simplifying the eternal connections to other parts of the entire circuit.

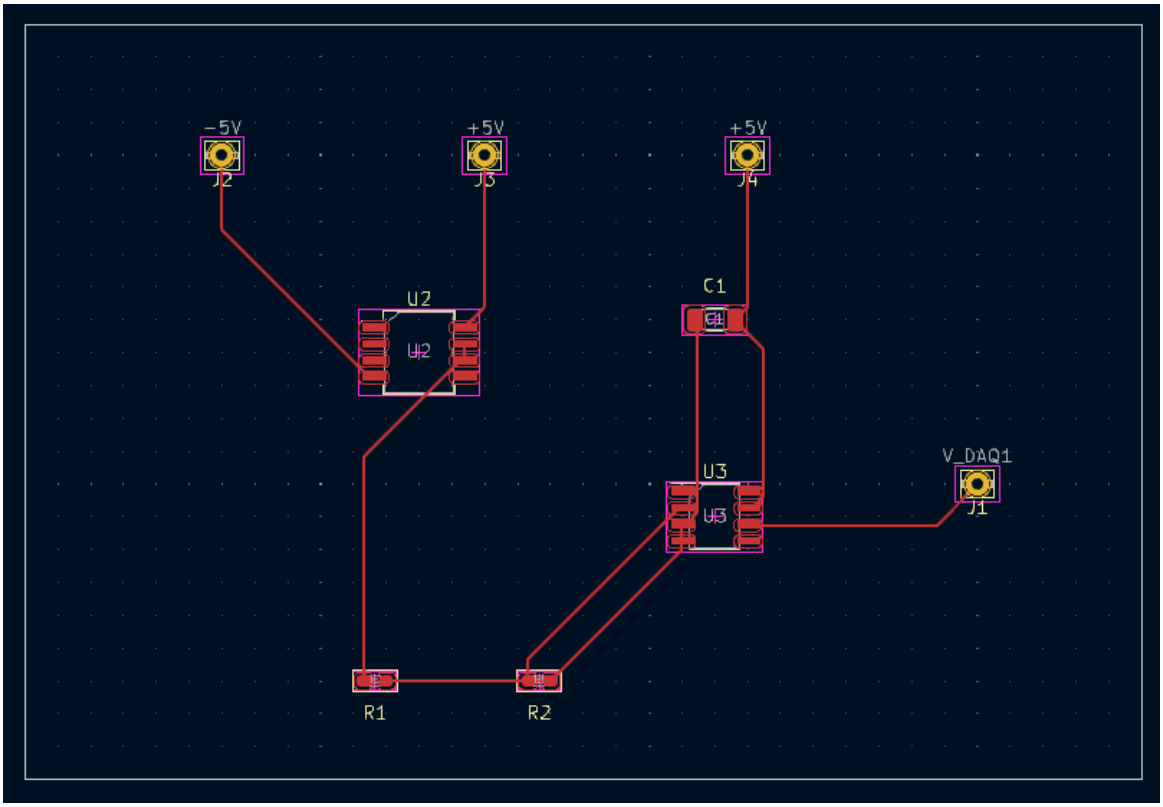

Figure 49 - PCB Layout of Voltage Measurement Circuit

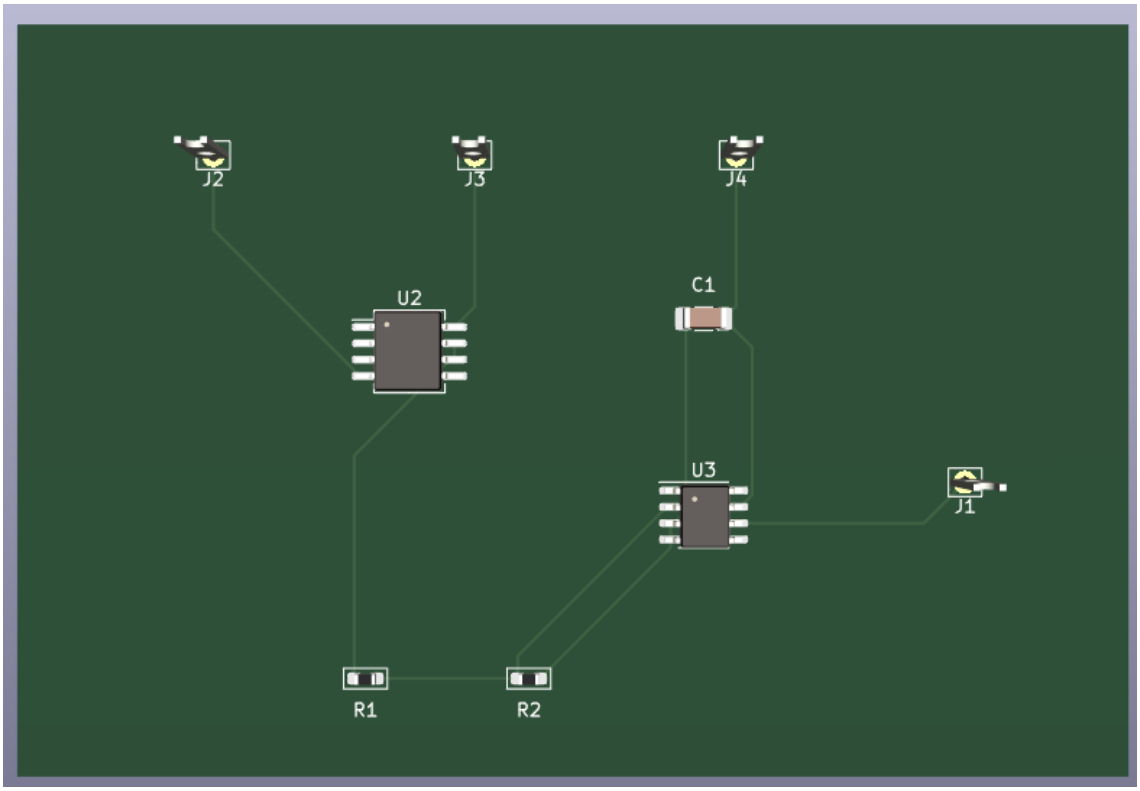

Figure 50 - 3D View of Voltage Measurement PCB

3.3.3 Current Measurement

Again, using KiCAD, the circuit schematic is automatically transferred onto the PCB building tool, where the components are translated into footprints to be positioned and connected on the PCB layout. A two-layered PCB was selected for this design. The top layer is the primary layer and is mainly utilised for electrical routing, while the bottom layer serves as a ground plane, not only providing a stable reference point for all signals but also enhances noise reduction. The bottom layer is also used for additional routing in areas where potential faults could have been caused by overlapping traces, that would result in the failure of the PCB. The PCB design uses colour coding for clarity of the layout: the red lines represent the traces on the first layer of the PCB and the blue lines represent the traces on the second layer of the board, with free standing vias in place to seamlessly connect these traces. Both traces are made from copper, for its excellent conductivity.

The TLV2774CN op amp is placed in the centre of the PCB, but due to the many connections to components on the PCB, the traces surrounding the op amp are narrower, so space around the device isn't compromised and the signal routes remain effective. Due to the inputs and outputs, the components are primarily arranged on the right side of the board. This minimises the trace lengths, so the voltage inputs can be placed on the outside of the board, prioritising organisation when the board is in operation. This PCB design also incorporates wide traces for high current paths, as well as enough space between traces and components to reduce the potential for EMI and short circuits, ensuring reliable and safe operation.

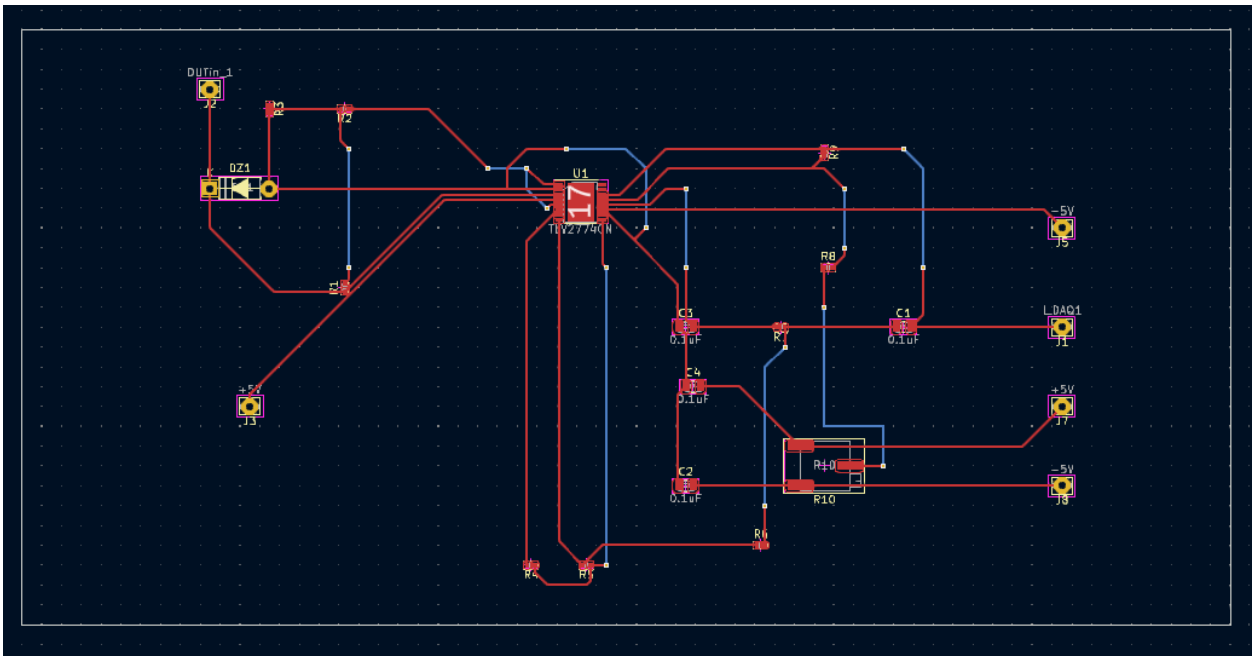

Figure 51 - PCB Layout of Current Measurement Circuit

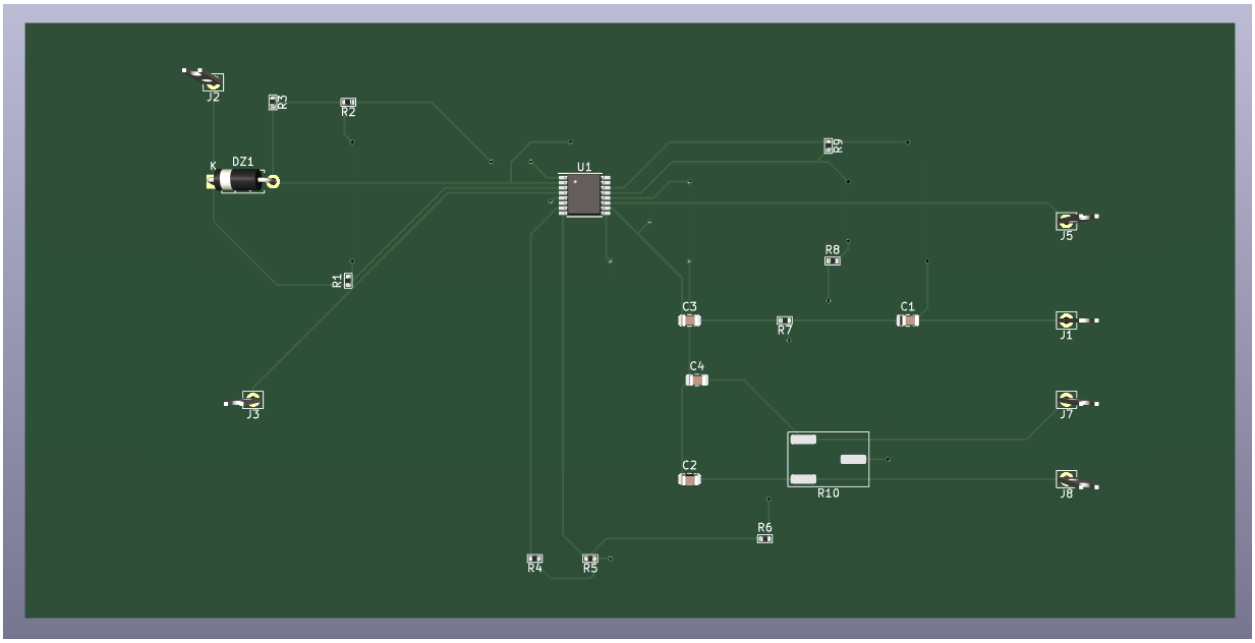

Figure 52 - 3D View of Current Measurement PCB

3.3.4 Power Supply

Using the wiring schematic for the power supply circuit constructed in KiCAD, the footprints of the circuit components can be transferred onto the PCB building tool to form the electrical routes necessary. Using a two-layer PCB, the layout of the power supply has been designed to optimise the accessibility of the terminal block connectors that are placed on the outskirts of the board, as they are responsible for supplying the necessary voltages and currents to each section of the PCB. This also maintains an organised layout, reducing the potential of signal interference from other components. At the centre of the PCB, the IA0505S DC-DC converter is placed as it is the most important component, due to its role as the core power supply unit for the entire circuit. This placement ensures that the distribution of the power is even and direct to each circuit of the PCB rig.

Surrounding the DC-DC converter is the RLB0914-6R08ML inductor is placed close to the inductors and converter, ensuring that it can effectively function without long trace lengths, which can introduce unwanted resistance and inductance. The capacitors are also situated close to the inductor and converter for the same reasoning. Using wide traces but also having sufficient spacing between the traces helps to prevent short circuits during operation, but also ensures safe operation.

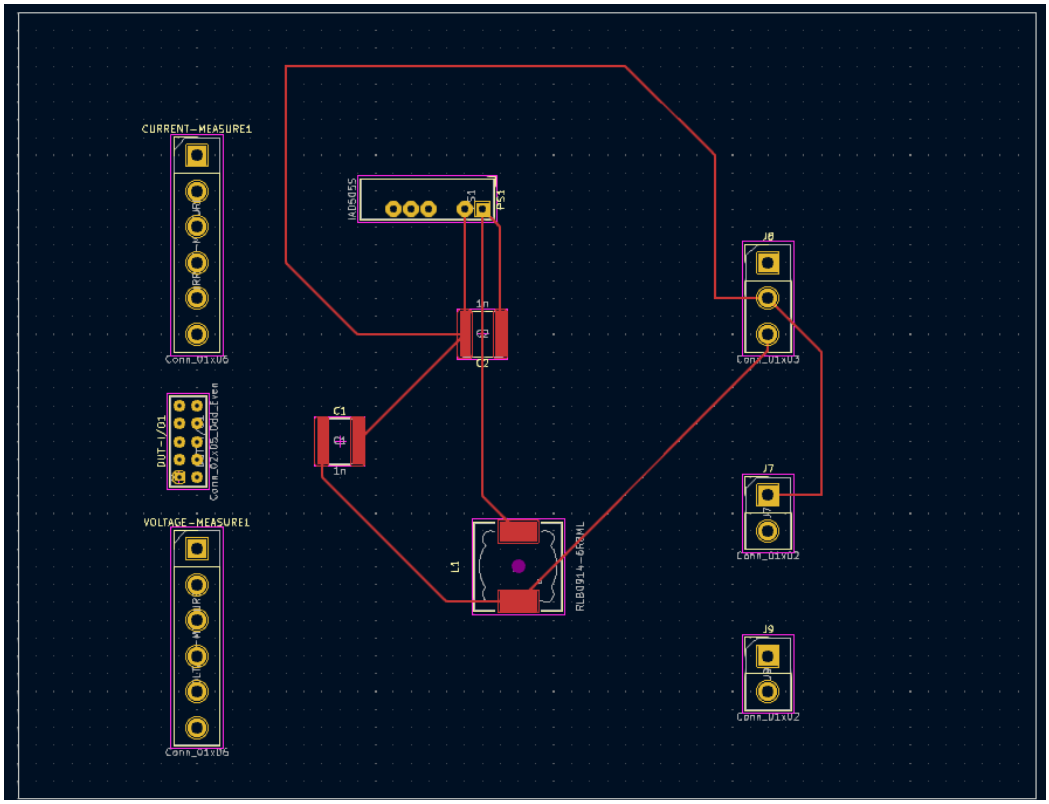

Figure 53 - PCB Layout of Power Supply on KiCAD

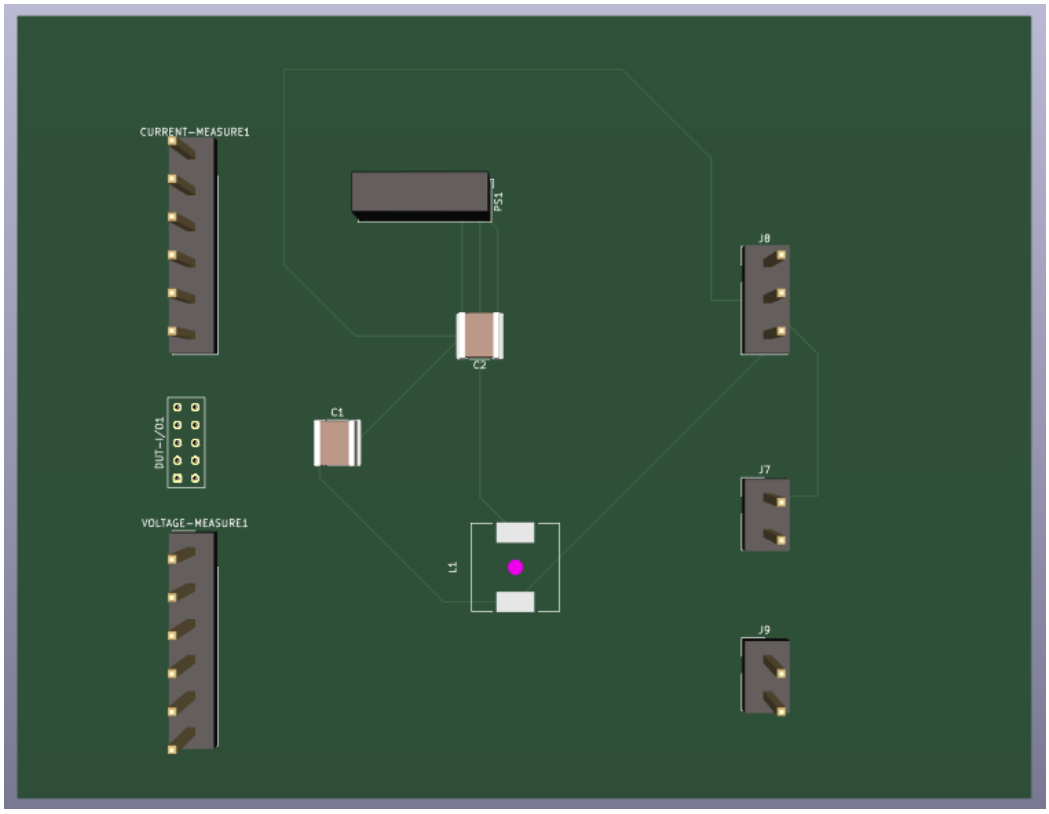

Figure 54 - 3D View of Power Supply PCB

3.3.5 Charge to Breakdown PCB

To enhance the overall functionality of the QBD experiment, all four of the circuits and PCB layouts were integrated into a single, large PCB. This integration simplifies the assembly process and improves the reliability and performance of the circuit by reducing the number of interconnections and potential failure points. The PCB of the QBD rig maintains the component placement and routing techniques, ensuring operation and efficient use of space, however, has three sets of the design, so multiple devices can undergo the test at one time.

Initial PCB Layout

To accommodate the complex routing and minimise the interference between the separate circuits, the PCB is designed as a dual layer board, arranged in the process of the QBD test. Located down the left of the board, the connector terminals are laced to allow easy access for external connections, such as the DUT, the power supplies and measurement outputs. Positioned immediately to the right of these outputs is the power supply circuit, which is connected to all the individual circuits on the PCB. This is followed by the current source configuration, which is placed first to minimise the distance between the current source and the MOSFET being tested to reduce the potential voltage drops and noise. The voltage measurement circuit is then placed here, as it is vital for maintaining the constant current source and detecting the breakdown point. It is also placed here to minimise the signal path lengths and reduce the EMI, ensuring accurate voltage readings during the experiment.

The current measurement circuit is positioned at the end of the circuit, which provides the data required to determine the QBD result, therefore the most important part of the circuit. The routings to the connector terminals for this part of the circuit are on the top layer of the board, to avoid any interference from other signals on the second layer of the board, ensuring an accurate result is acquired. Below the first set of circuits, two additional sets of the same layout are placed below, except the other two sets of circuits are connected to the original power supply so three devices can be tested at once. The separate circuits on the PCB are also spaced out to minimise interference between adjacent circuits, which also make assembly easier, as well as troubleshooting.

Fabrication and Assembly

Finalising the PCB design involves a thorough process to ensure that the board meets the standards and requirements necessary for the QBD experiment. This begins with checking for design regulations, to identify any issues such as trace width violations, spacing error and incorrect via placements, to ensure that all traces and components are correctly placed and connected to avoid any electrical failures. The next step is to prepare the design files for manufacturing by generating the Gerber files for each PCB layer, which contain the detailed information on the copper layers, solder mask and silkscreen layers. As well as this, the drill files are created to determine the locations and sizes of the holes that need to be drilled on the PCB. The bill of materials (BOM) is also created, in which the required components for assembly are listed, as well as their quantities and specifications.

Due to the complexity of this PCB, selecting an external PCB fabrication company is a crucial part for producing a high-quality board. All files were sent off to PCBWay to be manufactured, due to their quick turnaround times, low costs and high-quality manufacturing standards. The PCB took around three weeks to arrive, and five boards were ordered in total.

PCB Inspection and Testing

Although the PCB was thoroughly inspected and tested by PCBWay, the board was tested before QBD testing began to ensure the boards functionality and identify any potential issues. Beginning with a visual inspection, the board is checked for any visual defects. By comparing the component placement with the PCB diagram, the component, the placement and the orientation were verified to ensure that the device was correct, as well as the position, before examining the solder joints of the component, ensuring they were well formed. Any breaks in the copper traces were also checked for, to make sure there were no breaks or shorts in the circuit path.

The board also went under electrical testing, using a multimeter to measure the board continuity and verify that all connections have been correctly made, as well as verifying the resistor values of the circuit. The power supply lines were then checked, to ensure the correct voltage levels are flowing for the input and output pins on the separate circuits, as well as checking for any unexpected voltage drops. From this, the PCB was powered on, to check that the components were not overheating and that the expected voltages were present across the board. Each section of the QBD circuit (current source, voltage measurement, current measurement and power supply circuits) were tested individually to verify their correct operation. During this testing, it was discovered that the power distribution across the circuits was not operating as intended, as the voltage supplies for each circuit were interconnected, causing them to share the dame voltage supply, instead of using their individual voltage supplies as required. This was found as the voltage measurements at various points on the PCB indicated that the same voltage was being supplied to all circuits, instead of the intended isolated supplies, which caused interference between circuits, leading to incorrect measurements and unstable operation.

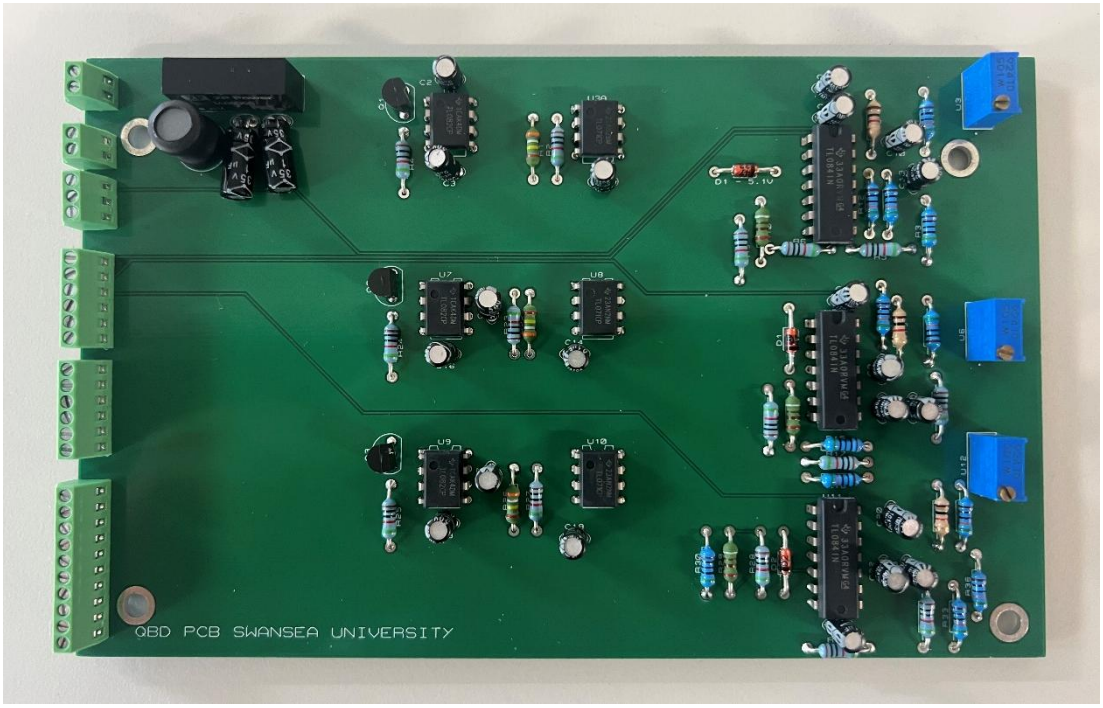

Figure 55 - Initial Charge to Breakdown PCB, Fabricated by PCBWay

To resolve this issue, an option to cut the power supply tracks of the individual circuits was possible, with new connections and tracks to the correct power supplies created that ensure that each circuit had its own isolated voltage supply. By using the PCB layout, the specific tracks where

the voltage supplies were incorrectly connected can be identified, before carefully cutting the tracks to disconnect the shared supply lines. Solder wire can then be used to create new tracks from the voltage supply pins to the corresponding circuit points, establishing the connections. However, due to the number of layers and tracks already on this board, this would've proved an extremely difficult and intricate task, so the decision was made to create a new QBD PCB from the beginning.

Adapted PCB Layout

With the knowledge of the problems of the previous PCB, another QBD testing set up was carefully designed to ensure efficient power distribution. Placing all power connection terminals on the left side of the board, it is easy to access and connect the external power supplies, allowing a clean and organised wiring set up. Along these terminals, this board has included an isolated power supply for the current source circuit, to prevent any interference to provide a stable and constant source to the DUT. At the top of the board, the power supply circuit is positioned, responsible for providing power to both the voltage measurement and current measurement circuits, so they receive stable power to produce accurate readings. Below the power supply circuit is the current source circuit and its individual power supply, which connects to the voltage measurement circuit to the right of it. This placement minimises the signal path lengths, reducing the potential noise ensuring reliable voltage measurements can be made. In addition, another Bourns trimmer resistor was also added, connected to the +5 V input, 0V and the non-inverting input of the TL082, to adjust the voltage input of the current source circuit, so various values of current can be produced to test the devices at different levels.

At the bottom of the board, the current measurement circuit is placed, where the current flowing through the DUT is measured, to ensure precise current monitoring during the QBD test. The connection terminals for the DUT are placed to the left of this circuit, where the gate connection is connected to the output of the current source circuit, so the gate of the device receives the necessary constant current for the breakdown testing, and the source of the DUT is connected to the input of the current measurement circuit, allowing for accurate measurement of the current flowing through the DUT. On the right side of the board, the voltage measurement and current measurement outputs are placed, keeping these connection terminals separate from the outputs, so the accurate results of the voltage and current can be easily obtained. For this circuit, each circuit has an individual ground plane, to provide stable references for each circuit and reduces noise, so all current and voltages are precise, as well as significant space between the circuits to reduce the chances of interference. As this is being built by hand, to save time only one set of the QBD testing apparatus is being built.

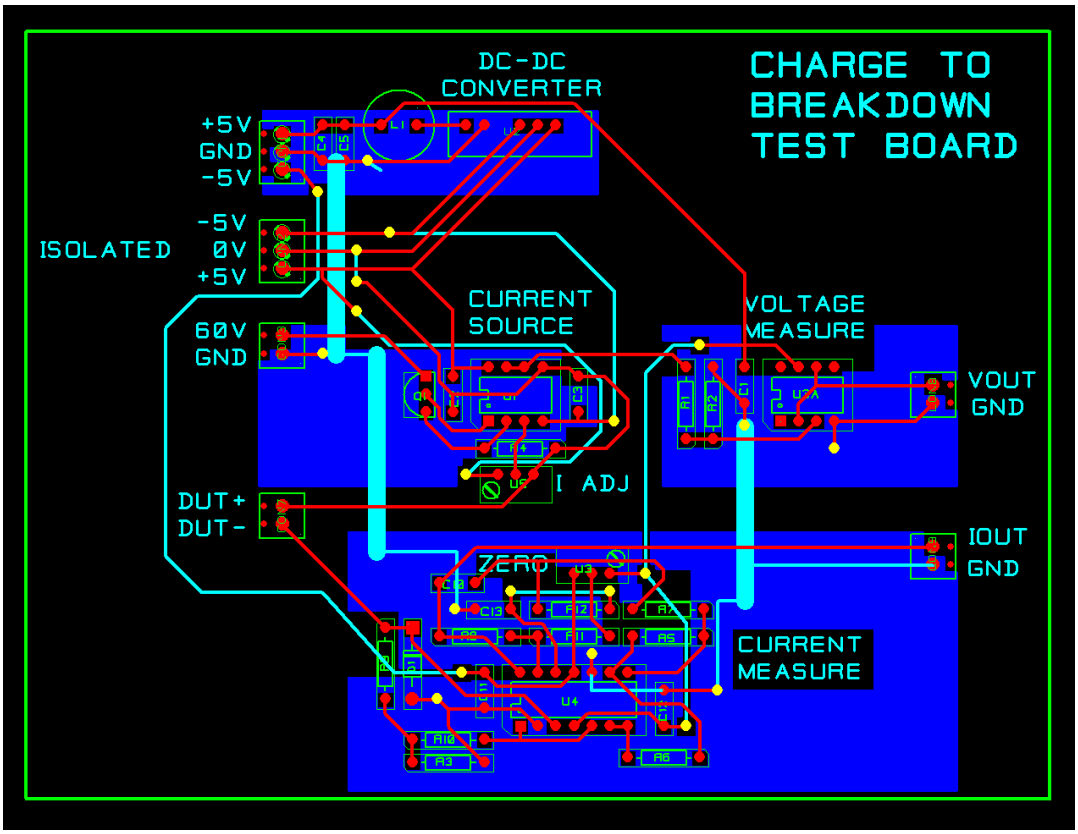

Figure 56 - Adapted PCB Layout of Charge to Breakdown Test Circuit, developed by Stephen Batcup

PCB Inspection and Testing

To ensure that this board is functioning correctly, the first step is to visually inspect the board, by checking the components are correctly placed and oriented on the PCB according to the design. The solder joints were carefully inspected for potential issues, including dry joints, which appear cracked and can disrupt electrical connections; solder bridges, which may cause short circuits on the tracks. Whilst under close inspection, the copper traces and pads were also examined for any signs of etching defects, such as incomplete etching and breaks in the traces from the soldering or drilling processes, and by using a multimeter, it was ensured that all the traces were correctly connected to avoid open circuits.

A multimeter was also used to verify that all the electrical connections were correct, according to the circuit schematic, as well as verifying each trace and via, to ensure that there are no open circuits, confirming that the power distribution of the circuits on the PCB was correct. Before powering the entire board, the power supply rails must be tested independently, by applying an input voltage and measuring the output levels, to test if they match the expected values of the QBD circuit. Upon verifying this, the board was powered, and each individual circuit of the board was tested. For the current source circuit, the output current was measured to ensure it was stable, however with the voltage measurement circuit, the expected voltages were applied to the circuit, before verifying that the output matched the expected readings. Similar to this, the current measurement circuit functionality was tested by passing the expected currents through the circuit and comparing the output readings.

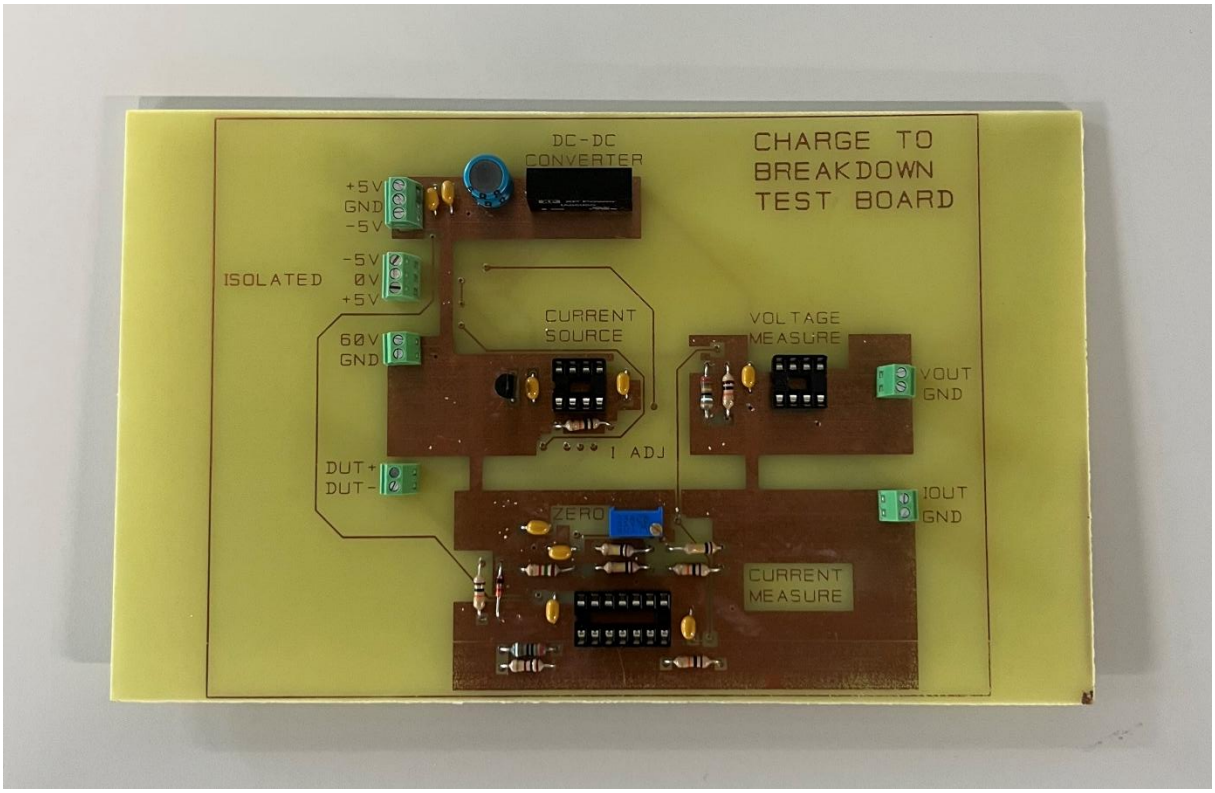

Figure 57 – Completed Charge to Breakdown PCB, Excluding ICs

4 Experimental Setup

For the Charge to Breakdown (QBD) testing in this study, a careful selection of MOSFETs was conducted to ensure relevance to the application in EVs and to provide insights into their reliability under electrothermal stress. The MOSFETs chosen for this testing are critical components in power electronics, particularly in EV inverters and converters, where they are subject to high electrical and thermal loads. Based on the criteria for this QBD experiment, the MOSFETs were first chosen for their voltage and current ratings, which must align with the operational requirements of EV power systems. High thermal conductivity and robustness to handle significant power dissipation were also essential to consider, as these characteristics ensure efficient heat management and durability under high demands of EV powertrain applications, where rapid and efficient power conversion is crucial for reliability. The last important consideration was the validity of datasheets and information from semiconductor manufacturers, which guaranteed that the chosen MOSFETs had a track record of dependability.

The selected MOSFETs are subjected to QBD testing to evaluate their reliability and endurance under cumulative charge stress. This testing is crucial for understanding several key aspects of their performance and longevity in high-power applications. A primary aspect is dielectric breakdown, which involves identifying the charge threshold at which the gate oxide layer fails, leading to device breakdown. This is essential for determining the maximum charge the MOSFETs can handle before experiencing final failure. Another critical aspect is thermal degradation, which assesses how thermal cycling and power dissipation impact the MOSFET's longevity and performance. By understanding the thermal limits and behaviour of the MOSFETs, the lifespan and reliability of MOSFETs in real-world applications can be predicted, in which they are subjected to varying thermal stresses. Additionally, the testing helps in understanding various failure mechanisms, such as thermal runaway and hot carrier injection, which are common to high-power EV applications, where MOSFETs operate under intense electrical and thermal stress.

4.1 Test Procedure

To test and confirm the functionality and stability of the QBD circuit, high value resistors can be used in place of MOSFETs to test the constant current source. By connecting one end of the resistor into the positive DUT output on the PCB, the other end of the resistor can be connected to an ammeter in series, which is connected to the ground of the PCB. The ammeter is used to confirm that there is a constant current flowing through the DUT, and that it is following Ohm's Law corresponding with the voltage across the device. The instrumentation for this is shown below.

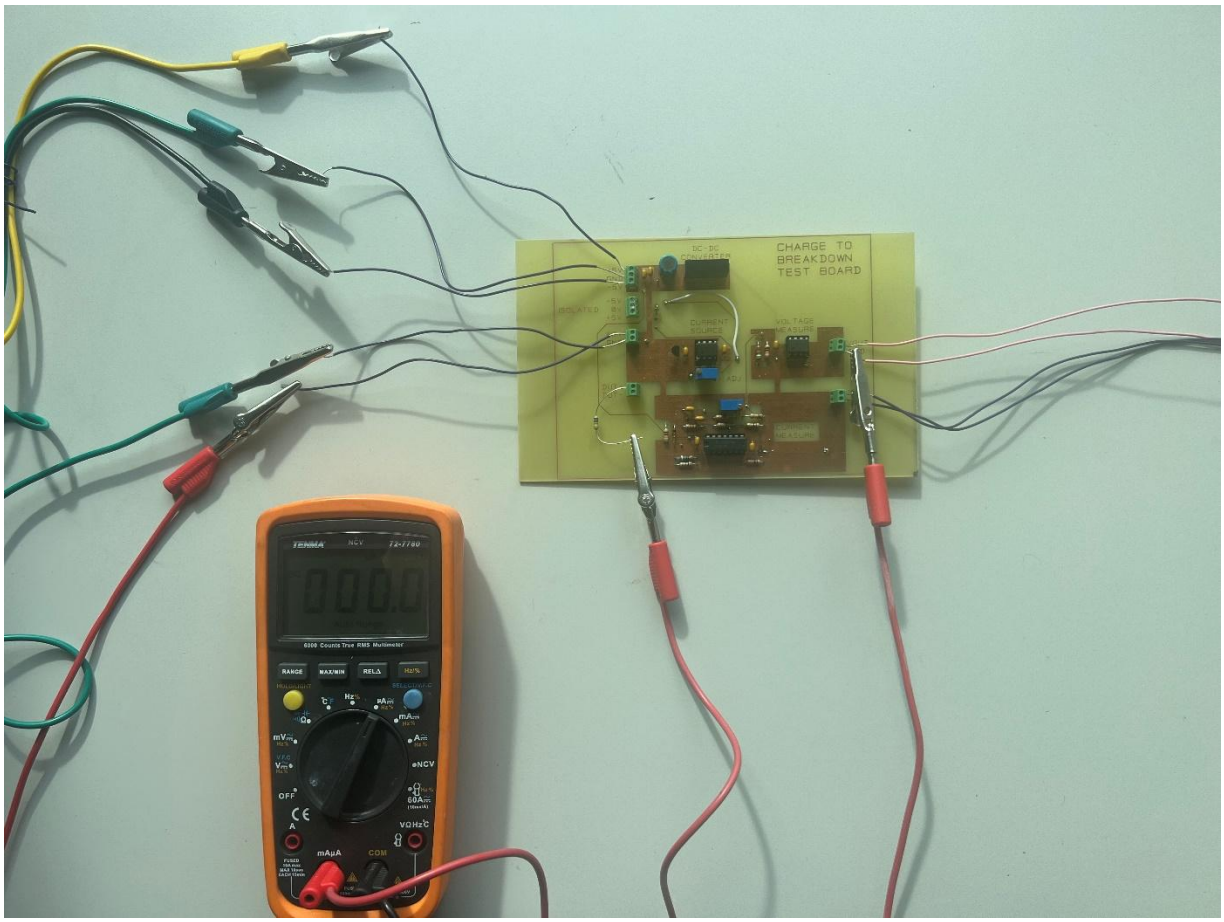

Figure 58 - Instrumentation of Test Procedure of Resistors

When the resistors are used as loads, the consistency of the output current can be measured, to ensure a stable current is maintained across resistors in the range of 1MΩ to 10MΩ. By applying the reference 5V voltage, -5V and ground voltage to the PCB power supply circuit, the voltage for the current source can be applied in the range 20V to 40V, before collecting the values for the voltage across the resistor and current through the resistor. The results for this are shown below, with each resistor value and their corresponding voltage and current through the devices.

Resistor	Input Voltage	Voltage Measured Across Device	Estimated Current Through Device	Current Measured Through Device
1MΩ	20V	19.80V	19.80µA	19.8µA
1MΩ	30V	29.70V	29.70µA	28.4µA
1MΩ	40V	39.62V	39.62µA	38.0µA

Table 1 - Input Voltage, Voltage Across Device, Estimated Current Through Device and Current Measured Through Device of 1MΩ Resistor

Resistor	Input Voltage	Voltage Measured Across Device	Estimated Current Through Device	Current Measured Through Device
2.2MΩ	20V	19.40V	8.818μA	8.6μA
2.2MΩ	30V	29.07V	13.21μA	12.9μA
2.2MΩ	40V	38.79V	18.18μA	17.3μA

Table 2 - Input Voltage, Voltage Across Device, Estimated Current Through Device and Current Measured Through Device of 2.2MΩ Resistor

Resistor	Input Voltage	Voltage Measured Across Device	Estimated Current Through Device	Current Measured Through Device
4.7MΩ	20V	19.42V	4.132μA	4.1μA
4.7MΩ	30V	29.75V	6.329μA	6.2μA
4.7MΩ	40V	38.92V	8.281μA	8.3μA

Table 3 - Input Voltage, Voltage Across Device, Estimated Current Through Device and Current Measured Through Device of 4.7MΩ Resistor

Resistor	Input Voltage	Voltage Measured Across Device	Estimated Current Through Device	Current Measured Through Device
6.8MΩ	20V	19.45V	2.860μA	2.7μA
6.8MΩ	30V	29.16V	4.288μA	4.1μA
6.8MΩ	40V	38.91V	5.722μA	5.5μA

Table 4 - Input Voltage, Voltage Across Device, Estimated Current Through Device and Current Measured Through Device of 6.8MΩ Resistor

Resistor	Input Voltage	Voltage Measured Across Device	Estimated Current Through Device	Current Measured Through Device
10MΩ	20V	19.97V	1.987μA	1.99μA
10MΩ	30V	29.96V	2.996μA	3.0μA
10MΩ	40V	39.98V	3.998μA	4.0μA

Table 5 - Input Voltage, Voltage Across Device, Estimated Current Through Device and Current Measured Through Device of 10MΩ Resistor

During the initial testing process, it was discovered that the voltage and current measurement circuits were not functioning correctly, leading inaccurate values for output current and voltage, in which the issue was traced back to incorrect circuit connections. However, by connecting a voltmeter across the DUT, it verified that the voltage flowing across the DUT was correct, as well as the current flowing through the device when connecting an ammeter in series with the DUT. This verified that the current source circuit is operating as intended and safely. The next planned step was to place the PCB in an environment with a temperature of 150°C, to replicate the operating conditions in EVs, to give precise QBD measurements on the reliability of MOSFETs in EV operations. Unfortunately, due to time constraints and various challenges along the way, this could not be carried out. As a result, the following test results are performed at room temperature. While these tests represent an initial exploration into stress testing and QBD analysis of MOSFETs in EV systems, the results gathered are a beginning point for further investigation under more rigorous conditions.

4.3 Analysis of SiC MOSFETs

Silicon Carbide Power C3M MOSFET Technology

Part Number: C3M0280090D

Manufacturer: Wolfspeed, Cree Inc.

Key Specifications

Drain-Source Voltage (VDS): 900V

The silicon carbide MOSFET used for this experiment is capable of withstanding a drain-source voltage of 900V, making it suitable for high-voltage applications commonly found in EV power systems. This high voltage rating ensures that the MOSFET can handle the significant voltage spikes that occur during the switching operations in EV inverters and converters.

Drain Current (ID) – 11.5A

With a continuous drain current rating of 11.5A, this MOSFET can manage substantial current loads, which are typical in high-power EV applications. This capability is crucial for maintaining efficient power transfer and ensuring the reliability of the powertrain components under demanding conditions.

RDS (on) – 280mΩ

The MOSFET features a low on-resistance of 280mΩ. This low resistance is essential for minimising conduction losses, therefore improving the overall efficiency of the power electronics system. Reduced conduction losses lead to lower heat generation during operation, which is beneficial for both performance and longevity.

Thermal Resistance - 40°C/W

The thermal resistance of 40°C/W indicates poor thermal performance, enabling ineffective heat dissipation from the MOSFET junction to the ambient environment. This characteristic is particularly important in EV applications, where high power dissipation can lead to significant thermal stress. Effective thermal management helps in maintaining the performance of the device and helps to prevent thermal runaway.

As SiC devices are the most prominent in advancing MOSFET technologies for EVs, the C3M0280090D SiC MOSFET was selected for this due to their superior switching speeds. With an exceptional VDS of 900V, in which this value determines the on-resistance and drain current for the MOSFET, which are 280mΩ and 11.5A respectively. These values are significant for the dependability of EVs, as they are directly proportional to each other. As a result of this, the RDS (on) of the SiC MOSFET determines the power dissipation in the MOSFET, and therefore the switching losses, hence the degradation rate and effectiveness. As the value for on-resistance is so low, the voltage-drop across the device decreases, so there is less power dissipation and better thermal management within the battery management system, as the device operates at lower operating temperatures, resulting in a longer lifespan of the MOSFET and therefore making electric vehicles more efficient.

Sic MOSFETs hold high switching frequency technologies, enabling more compact and lightweight power electronics design, which allows for the use of smaller passive components, such as inductors and capacitors. This allows for more space between components, reducing the chances of thermal stresses, but also improving power conversion efficiency and resulting in faster

response times. However, SiC MOSFETs tend to struggle at the high temperatures required for the power conversion system of electric vehicles. The thermal resistance of this device is 40°C/W, yet the maximum junction temperature can reach a maximum of 500°C in electric vehicle applications, especially in operation systems such as the battery management system, which require high switching frequencies. These high temperatures can cause the threshold voltage of SiC MOSFETs to shift positively, gradually increasing the on-state resistance, decreasing the efficiency and therefore making them less reliable.

Overall, the 900V SiC MOSFET is an ideal choice for the QBD test, providing valuable insights into the device's reliability and performance under high-stress conditions. Its high voltage and current handling capabilities, combined with superior thermal and electrical characteristics, make it a robust and efficient component for modern electric vehicle applications.

Experimental Procedure

To set up the QBD test board, it must be connected to the necessary input power supplies. By connecting the +5V, -5V and ground inputs for the power supply circuit, a 40V voltage is applied to the gate of the silicon MOSFET to assess its gate oxide reliability under electrical stress. This supplies the necessary voltage for the current source circuit on the PCB, before connecting the gate of the SiC MOSFET to the positive DUT input and the source of the MOSFET to the negative DUT input, which establishes the final links for the experiment to begin, allowing for the precise control of the current delivered to the SiC MOSFET, essential for accurate QBD testing.

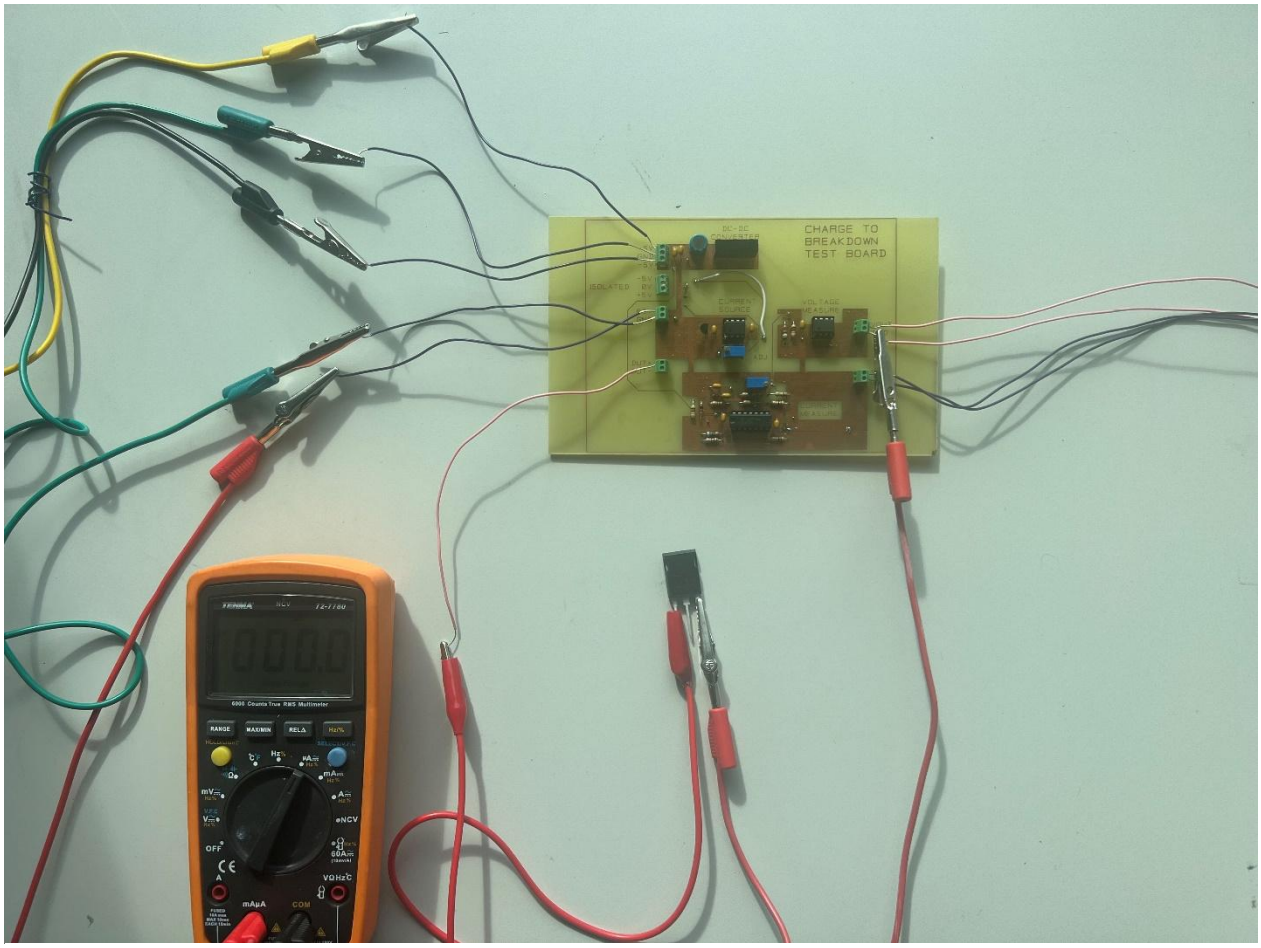

Figure 59 - Charge to Breakdown Instrumentation for SiC MOSFETs

Once the setup is complete, the set-up current of the current source circuit can be verified using a multimeter, which is found to be 0.5mA. As a current is applied to the device, the SiC MOSFET undergoes a severe electrical stress, which is carefully monitored to determine the overall stress timing of the device. For the C3M0280090D SiC MOSFET, the stress time was found to be 270 seconds. This process can be repeated for a second SiC MOSFET, where results of the QBD experiment for the SiC MOSFET are presented below. This data provides a clear indication of the SiC MOSFETs behaviour under the multiple levels of electrical stress. Using the QBD equation, the set up current and total stress time can be used to produce the QBD value for both experiments:

$$Q_{BD} = \int_0^{268} 0.0005 \cdot dt = 0.134C \quad (22)$$

$$Q_{BD} = \int_0^{347} 0.0005 \cdot dt = 0.1735C \quad (23)$$

MOSFET	Supply Voltage	Setup Current	Total Stress Time	Breakdown Current	Charge-to-Breakdown
C3M0280090D	40V	0.5mA	268s	506µA	0.134C
C3M0280090D	40V	0.5mA	347s	520.3µA	0.174C

Table 6 - Charge-to-Breakdown Results of Silicon Carbide MOSFET

4.4 Analysis of GaN Cascode Si MOSFET

650 V, 35 mΩ Gallium Nitride (GaN) Cascode Si MOSFET

Part Number: GAN041-650WSBQ

Manufacturer: Nexperia

Key Specifications

Drain-Source Voltage (VDS) – 650V

For the charge-to-breakdown experiment, a silicon MOSFET is selected. The chosen Si MOSFET has a rated drain-source voltage of 650V, making it suitable for high-voltage applications such as electric vehicle (EV) power systems. Whilst the VDS rating is comparable to alternative wide-bandgap devices, the reliability of the MOSFET and well-characterised failure mechanisms make it a valuable component for this experiment.

Drain Current (ID) – 47.2A

With a drain current rating of 47.2A, which is significantly larger than the SiC MOSFET rating, the Si MOSFET is capable of sustaining high-power loads, making it well-suited for demanding EV applications. This rating ensures the MOSFET can handle the substantial current flow required in power electronics, particularly in traction inverters and onboard chargers, where components are subjected to high currents due to the heavy loads imposed by the electric motor.

RDS (on) – 35mΩ

The chosen silicon MOSFET has a RDS (on) of 35mΩ, which is optimised for minimising conduction losses. A lower RDS (on) contributes to higher efficiency in power conversion systems, reducing heat dissipation and improving thermal performance in EV applications.

Thermal Resistance - 40°C/W

The Si MOSFET selected for this study has a thermal resistance of 40°C/W. While its electrical performance is suitable for high frequency switching applications, its thermal characteristics must also be considered. The ability to operate at elevated temperatures is essential for reliability in EVs, as power devices experience significant thermal stresses during operation.

The Si MOSFET was selected for this investigation due to its well-established reliability and suitability for high-power applications, making it a viable candidate for EV operations. The drain-source voltage rating of 650V and a continuous drain current of 47.2A ensure that it can operate reliably under the harsh electrical environments of EV powertrains, particularly in traction inverters and DC-DC converters. Additionally, with an RDS(on) value of 35mΩ, the device achieves relatively low conduction losses, minimising resistive heating and improving overall system efficiency.

However, thermal management remains a critical consideration, as Si MOSFETs have higher conduction and switching losses compared to WBG devices. Since the thermal resistance of the SiC and Si MOSFETs is the same, this device in high-stress environments such as EVs can cause premature breakdown, due to the high switching speeds that result in a shift in the threshold voltage, where failure mechanisms occur, decreasing the reliability of these devices and the entire system. In summary, the Si MOSFET was also selected for this experiment due to its superior electrical characteristics, that make it a compelling choice for improving efficiency by reducing losses, and ensuring reliable operation in the harsh conditions of electric vehicle applications.

Experimental Procedure

For the GaN Cascade Si MOSFET, the same procedure is used. By connecting the gate of the Si MOSFET to the positive DUT input of the test board and the source of the device to the negative DUT input of the QBD rig, the experiment can begin. A 40V voltage is applied to the gate of the silicon MOSFET to assess its gate oxide reliability under electrical stress. The stress time can also be monitored, as well as the current flowing through the Si MOSFET, so the durability of the gate oxide of the device can be tested to prove its reliability. The complete results of the GaN Cascade Si MOSFET are shown below in Table 7.

MOSFET	Supply Voltage	Setup Current	Maximum Current Through Device	Total Stress Time
GAN041-650WSBQ	40V	0.5mA	148.4mA	492s
GAN041-650WSBQ	40V	0.5mA	114.2mA	519s

Table 7- Charge-to-Breakdown Results of Gallium Nitride Cascade Si MOSFET.

5 Limitations and Future Considerations

One of the main limitations of this study is the relatively small sample size of tested devices. Only two SiC MOSFETs and two Si MOSFETs were analysed, which means the results may not fully represent all MOSFETs of these types. The QBD values obtained are specific to the tested planar-gate MOSFETs, and different structures, such as trench-gate SiC MOSFETs, may exhibit different reliability characteristics. Additionally, the testing was conducted at room temperature, which does not account for real-world variations in operating conditions, such as high-temperature operation in EV operations or extreme cold conditions during winter starts. The results provide valuable insight into oxide deterioration, but further tests under diverse conditions are necessary to confirm these findings.

Temperature plays a critical role in gate oxide reliability and QBD performance. At high temperatures, the increased thermal energy accelerates oxide degradation, leading to faster charge trapping and a reduction in QBD values [131]. Elevated temperatures can also cause an increase in leakage currents, which may prematurely trigger gate oxide breakdown. In an EV context, where power losses and rapid switching cycles generate substantial heat, these effects can significantly impact the longevity of MOSFETs [2].

In contrast, cryogenic conditions can have the opposite effect on QBD values. At extremely low temperatures, the on-resistance of MOSFETs decreases, which improves the efficiency due to the reduction in power dissipation, due to the decreased development of failure mechanisms that attribute to oxide breakdown [132]. However, whilst most degradation mechanisms are thermally activated, designing a circuit to operate at extremely low temperatures could potentially introduce other challenges related to parasitic effects and material properties [133].

By studying the impact of both high and low temperatures on MOSFET degradation, as well as using a larger batch of MOSFETs from different manufacturers and designs, future research could provide more accurate lifetime models and reliability predictions for power electronics in EVs and other demanding applications.

6 Results and Discussions

6.1 Test Procedure

Using resistors in the range of 1M-10M, the goal was to determine the functionality and stability of the current source circuit. This was achieved by measuring the consistency of the current through each resistor when different voltages applied across the device. The results from the experiment are shown in the graph below.

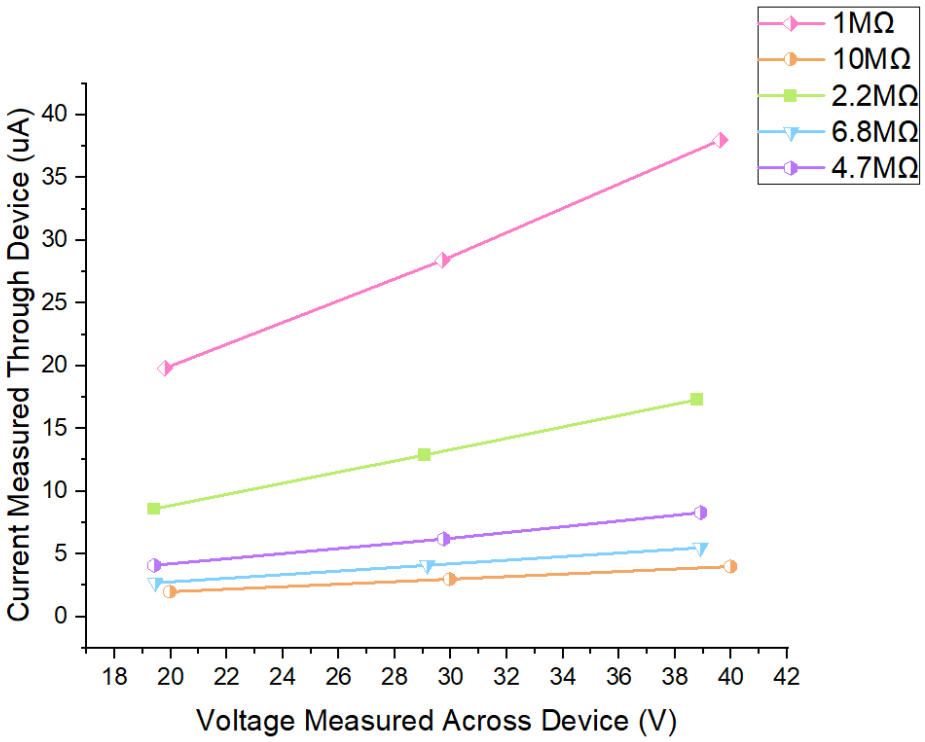

Figure 60 - Line Graph of Current Measured Through Resistors Against Voltage Measured Across Resistors

The core function of the current source circuit is to produce and maintain a constant, stable current output, regardless of variations in the supply voltage. It can be interpreted from the graph that this has been achieved, as the results showed as the voltage across the resistor was elevated, the current through the DUT also increased, indicating that the circuit is following Ohm's Law. This pattern repeats for each resistor that was used in this test procedure, indicating that the current source is effectively regulating the current, as intended. The expected results for this experiment are shown in the graph below. With the experiment results closely matching the expected values, the reliability of the current source circuit created is highlighted. The linearity of the results for the varying resistors also confirm that the current source is correctly regulating the current through the resistors, independent of the varying load resistance, indicating the circuit is performing correctly within its designed parameters.

Testing the current source using a range of high value resistors also proved that the current source maintained the desired current across the different loads, demonstrating its ability to handle various load conditions without significant fluctuation. The results indicate minimal noise is produced in both the current and voltage measurements, compared to the expected results, proving the current source provides a clean and stable output. Finally, the close alignment between the measured results and the theoretical expectations indicates that the circuit components are functioning within their tolerances, and that the design is robust against thermal and other environmental variations.

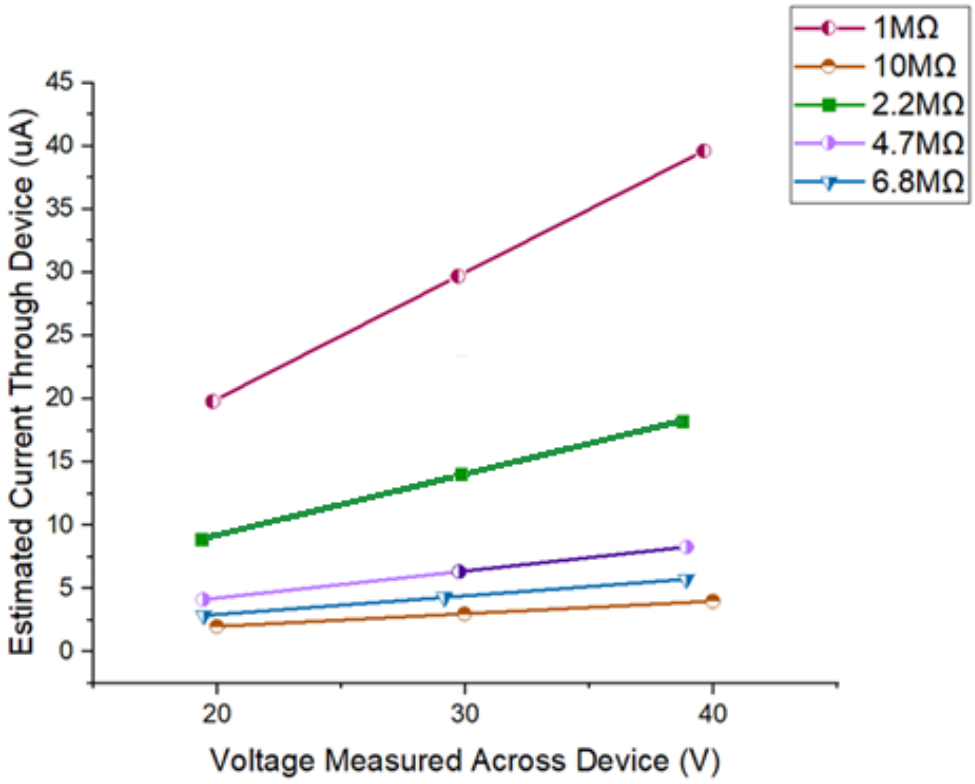

Figure 61 - Line Graph of Expected Current Through Resistors Against Voltage Measured Across the Device.

6.2 SiC MOSFETs

Since the circuit was not thermally regulated by using a hot plate, it was expected that by placing the MOSFETs into the QBD instrumentation, the MOSFETs would gradually charge up without reaching thermal breakdown. However, the observed results for both MOSFETs indicated that both devices reached gate oxide breakdown at room temperature. During the experiment, the current through the MOSFETs was monitored, while the constant current was applied to the gate of the DUT. For the SiC MOSFETs under testing, the results from the experiment are shown in Figure 62 and 63.

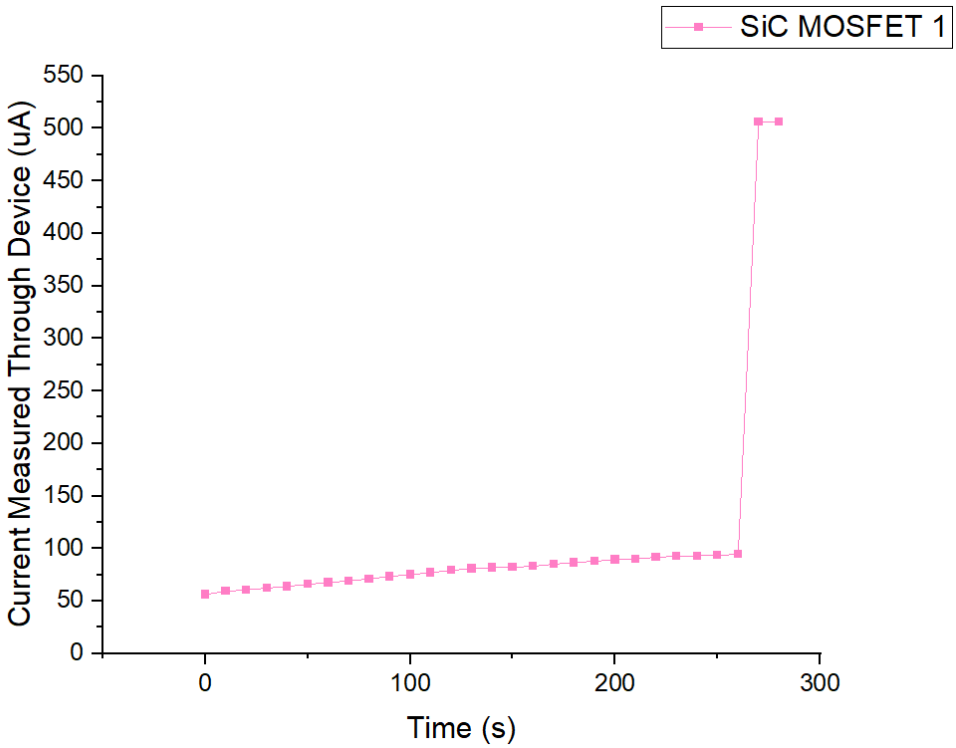

Figure 62 – Graph of Results of First Charge-to-Breakdown Experiment of SiC MOSFET

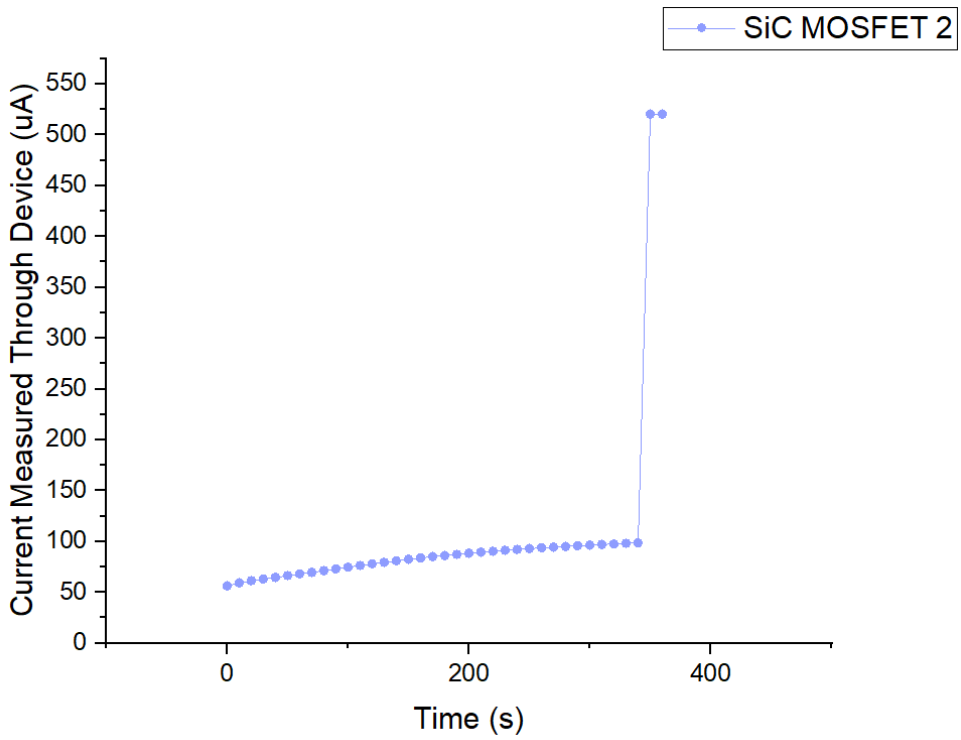

Figure 63 - Graph of Results of Second Charge to Breakdown Experiment of SiC MOSFET

Initially, the current through the SiC MOSFET increased linearly, as expected, steadily climbing until reaching a value of 94.5μA. This linear rise indicated that the MOSFET was functioning normally within its operating range, with the current gradually increasing with the applied voltage. At this point, the current abruptly spiked to 506μA, signifying that the MOSFET had reached breakdown. This took a total time of 268 seconds, resulting in a QBD value of 0.134C for the first MOSFET. A similar procedure was followed for the second SiC MOSFET, where the current again increased linearly until reaching a value of 98.7μA before rapidly increasing to 520.4μA. The time to breakdown for this MOSFET was 347 seconds, producing a QBD value of 0.174C—0.04C higher than the first MOSFET under testing.

The QBD value, representing the total charge the MOSFET can withstand before failure, is key to understanding the long-term reliability of these devices. In the context of EV applications, a longer breakdown time and a higher QBD value suggest that the second MOSFET exhibited greater endurance before breakdown. This indicates a better ability to handle prolonged electrical stress, which is crucial in high-frequency switching applications. With this endurance, less power is dissipated as heat, reducing thermal energy transfer and minimising the risk of premature failure, making these MOSFETs reliable candidates for EV power systems.

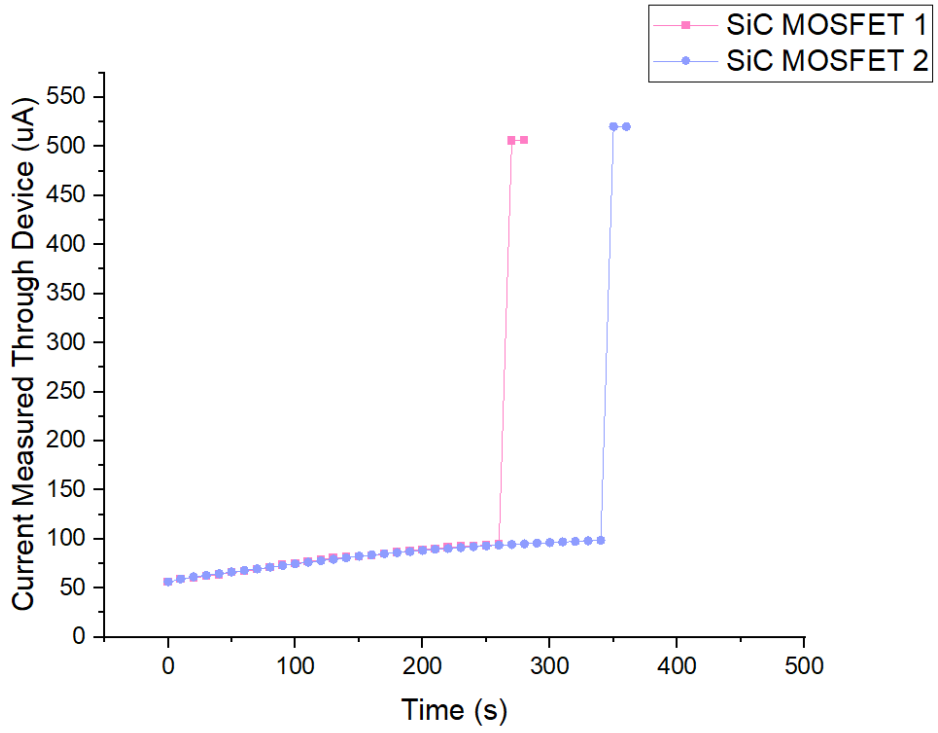

Figure 64 - Line Graph of Both Results of SiC MOSFET Charge-to-Breakdown Experiment

Although the first experiment produced a QBD value of 0.134C, indicating that breakdown occurred sooner under identical conditions, it still demonstrates reasonable stress tolerance. The variation in QBD values between the two SiC MOSFETs may be attributed to differences in material quality, such as inconsistencies in the gate oxide layer, leading to different charge endurance levels. This highlights the importance of quality control during MOSFET manufacturing, as variations in material properties could significantly impact reliability. The results from the QBD experiment emphasise the critical role of gate oxide integrity in determining MOSFET reliability, particularly in high-power applications. The charge accumulation in the gate oxide over time leads to degradation, ultimately resulting in breakdown, which can compromise overall device performance.

The experiment was conducted at room temperature, meaning no additional thermal stress was applied to replicate harsh operating conditions. Despite this, both SiC MOSFETs exhibited a consistent linear increase in current before failure, suggesting stable performance under normal conditions. While the QBD values confirm that SiC MOSFETs can endure prolonged electrical stress, further studies under elevated temperatures and harsher conditions would be necessary to assess their performance in real-world EV environments. Nonetheless, the results suggest that these MOSFETs possess the necessary gate oxide durability for high-power applications, where maintaining long-term reliability is essential for efficiency and operational longevity.

6.3 GaN Cascade Si MOSFETs

For the Si MOSFETs, the same procedure was carried out. However, the outcome of the test aligned with expectations—the MOSFETs did not reach gate oxide breakdown at room temperature but instead transitioned into an 'on' state operation mode. The first Si MOSFET under testing took 492 seconds to reach a maximum current of 148.4mA, whereas the second took 519 seconds, reaching a maximum current of 114.2mA. This behaviour highlights the significant influence of thermal conditions on the breakdown of Si MOSFETs. The results for this are shown in Figure 65 and 66.

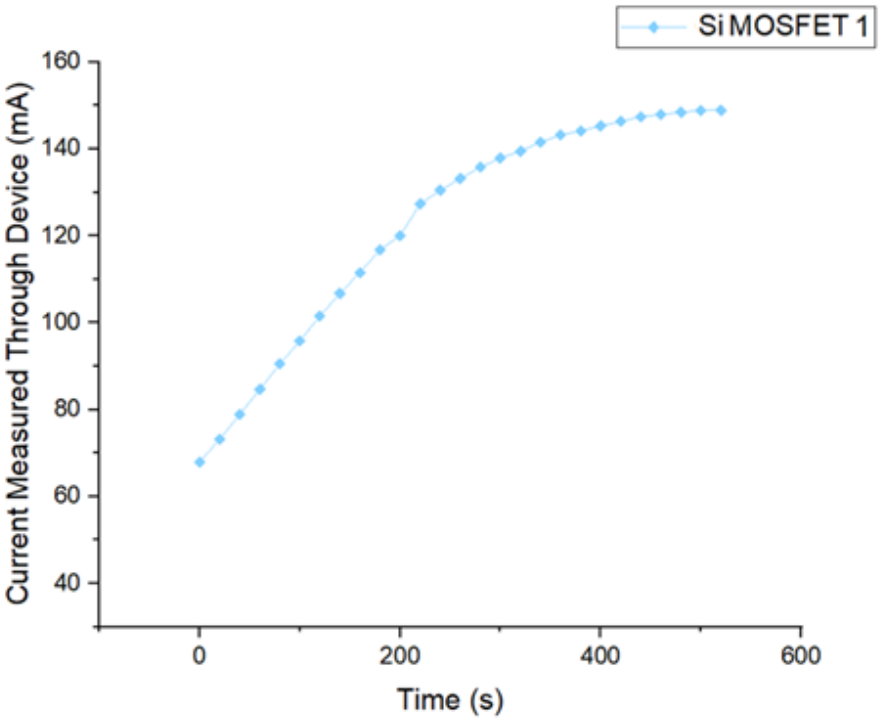

Figure 66 - Line Graph of Results of First GaN Cascade Si MOSFET Experiment

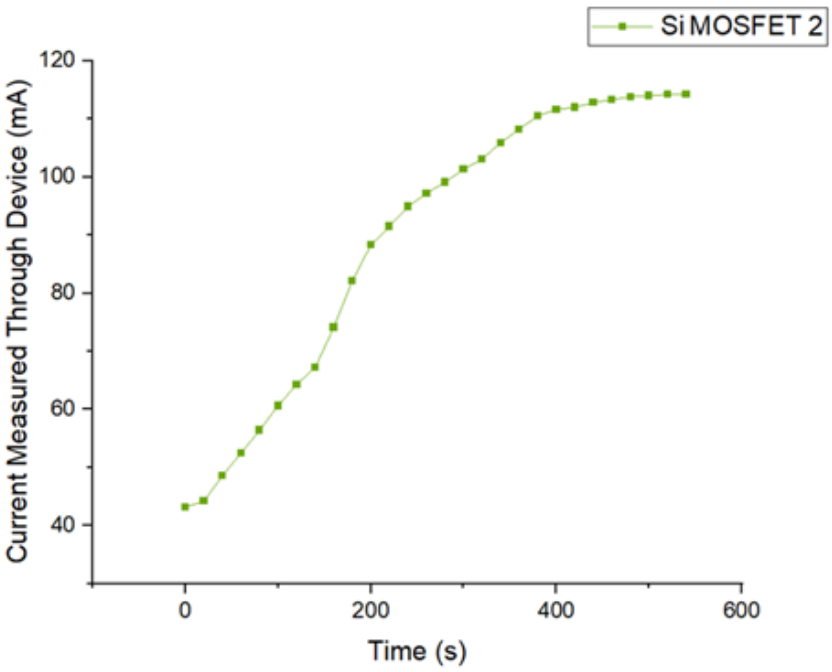

Figure 65 - Line Graph of Results of Second GaN Cascade Si MOSFET Experiment

From the graphs, it can be seen that both devices initially exhibited an increase in current before levelling off, indicating that the MOSFET had reached an operational state. In the experiment of the first Si MOSFET, the current increased steadily until reaching 90mA, after which the device continued to show variations, indicating that the device has not settled into a steady state mode, indicating that while the current showed signs of stability, variations were still present, implying underlying instabilities affecting the behaviour of the MOSFET. However, during the second experiment, the current behaviour was less gradual, displaying multiple transitions rather than a smooth incline. This could indicate inconsistencies in the gate oxide or variations in the threshold voltage, both of which influence the MOSFET's ability to reliably maintain its operation.

When comparing the two Si MOSFETs' behaviour under QBD testing, the variation in their current incline represents their potential reliability in EV applications. In the first experiment, the linear behaviour suggests consistent electrical performance, which is crucial for maintaining stable power delivery in EV systems. This demonstrates more efficient operation under high switching conditions, reducing the likelihood of unexpected power fluctuations, which in turn minimises thermal stress on the device and reduces the risk of premature breakdown—ultimately contributing to a more efficient EV system.

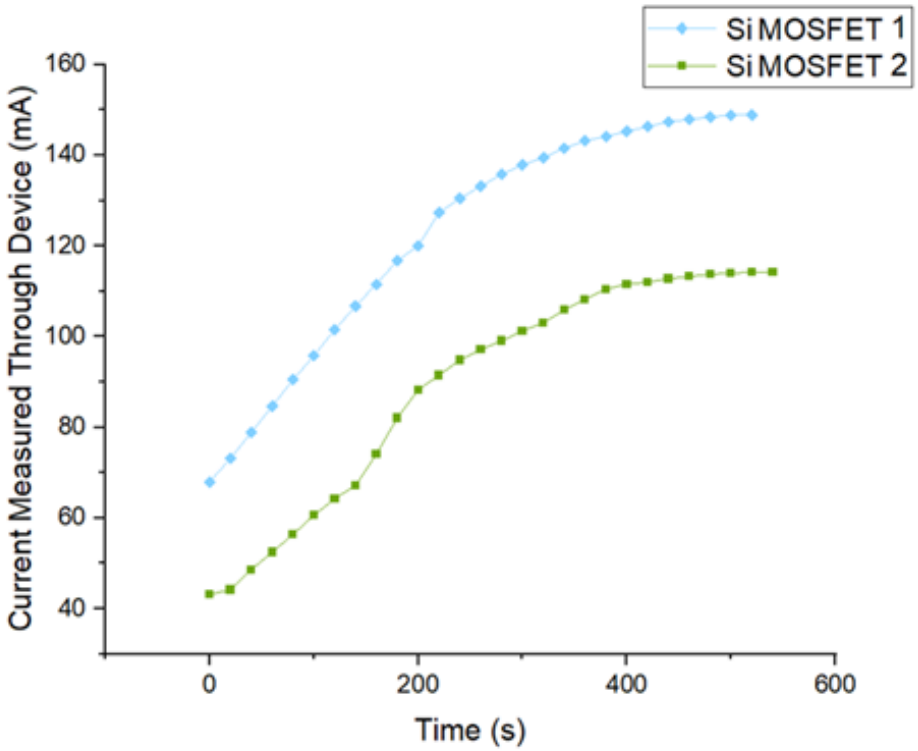

Figure 67 - Line Graph of Both Results of Si MOSFET Charging Experiment

In contrast, the second MOSFET exhibited a less linear increase in current. This could indicate minor inconsistencies in the gate oxide, as the device reached a lower steady-state current, which could impact its performance in EV applications. This non-linear behaviour may also suggest a less reliable device, as it could experience increased electrical stress over time, particularly in high-temperature and high-power environments, potentially leading to premature breakdown and reduced efficiency in the vehicle. The variation in results between the two Si MOSFETs may stem from factors such as manufacturing inconsistencies or differences in threshold voltage and gate voltage quality, even though both devices are identical. This highlights the importance of uniform gate oxide quality for predictable MOSFET performance, ensuring long-term reliability in EV power systems.

The absence of breakdown during the QBD experiment, though expected due to the lack of thermal stresses, supports the objective of assessing the reliability of MOSFETs under QBD conditions, demonstrating their ability to sustain prolonged current flow without immediate failure. This is crucial for EVs, where fast switching speeds reduce power losses, thereby decreasing thermal energy production and optimising reliability of not only the device but the entire vehicle.

7 Conclusion

This study aimed to evaluate the reliability of SiC and Si MOSFETs under QBD testing to assess their suitability for EV applications, and provided valuable insights into their reliability and performance under prolonged electrical stress. Considering the functionality of the test circuit, the current source circuit for the QBD experiment demonstrated excellent performance in maintaining a stable current when resistors were used as a load. The linearity of the measured results in comparison with the expected results provides strong evidence of the circuits accuracy and reliability, however resistors lack complexity compared to MOSFETs. The experiment findings suggest that the circuit is well-suited for charge-to breakdown testing.

The results of the QBD experiment demonstrated that SiC MOSFETs reached gate oxide breakdown at room temperature, highlighting their susceptibility to charge accumulation over time. In contrast, Si MOSFETs did not undergo breakdown during testing but instead transitioned into an 'on' state, suggesting a more reliable gate oxide under the given conditions. The results also presented that Si MOSFETs exhibited better gate oxide durability and lower thermal stress, maintaining an operational state without reaching breakdown. The high frequency switching capability and efficient thermal management contributed to reduced charge accumulation, minimising the likelihood of premature failure. In contrast, SiC MOSFETs, despite their ability to handle higher voltages, experienced earlier gate oxide breakdown due to increased thermal and electrical stress.

These findings suggest that Si MOSFETs may be more reliable for applications requiring high-frequency operation and lower thermal stress, whereas SiC MOSFETs are better suited for high-power conditions but require improved thermal management strategies to enhance their longevity. This distinction is crucial for optimising power electronics in EVs, where balancing efficiency, durability, and power handling is essential. Future studies could investigate the long-term performance of these MOSFETs under varying thermal and electrical conditions, as well as the impact of different gate oxide materials and manufacturing processes on their breakdown behaviour. Additional testing at elevated temperatures would provide a more comprehensive understanding of their real-world performance in EV power systems.

Ultimately, the selection of semiconductor devices in EV applications should be based on a balance between power efficiency, reliability, and thermal management considerations, ensuring optimal performance and longevity in demanding automotive environments.

Bibliography

[1] Pod Point, "2030 Diesel and Petrol Car Ban in the UK: Everything You Need to Know," Pod Point, 01 02 2025. [Online]. Available: https://pod-point.com/guides/2035-diesel-and-petrol-car-ban-in-the-uk-everything-you-need-to-know#:~:text=What%20will%20happen%20to%20petrol,to%20purchase%20a%20used%20EV.. [Accessed 06 02 2025].

[2] B. Shi, A. I. Ramones, Y. Liu, H. Wang, S. Pischinger and J. Andert, "A review of silicon carbide MOSFETs in electrified vehicles: Application, challenges, and future development," *IET Power Electronics,* vol. 16, no. 12, pp. 2103-2120, 2023.

[3] B. Damestani, "Power Electronics in EVs: A Complete Guide to the Brain Behind Electric Cars," Stedmans Garage , 03 02 2025. [Online]. Available: https://stedmansgarage.co.uk/electric-vehicles/power-electronics-in-evs/#:~:text=A%20traction%20inverter%20is%20a%20crucial%20component,the%20motor%20shaft%20angle%20continuously%20and%20calculating. [Accessed 06 02 2025].

[4] A. Ibrahim, J.-P. Ousten, R. Lallemand and Z. Khatir, "Power Cycling Issues and Challenges of SiC-MOSFET Power Modules in High Temperature Conditions," *Microelectronics Reliability,* 2016.

[5] J. Wang and X. Jiang, "Review and analysis of SiC MOSFETs' ruggedness and reliability," *IET Power Electronics Special Issue: WBG Semiconductor Power Electronics for Industrial and Automative Applications,* vol. 13, no. 3, pp. 445-455, 2020.

[6] Q. Yu, "Comparative Analysis of Sic and Gan: Third-Generation Semiconductor Materials," *Highlights in Science Engineering and Technology,* no. 81, pp. 484-490, 2024.

[7] S. Goel, R. Sharma and A. K. Rathore, "A review on barrier and challenges of electric vehicle in India and vehicle to grid optimisation," *Transportation Engineering,* vol. 4, p. Article Number 100057, 2021.

[8] F. Alanazi, "Electric Vehicles: Benefits, Challenges, and Potential Solutions for Widespread Adaptation," *Towards a Sustainable Future: The Role of Electric Vehicles and Smart Grids in the Energy Transition,* vol. 13, no. 10, 2023.

[9] S. Kumar, *Battery charging topology, infrastructure, and standards for electric vehicle applications: A comprehensive review,* IET, 2021.

[10] D. D. Friel, "16 - Electronic Options for Lithium-Ion Batteries," in *Lithium-Ion Batteries; Advancements and Applications*, Fremont, CA, Elsevier, 2014, pp. 361-386.

[11] U.S. Department of Energy, "Batteries for Electric Vehicles," Energy Efficiency and Renewable Energy, 2024. [Online]. Available: https://afdc.energy.gov/vehicles/electric-batteries#:~:text=Lithium%2DIon%20Batteries,-Lithium%2Dion%20batteries&text=They%20also%20have%20a%20high,a%20challenge%20for%20the%20industry.. [Accessed 03 02 2025].

[12] P. Sisson, “How does an EV battery actually work?,” MIT Technology Review, 17 February 2023. [Online]. Available: https://www.technologyreview.com/2023/02/17/1068037/how-do-ev-batteries-work/. [Accessed 3 January 2024].

[13] Office of Energy Efficiency & Renewable Energy, “How Lithium-Ion Batteries Work,” U.S. Department of Energy, 28 02 2023. [Online]. Available: https://www.energy.gov/energysaver/articles/how-lithium-ion-batteries-work. [Accessed 5 02 2024].

[14] K. D. S. Priya, B. Triveni, G. Sirisha, V. M. Rao and J. V. S. Kumar, “Review on Converters used in Electric Vehicles,” *International Journal of Research Publication and Reviews,* vol. 5, no. 1, pp. 440-454, 2024.

[15] Sustainable Energy Authority of Ireland, “How Electric Vehicles Work,” 2017. [Online]. Available: https://www.seai.ie/technologies/electric-vehicles/what-is-an-electric-vehicle/how-electric-vehicles-work/#:~:text=An%20inverter%20is%20a%20device,frequency%20of%20the%20alternating%20current.. [Accessed 3 January 2024].

[16] X. Shu, Y. Guo, W. Yang, K. Wei, Y. Zhu and H. Zou, “A Detailed Reliability Study of the Motor System in Pure Electric Vans by the Approach of Fault Tree Analysis,” *IEEE Access,* vol. 8, pp. 5295-5307, 2019.

[17] RS Components, “How Does an Electric Motor Work?,” RS Components, 23 04 2023. [Online]. Available: https://uk.rs-online.com/web/content/discovery/ideas-and-advice/how-does-electric-motor-work. [Accessed 10 02 2024].

[18] BESTAS, “What is a DC-DC Converter? Selection, Functionality, and Types,” BESTAS, 20 November 2024. [Online]. Available: https://www.bestas.com.tr/en/blog/a-comprehensive-guide-to-dc-dc-converters-selection-functionality-and-types#:~:text=How%20Does%20a%20DC%2DDC,voltage%20output%20without%20unwanted%20fluctuations.. [Accessed 03 02 2025].

[19] V. S. Kosuru, “DC-DC Converter and its Use in Electric Vehicles,” Power Electronics News, 28 March 2023. [Online]. Available: https://www.powerelectronicsnews.com/dc-dc-converter-and-its-use-in-electric-vehicles/#:~:text=DC%2DDC%20converter%20is%20an,another%20based%20on%20circuit%20requirements.. [Accessed 3 January 2024].

[20] R. Hou, J. Guo, L. Dorn-Gomba and A. Emadi, “Power Eelectronic Systems and Control in Automobiles,” *Control of Power Eelectronic Converters and Systems,* vol. 2, pp. 309-332, 2018.

[21] A. Olabi, H. M. Maghrabie, O. H. K. Adhari, E. T. Sayed, B. A. Yousef, T. Salameh, M. Kamil and M. A. Abdelkareem, “Battery Thermal Management Systems: Recent Progress and Challenges,” *International Journal of Thermofluids,* vol. 15, p. Article Number 100171, 2022.

[22] Amphenol Sensors, “How Battery Thermal Management Systems Impact EV Battery Performance,” Amphenol Sensors, 26 01 2022. [Online]. Available: https://blog.amphenol-sensors.com/blog/battery-thermal-management-systems-and-

ev-battery-performance#:~:text=Lithium%2Dion%20battery%20cells%20perform,to%20quickly%20fill%20the%20cell.. [Accessed 03 02 2024].

[23] A. Cheng, Y. Xin, H. Wu, L. Yang and B. Deng, "A Review of Sensor Applications in Electrical Vehicle Thermal Management Systems," *Advancements in New Energy Vehicle Technology,* vol. 16, no. 5139, pp. 2-29, 2023.

[24] Microtronik, "ECU Key Components and Functions," Microtronik, 11 2024. [Online]. Available: https://www.microtronik.com/technical-info/hexprog/ecu-key-components-and-functions#:~:text=The%20Engine%20Control%20Unit%20(ECU)%20serves%20as%20the%20brain%20of,further%20to%20provide%20additional%20torque.. [Accessed 03 02 2025].

[25] "Understanding the role of the ECU in an electric vehicle," Energy5, 2023 December 2023. [Online]. Available: https://energy5.com/understanding-the-role-of-the-ecu-in-an-electric-vehicle. [Accessed 6 January 2024].

[26] H. DeLeon, "What is Semiconductor Technology and Why Is It Important?," Corporate Training, 11 04 2023. [Online]. Available: https://corporatetraining.usf.edu/blog/what-is-semiconductor-technology-and-why-is-it-important#:~:text=Overall%2C%20semiconductors%20are%20a%20crucial,implants%20and%20devices%2C%20use%20semiconductors.. [Accessed 03 02 2025].

[27] Computer History Museum, "1947: INVENTION OF THE POINT-CONTACT TRANSISTOR," Computer History Museum, 2024. [Online]. Available: https://www.computerhistory.org/siliconengine/invention-of-the-point-contact-transistor/. [Accessed 01 06 2024].

[28] Wikipedia, "History of the Transistor," Wikipedia, 08 2022. [Online]. Available: https://en.wikipedia.org/wiki/History_of_the_transistor#:~:text=John%20Bardeen%2C%20Walter%20Brattain%20and%20William%20Shockley,to%20the%20first%20widespread%20use%20of%20transistors.. [Accessed 03 02 2025].

[29] M. Riordan, "The Incredible Shrinking Transistor," MIT Technology Review, 1997. [Online]. Available: https://www.technologyreview.com/1997/11/01/237128/the-incredible-shrinking-transistor/. [Accessed 1 06 2024].

[30] R. Mitchell, "The History of the Microchip: How a Tiny Device Changed the World," Electropages, 22 11 2023. [Online]. Available: https://www.electropages.com/blog/2023/11/history-of-the-microchip#:~:text=functionality%20and%20reliability.-,The%20Advantages%20of%20Transistors,and%20portability%20of%20electronic%20devices.. [Accessed 03 02 2025].

[31] C. E. Rowland, J. B. Delehanty, C. L. Dwyer and I. L. Medintz, "Growing applications for bioassembled Förster resonance energy transfer cascades," *Materials Today,* vol. 20, no. 3, pp. 131-141, 2017.

[32] C. Tardi, “What Is Moore's Law and Is It Still True?,” Investopedia, 02 04 2024. [Online]. Available: https://www.investopedia.com/terms/m/mooreslaw.asp. [Accessed 03 02 2025].

[33] All About Circuits, “Introduction to Bipolar Junction Transistors (BJT),” All About Circuits, [Online]. Available: https://www.allaboutcircuits.com/textbook/semiconductors/chpt-4/bipolar-junction-transistors-bjt/. [Accessed 2 06 2024].

[34] E. Ashely, “What is FET: A Guide on FET,” RS Design Spark, 23 06 2021. [Online]. Available: https://www.rs-online.com/designspark/what-is-fet-a-detailed-guide-on-fet#:~:text=Definition:,between%20source%20and%20drain%20terminals.. [Accessed 03 02 2025].

[35] F. G. Turnbull, “14 - Power Electronics—Rectifiers, Filters, and Power Supplies,” in *Reference Data For Engineers*, Newnes, 2002, pp. 14-51.

[36] R. Mitchell, “How Do Microchips Work: Understanding the Core of Computing,” Electropages, 18 12 2023. [Online]. Available: https://www.electropages.com/blog/2023/12/how-do-microchips-work#:~:text=FETs%20are%20known%20for%20their,and%20space%2Dsaving%20are%20critical.. [Accessed 03 02 2025].

[37] S. Kurinec, *Encyclopedia of Materials: Science and Technology: Junction Field Effect Transistors,* Elsevier, 2001.

[38] All About Circuits, “Introduction to Junction Field-effect Transistors (JFET),” All About Circuits, [Online]. Available: https://www.allaboutcircuits.com/textbook/semiconductors/chpt-5/junction-field-effect-transistors-jfet/. [Accessed 2 06 2024].

[39] Wikipedia, “Gate Oxide,” Wikipedia, 25 01 2025. [Online]. Available: https://en.wikipedia.org/wiki/Gate_oxide#:~:text=The%20gate%20oxide%20is%20the,%22%20or%20%22gate%20conductor%22.. [Accessed 03 02 2025].

[40] G. Wright, “metal-oxide semiconductor field-effect transistor (MOSFET),” Tech Target, 2022. [Online]. Available: https://www.techtarget.com/whatis/definition/MOSFET-metal-oxide-semiconductor-field-effect-transistor. [Accessed 2 06 2024].

[41] Electronics Tutorials, “The MOSFET,” Electronics Tutorials, 2021. [Online]. Available: https://www.electronics-tutorials.ws/transistor/tran_6.html#:~:text=The%20more%20common%20Enhancement%2Dmode,normally%20open%20non%2Dconducting%20channel.. [Accessed 03 02 2025].

[42] R. Teja, “Introduction to MOSFET | Enhancement, Depletion, Amplifier, Applications,” Electronics Hub, 02 04 2024. [Online]. Available: https://www.electronicshub.org/mosfet/. [Accessed 2 06 2024].

[43] RS Components, “A Complete Guide to IGBTs,” RS Components, 24 01 2023. [Online]. Available: https://uk.rs-online.com/web/content/discovery/ideas-and-advice/igbts-guide. [Accessed 03 06 2024].

[44] Cadence PCB Solutions, “Heterojunction Bipolar Transistors,” Cadence PCB Solutions, 2024. [Online]. Available: https://resources.pcb.cadence.com/blog/2024-heterojunction-bipolar-transistors. [Accessed 3 06 2024].

[45] I. Abbasi, “A to Z of Thin-Film Transistors,” AZO Materials, 25 05 2022. [Online]. Available: https://www.azom.com/article.aspx?ArticleID=21702. [Accessed 04 06 2024].

[46] M. Clancy, “Thin Film Transistor: Definition, Structure, and More,” Korvus Technology, 25 05 2022. [Online]. Available: https://korvustech.com/thin-film-transistor/. [Accessed 4 06 2024].

[47] R. Pakdel, M. Yavarinasab, M. R. Zibad and M. R. Almohaddesn, “Design and Implementation of Lithium Battery Management System for Electric Vehicles,” in *2022 9th Iranian Conference o Renewable Energy and Distributed Generation (ICREDG)*, Mashhad, Iran, 2022.

[48] Renesas, “Battery Management System Tutorial,” Renesas Electronics America Inc. (REA), 2018.

[49] “EV Traction Inverter Development - Evolution of Traction Inverters (Part 2 of 3),” EXRO, [Online]. Available: https://www.exro.com/industry-insights/ev-traction-inverter-development. [Accessed 05 02 2024].

[50] H. Gao, D. Hai, Y. Jin and F. Zheng, “Improved Short-Circuit Protection Method for SiC MOSFET Split-Output Power Module Achieving Ultra-Low Fault Dissipated Energy,” *IEEE Transactions on Power Electronics,* vol. 99, pp. 1-11, 2023.

[51] S. Kivrak, T. Ozer, Y. Oguz and E. B. Erken, “Battery Management System Implementation with the Passive Control Method Using MOSFET as a Load,” *Measurement and Control,* vol. 53, no. 1-2, pp. 205-213, 2019.

[52] Monolithic Power, “Battery Balancing: A Crucial Function of Battery Management Systems,” Monolithic Power, 2025. [Online]. Available: https://www.monolithicpower.com/en/learning/resources/battery-balancing-a-crucial-function-of-battery-management-systems. [Accessed 03 02 2025].

[53] A. Velcescu and C. Radici, “ IAN50004 - Using power MOSFETs in DC motor control applications,” Nexperia, 28 09 2021. [Online]. Available: https://www.nexperia.com/applications/interactive-app-notes/IAN50004_using-power-MOSFETs-in-DC-motor-control-applications. [Accessed 03 02 2025].

[54] B. Shi, A. I. Ramones, Y. Liu, H. Wang, Y. Li, S. Pischinger and J. Andert, “A review of silicon carbide MOSFETs in electrified vehicles:Application, challenges, and future development,” *IET Power Electronics,* vol. 16, no. 12, pp. 1943-2120, 2023.

[55] S. A. Lombardo, J. Stathis, B. P. Linder, K. L. Pey, F. Palumbo and C. H. Tung, "Dielectric breakdown mechanisms in gate oxides," *Journal of Applied Physics,* vol. 98, no. 12, 2005.

[56] O. V. H. Gonzalez, *Charge Trapping Dynamics Associated to MOSFET Degradation: An Experimental Approach with Magnetic Fields,* Tonantzintla, Puebla: National Institute for Astrophysics, Optics and Electronics, 2019.

[57] D. J. DiMaria and J. Stathis, "Anode hole injection, defect generation, and breakdown in ultrathin silicon dioxide films," *Journal of Applied Physics,* vol. 89, no. 9, pp. 5015-5024, 2001.

[58] A. Aassime, "High field electron trap generation and oxide breakdown in thin silicon dioxide layers," *Thin Solid Films,* vol. 385, no. 1-2, pp. 252-285, 2001.

[59] M.-J. Chen, T.-K. Kang, C.-H. Liu and Y. J. Chang, "Oxide thinning percolation statistical model for soft breakdown in ultrathin gate oxides," *Applied Physics Letters,* vol. 77, no. 4, pp. 555-557, 2000.

[60] Y. S. Chauhan, C. Hu, S. Vanugopalan, J. P. Duarte, S. Khandelwal, D. Lu and N. Payvadosi, "Chapter 5 - Leakage Currents," in *FinFET Modeling for IC Simulation and Design - Using the BSIM-CMG Standard*, London, Academic Press, 2015, pp. 127-142.

[61] H. Jafari, S. A. h. Feghhi and S. Boorboor, "The effect of interface trapped charge on threshold voltage shift estimation for Gamma irradiated MOS device," *Radiation Measurements,* 2014.

[62] J. A. O. Gonzalez and L. Alatise, "Impact of BTI Induced Threshold Voltage Shifts in Shoot-through Currents from Crosstalk in SiC MOSFETs," *IEEE Transactions on Power Electronics,* vol. 26, no. 3, 2020.

[63] T. Chan, J. Chen, P. K. Ko and C. Hu, "The Impact of Gate Induced Drain Leakage Current on MOSFET Scaling," in *International Electron Devices Meeting*, Washington D.C. , 1987.

[64] J. Robertson, "High dielectric constant gate oxides for metal oxide Si transistors," *Reports on Progress in Physics,* vol. 69, no. 2, pp. 327-396, 2006.

[65] J. Robertson, "High Dielectric Constant Oxides," *The European Physical Journal Applied Physics,* vol. 28, pp. 265-291, 2004.

[66] M. V. Rossum, "Integrated Circuits," *Encyclopedia of Condensed Matter Physics,* pp. 394-403, 2005.

[67] "Rapid Thermal Anneal (RTA), Rapid Thermal Processing (RTP)," Semiconductor Engineering, 2024. [Online]. Available: https://semiengineering.com/knowledge_centers/manufacturing/process/rapid-thermal-anneal-rta-rapid-thermal-processing-rtp/. [Accessed 10 06 2024].

[68] Y. S. Song, K. Y. Kim, T. Y. Yoon, S. J. Kang, G. Kim, S. Kim and J. H. Kim, "Reliability improvement of self-heating effect, hot-carrier injection, and on-current variation by electrical/thermal co-design," *Solid-State Electronics,* vol. 197, p. Article Number 108436, 2022.

[69] M.-H. Jaung and Y.-M. Chiu, “Effects of a lightly-doped-drain (LDD) implantation condition on the device characteristics of polycrystalline-Si thin-film transistors,” *Semiconductor Science and Technology,* vol. 21, no. 3, p. Article Number 291, 2006.

[70] D. Akinyele and D. Callahan, “Fabrication techniques such as molecular beam epitaxy,” August 2024. [Online]. Available: https://www.researchgate.net/publication/383177990_Fabrication_techniques_such_as_molecular_beam_epitaxy. [Accessed 21 August 2024].

[71] P. O. Oviroh, R. Akbarzadeh, D. Pan, R. A. M. Coetzee and T.-C. Jen, “New development of atomic layer deposition: processes, methods and applications,” *Sci Technol Adv Mater.,* vol. 20, no. 1, pp. 465-496, 2019.

[72] A.-M. El-Sayed, M. Watkins, T. Grasser, V. Afanas'ev and A. L. Shluger, “Hydrogen-Induced Rupture of Strained Si—O Bonds in Amorphous Silicon Dioxide,” *Physical Review Letters,* vol. 114, no. 11, p. Article Number 115503, 2015.

[73] N. Waldron, “Chapter 7 - III-V Devices and Technology for CMOS,” in *High Mobility Materials for CMOS Applications*, Woodhead Publishing Series in Electronic and Optical Materials, 2018, pp. 231-280.

[74] H. Mostafa, M. Anis and M. Elmasry, “Adaptive Body Bias for Reducing the Impacts of NBTI and Process Variations on 6T SRAM Cells,” *IEEE Transactions on Circuits and Systems I Regular Papers,* vol. 12, no. 58, pp. 2859-2871, 2012.

[75] S. A. Parke, J. E. Moon, H.-J. C. Wann, P. K. Ko and C. Hu, “Design for suppression of gate-induced drain leakage in LDD MOSFET's using a quasi-two-dimensional analytical model,” *IEEE Transactions on Electron Devices,* vol. 39, no. 7, pp. 1694-1703, 1997.

[76] Y. Chen, Y. Song, B. Wo, F. Liu, Y. Deng, P. Kang, X. Huang, Y. Wu, D. Gao and K. Xu, “Optimization of Impact Ionization in Metal–Oxide–Semiconductor Field-Effect Transistors for Improvement of Breakdown Voltage and Specific On-Resistance,” *Electronics,* vol. 13, no. 20, p. 4101, 2024.

[77] TUV SUD, “What Is Reliability Engineering and Why Does It Matter,” TUV SUD, 9 08 2023. [Online]. Available: https://www.tuvsud.com/en-in/resource-centre/blogs/what-is-reliability-engineering-and-why-does-it-matter#:~:text=In%20engineering%2C%20reliability%20is%20a%20critical%20factor,reaching%20this%20steady%20overall%20performance%20and%20dependability.. [Accessed 03 02 2025].

[78] A. Pamidimukkala, S. Kermanshachi, J. M. Rosenberger and G. Hladik, “Barriers and motivators to the adoption of electric vehicles: A global review,” *Green Energy and Intelligent Transportation,* vol. 3, no. 2, 2024.

[79] F. H. Gandoman, T. Kalogiannis, M. Berecibar, J. V. Mierlo and P. V. d. Bossche, “Quantitative analysis techniques for evaluating the,” in *2020 IEEE Vehicle Power and Propulsion Conference (VPPC)* , 2020.

[80] Exro, “Battery Degradation,” Exro, [Online]. Available: https://www.exro.com/industry-insights/battery-degradation-

explained#:~:text=Battery%20Degradation:%20A%20Deep%20Dive%20Battery%20degradation,you%20as%20far%20as%20it%20initially%20did.. [Accessed 03 02 2025].

[81] A. J. Niri, G. A. Poelzer, S. E. Zhang, J. Rosenkranz, M. Pettersson and Y. Ghorbani, "Sustainability challenges throughout the electric vehicle battery value chain," *Renewable and Sustainable Energy Reviews,* vol. 191, 2024.

[82] S. Shahid and M. Agelin-Chaab, "A review of thermal runaway prevention and mitigation strategies for lithium-ion batteries," *Energy Conversion and Management: X,* vol. 16, 2022.

[83] M. Zwicker, M. Moghadam, W. Zhang and C. Nielsen, "Automotive Battery Pack Manufacturing - A Review of Battery to Tab Joining," *Journal of Advanced Joining Processes,* vol. 1, p. Article Number 100017, 2020.

[84] L. Nagal, "Motor Winding Resistance - How to Test It," Tyto Robotics, 04 04 2023. [Online]. Available: https://www.tytorobotics.com/blogs/articles/motor-winding-resistance-how-to-test-it#:~:text=2.,the%20bearings%20or%20drive%20circuitry.. [Accessed 03 02 2025].

[85] M. S. Mastoi, S. Zhuang, H. M. Munir, M. Haris, M. Hassan, M. Algarni and B. Alamri, "A study of charging-dispatch strategies and vehicle-to-grid technologies for electric vehicles in distribution networks," *Energy Reports,* vol. 9, pp. 1777-1806, 2023.

[86] T. Rahman and T. Alharbi, "Exploring Lithium-Ion Battery Degradation: A Concise Review of Critical Factors, Impacts, Data-Driven Degradation Estimation Techniques, and Sustainable Directions for Energy Storage Systems," *Batteries,* vol. 10, no. 7, p. 220, 2024.

[87] F. Iannuzzo, "Reliability Challenges of Automotive-Grade Silicon Carbide Power MOSFETs," EE Power, 2021. [Online]. Available: https://eepower.com/technical-articles/reliability-challenges-of-automotive-grade-silicon-carbide-power-mosfets/#. [Accessed 10 January 2024].

[88] J. Gambino, "Process Technology for Copper Interconnects," in *Handbook of Thin Film Deposition (Third Edition)*, Elsevier , 2012, pp. 221-269.

[89] E. N. Cho, Y. H. Shin and I. Yun, "An analytical avalanche breakdown model for double gate MOSFET," *Microelectronics Reliability,* vol. 55, no. 1, pp. 38-41, 2015.

[90] H. Zhuang, R. Bauer and M. Dinkel, "Electromigration in Power Devices," in *International Symposium on Microelectronics*, 2020.

[91] A. Heryanto, "Effect of stress migration on electromigration for nano scale advanced interconnects," Nanyang Technological University, Singapore, 2012.

[92] J. Hurtarte, "Silicon Carbide And Gallium Nitride Bring New Challenges For Semiconductor Test," Semiconductor Engineering, 12 11 2024. [Online]. Available: https://semiengineering.com/silicon-carbide-and-gallium-nitride-bring-new-challenges-for-semiconductor-test/. [Accessed 03 02 2025].

[93] D. A. Barkley, “Gen 4 Silicon Carbide Technology: Redefining Performance and Durability in High-Power Applications,” Wolfspeed, 2025 01 22. [Online]. Available: https://www.wolfspeed.com/knowledge-center/article/gen-4-silicon-carbide-technology-redefining-performance-and-durability-in-high-power-applications/#:~:text=For%20example%2C%20in%20electric%20vehicles,based%20on%20their%20specific%20needs.. [Accessed 03 02 2025].

[94] Z. Zhang, J. Wei, M. Zhang, J. Zhang, W. Hu and L. Zhang, “An eGaN HEMT-Based High Power Density Controller for Permanent Magnet Synchronous Motor,” in *26th International Conference on Electrical Machines and Systems*, 2023.

[95] M. Ohring and L. Kasprzak, Reliability and Failure of Electronic Materials and Devices, Elsevier, 2011.

[96] B. H. Lee, J. Oh, H. H. Tseng, R. Jammy and H. Huff, “Gate stack technology for nanoscale devices,” *Materials Today,* vol. 9, no. 6, pp. 32-40, 2006.

[97] R. K. Ratnesh, .. Goel, G. Kaushik, H. Garg, Chandan, M. Singh and B. Prasad, “Advancement and challenges in MOSFET scaling,” *Materials science in semiconductor processing,* vol. 134, no. 106002, 2021.

[98] M.Durairaj, R. Kumar, K. Kumar, S. Bharathi, V.Sharanya and T.Sathish, “A Comprehensive Review of MOSFET Device Scaling,” *Journal of Science, Computing and Engineering Research (JSCER),* vol. 6, no. 3, 2023.

[99] Y. Wang, H. Liang, H. Zhang, D. Li, Y. Li, M. Yi and Z. Huang, “A new characterization model of FinFET self-heating effect based on FinFET characteristic parameter,” *Microelectronic Engineering,* vol. 287, 2024.

[100] K. Derbyshire, “What's Different About Next-Gen Transistors,” Semiconductor Engineering, 20 October 2022. [Online]. Available: https://semiengineering.com/whats-different-about-next-gen-transistors/. [Accessed 24 May 2024].

[101] F. Hosseinabadi, S. Chakraborty, S. K. Bhoi, G. Prochart, D. Hrvanovic and O. Hegazy, “A Comprehensive Overview of Reliability Assessment Strategies and Testing of Power Electronics Converters,” *IEEE Open Jounal of Power Electronics,* vol. 99, pp. 1-42, 2024.

[102] P. Moens, J. Franchi, J. Lettens, L. D. Schepper, M. Domeij and F. Allerstam, “A Charge-to-Breakdown (QBD) Approach to SiC Gate Oxide Lifetime Extraction and Modeling,” in *2020 32nd International Symposium on Power Semiconductor Devices and ICs (ISPSD)*, Vienna, 2020.

[103] S. Zhu, T. Liu, L. Shi, M. Jin, H. L. R. Maddi, M. H. White and A. K. Agarwal, “Comparison of Gate Oxide Lifetime Predictions with Charge-to-Breakdown Approach and Constant-Voltage TDDB on SiC Power MOSFET,” in *8th Workshop on Wide Bandgap Power Devices and Applications (WiPDA)*, Redondo Beach, CA, 2021.

[104] M. Baghdadi, E. Elwarraki, I. A. Ayad and N. Mijlad, “Behavioral electrothermal modeling of MOSFET for energy conversion circuits simulation using MATLAB/Simulink,” *Microelectronics Reliability,* vol. 154, p. Article Number 115340, 2024.

[105] C. Morel and N. Rizoug, “Electro-Thermal Modeling, Aging and Lifetime Estimation of Power Electronic MOSFETs,” *Civil Engineering Research Journal,* vol. 14, no. 1, pp. 1-3, 2023.

[106] W.-C. Lin, W.-C. Yu, B.-R. Chen, Y.-S. Hsiao, Z.-H. Huang, C.-L. Hung, Y.-K. Hsiao, N.-J. Yeh, H.-C. Kuo, C.-C. Tu and T.-L. Wu, “Investigation of the time dependent gate dielectric stability in SiC MOSFETs with planar and trench gate structures,” *Microelectronics Reliability,* vol. 150, no. 4, p. Article Number 115141, 2023.

[107] H. Lin, E. Bouyssou and L. Ventura, “TDDB Characterizations of BST Capacitors Exhibiting Bimodal Weibull Distribuitions,” in *2011 IEEE International Integrated Reliability Workshop*, South Lake Tahoe, CA, 2011.

[108] S.-I. Hayashi and K. Wada, “Accelerated aging test for gate-oxide degradation in SiC MOSFETs for condition monitoring,” *Microelectronics Reliability,* vol. 114, no. 31, p. Article Number 113777, 2020.

[109] L. Yang and A. Castellazzi, “High temperature gate-bias and reverse-bias tests on SiC MOSFETs,” *Microelectronics Reliability,* vol. 53, no. 9-11, pp. 1771-1773, 2013.

[110] J. Caldwell, “Accurate Constant-Current, Constant-Voltage 20A Power Supply Ensures Safe Charging of Supercaps and Li-Ion Batteries,” Analog Devices, 1 10 2010. [Online]. Available: https://www.analog.com/en/resources/technical-articles/power-supply-ensures-safe-charging-of-surpercaps-and-liion-batteries.html#:~:text=India-,Accurate%20Constant%2DCurrent%2C%20Constant%2DVoltage%2020A%20Power%20Supply%20Ensures,Supercaps%20and%20Li%2DI. [Accessed 03 02 2025].

[111] M. Zamora, “Precision Current Sources and Sinks Using Voltage,” Texas Instruments, 2020.

[112] F. Z. Peng, “Impedance sources (Z sources) with inherent fault protection for resilient and fire-free electricity grids,” *Scientific Reports,* 2024.

[113] “Active Transistor Constant Current Source,” Electronics Notes, [Online]. Available: https://www.electronics-notes.com/articles/analogue_circuits/transistor/active-constant-current-source.php. [Accessed 31 May 31].

[114] Wikipedia, “Bipolar Junction Transistor,” Wikipedia, [Online]. Available: https://en.wikipedia.org/wiki/Bipolar_junction_transistor#:~:text=This%20effect%20can%20be%20used%20to%20amplify,to%20the%20low%20impedance%20at%20the%20base.. [Accessed 03 02 2025].

[115] Doug Mercer, “The Current Mirror,” Analog Devices, 17 September 2021. [Online]. Available: https://wiki.analog.com/university/courses/electronics/text/chapter-11#basic_principles. [Accessed 31 May 2024].

[116] Analog Devices, “Class A NPN Emitter-Follower Amplifier,” Analog Devices, 26 10 2016. [Online]. Available: https://wiki.analog.com/university/courses/engineering_discovery/lab_11#:~:text=In%20the%20emitter%2Dfollower%20amplifier,that%20for%20large%20%CE%B2%20we. [Accessed 03 02 2025].

[117] B. Chaudhary, “Emitter Follower : Working, Characteristics and Its Applications,” Semiconductor For U, 16 September 2022. [Online]. Available: https://www.semiconductorforu.com/emitter-follower-working-characteristics-and-its-applications/. [Accessed 31 May 2024].

[118] R. Keim, “The Basic MOSFET Constant-Current Source,” All About Circuits, 06 June 2016. [Online]. Available: https://www.allaboutcircuits.com/technical-articles/the-basic-mosfet-constant-current-source/. [Accessed 31 May 2014].

[119] “Learn Analog Circuits: Types and Applications of Current Mirrors,” All About Circuits, 03 April 2019. [Online]. Available: https://www.allaboutcircuits.com/technical-articles/learn-analog-circuits-introduction-to-current-mirrors-types-applications/. [Accessed 31 May 2024].

[120] S. Gupta, “Design a Voltage Controlled Current Source Circuit using Op-Amp,” Circuit Digest, 29 January 2020. [Online]. Available: https://circuitdigest.com/electronic-circuits/voltage-controlled-current-source-circuit-using-op-amp. [Accessed 31 05 2024].

[121] S. Pai and V. Sethia, “Reducing Excessive Heat with Dynamic Power Control for Current Output Digital-to-Analog Converters,” Analog Devices, 04 09 2024. [Online]. Available: https://www.analog.com/en/resources/technical-articles/reducing-excessive-heat-with-dynamic-power-control-for-current-output.html#:~:text=When%20current%20source/sink%20digital,the%20functioning%20of%20the%20IDAC.. [Accessed 03 02 2025].

[122] RS Components, “A Complete Guide to Voltage References,” RS Components, 01 02 2024. [Online]. Available: https://uk.rs-online.com/web/content/discovery/ideas-and-advice/voltage-references-guide. [Accessed 03 02 2025].

[123] Texas Instruments, *TL082 Wide Bandwidth Dual JFET Input Operational Amplifier,* Dallas, TX: Texas Instruments, 2013.

[124] Microchip, *LND150/LND250 N-Channel Depletion-Mode DMOS FETs,* Chandler, AZ: Microchip, 2018.

[125] Texas Instruments, “TL071,” September 1978. [Online]. Available: https://www.ti.com/product/TL071. [Accessed 22 May 2024].

[126] Texas Instruments, “TLV2774CN,” January 1998. [Online]. Available: https://www.digikey.co.uk/en/products/detail/texas-instruments/TLV2774CN/277550. [Accessed 23 May 2024].

[127] Vishay Semiconductors, “BZT03-Series: Zener Diodes with Surge Current Specification,” 11 September 2019. [Online]. Available: https://www.vishay.com/docs/85599/bzt03.pdf. [Accessed 24 May 2024].

[128] Bourns, “3269 – 1/4 ″ Square SMD Trimpot® Trimming Potentiometer,” 31 March 2015. [Online]. Available: https://www.digikey.co.uk/en/products/detail/bourns-inc/3269W-1-105LF/1817519. [Accessed 24 May 2024].

[129] B. Carter and R. Mancini, “Active Filter Design Technques,” in *Op Amps For Everyone*, Newnes, 2918, pp. 199-258.

[130] Bourns, “RLB Series Radial Lead Inductors,” 31 March 2015. [Online]. Available: RLB Series Radial Lead Inductors. [Accessed 26 May 2024].

[131] XP Power, “IA Series DC-DC Converter,” 22 March 2022. [Online]. Available: https://www.xppower.com/portals/0/pdfs/SF_IA.pdf. [Accessed 26 May 2024].

[132] C. Chen, Y. Cai, P. Sun and Z. Zhao, “Threshold voltage instability of SiC MOSFETs under very-high temperature and wide gate bias,” *IET Power Electronics,* vol. 17, no. 15, pp. 2393-2404, 2024.

[133] J.-M. Yu, D.-H. Wang, J.-Y. Ku, J.-K. Han, D.-H. Jung, J.-Y. Park and Y.-K. Choi, “Low-temperature deuterium annealing to improve performance and reliability in a MOSFET,” *Solid-State Electronics,* vol. 197, 2022.

[134] R. Anderson and J. Hill, “Low Temperature Electronics,” *Microelectronics Journal,* vol. 19, no. 4, pp. 7-12, 1988.

[135] M. Falter, “Advanced Packaging Innovations Improve Power MOSFET Performance,” EE Power, 04 11 2023. [Online]. Available: https://eepower.com/new-industry-products/advanced-packaging-innovations-improve-power-mosfet-performance/#. [Accessed 20 01 2024].

[136] K.-i. Moon, “The Role of Interconnection in the Evolution of Advanced Packaging Technology,” EE Times, 18 08 2023. [Online]. Available: https://www.eetimes.com/the-role-of-interconnection-in-the-evolution-of-advanced-packaging-technology/#:~:text=However%2C%20copper%2Dto%2Dcopper,in%20importance%20in%20the%20future.. [Accessed 20 01 2024].

[137] J. P. Gambino, S. A. Adderly and J. U. Knickerbocker, “An overview of through-silicon-via technology and manufacturing challenges,” *Microelectronic Engineering,* vol. 135, pp. 73-106, 2015.

[138] “Strengthening HBM Market Leadership: Meet the SK hynix Team Behind the World’s First 12-Layer HBM3,” SK Hynix, 19 05 2023. [Online]. Available: https://news.skhynix.com/meet-the-sk-hynix-team-behind-the-worlds-first-12-layer-hbm3/. [Accessed 29 01 2024].

[140] S. Halder, K. Bhuvir, S. Bhattacharjee, J. Nakka, A. Panda and M. Ghosh, “Performance Analysis of WBG Inverter Fed Electric Traction Drive System for EV Application,” in *2023 IEEE IAS Global Conference on Renewable Energy and Hydrogen Technologies (GlobConHT)*, Male, Maldives, 2023.

[141] L. Yang and A. Castellazzi, *High temperature gate-bias and reverse-bias tests on SiC MOSFETs,* 2013.

[143] ITW Performance Polymers, “Use of Adhesives in an EV Battery,” ITW Performance Polymers, [Online]. Available: https://itwperformancepolymers.com/blog/use-of-adhesives-in-an-ev-battery. [Accessed 31 05 2024].

[144] D. Edmunds, “EV Motors Explained,” 5 April 2022. [Online]. Available: https://www.caranddriver.com/features/a39493798/ev-motors-explained/. [Accessed 31 May 2024].

[145] X. Sun, Z. Li, X. Wang and C. Li, *Technology Development of Electric Vehicles: A Review,* Guangdong: MDPI Energies, 2020.

[146] “DIYGuru,” [Online]. Available: https://diyguru.org/resources/article/electric-power-control-unit/. [Accessed 31 May 2024].

[147] K. Derbyshire, *What's Different About Next-Gen Trasnsistors,* Semi Engineering, 2022.

[148] Semiconductor Samsung, *TSV (Through Silicon Via),* Samsung, 2014.

[149] S. M. Kerner, *IBM advances chiplets with hybrid bonding for thinner, smaller connections,* SDX Central, 2023.

[150] M. Falter, *Advanced Packaging Innovations Improve Power MOSFET Performance,* EEPower, 2023.

[151] J. Bryant, *Current-Output Circuit Techniques Add Versatility to Your Analog Toolbox,* ADI Analog Dialogue , 2014.

[152] *Emitter Follower and Darlington Amplifier,* Tutorials Point, 2024.

[153] w. t. e. s. o. A. D. Hank Zumbahlen, “Chapter 8 - Analog Filters,” in *Linear Circuit Design Handbook*, Newnes, 2008, pp. 581-679.

[154] *TL082 Wide Bandwidth Dual JFET Input Operational Amplifier,* Dallas, Texas: Texas Instruments, 2013.

[155] *N-Channel Depeletion-Mode DMOS FETs,* Chandler, Arizona: Microchip Technology Inc., 2018.

[156] *TL07xx Low Noise FET-Input Operatonal Amplifiers,* Dallas, Texas: Texas Instruments , 2013.

[157] *TLV277x, TLV277xA Family of 2.7-V High-Slew-Rate Rail-To-rail Output Operational Amplifiers with Shutdown,* Dallas, Texas: Texas Instruments, 2013.

[158] *BZT03-Series Zener Diodes with Surge Current Specification,* Malvern, Pennsylvania: Vishay, 2019.

[159] *3269 - 1/4" Sqaure SMD Trimpot Trimming Potentiometer,* Riverside, California : Bourns Inc., 2015.

[160] B. Carter and R. Mancini, *Active Filter Design Techniques,* Newnes, 2018.

[161] M. Kamran, “Chapter 10 - Electric Vehicles and Smart Grids,” in *Fundamentals of Smart Grid Systems*, Islamabad, Pakistan, Academic Press, 2023, pp. 431-460.

[162] F. Iannuzzo, “Reliability Challenges of Automotive-grade Silicon Carbide Power MOSFETs,” EE Power, 11 June 2021. [Online]. Available:

https://eepower.com/technical-articles/reliability-challenges-of-automotive-grade-silicon-carbide-power-mosfets/#. [Accessed 24 08 2024].

[163] CREE, "C3M0280090D Silicon Carbide Power MOSFET," November 2015. [Online]. Available: https://docs.rs-online.com/1b50/0900766b8149fd50.pdf. [Accessed 25 June 2024].

[164] Nexperia, "GAN041-650WSB 650 V, 35 mΩ Gallium Nitride (GaN) FET in a TO-247 package," 12 January 2021. [Online]. Available: https://docs.rs-online.com/ea35/A700000008812991.pdf. [Accessed 26 June 2024].

[165] X. Liang, J. Zhao, Q. Zheng, J. Cui, S. Yang, B. Wang, D. Zhang, X. Yu and Q. Guo, *Impact of heavy-ion irradiation on gate oxide reliability of silicon carbide power MOSFET,* 2021.

[166] K. Tang, W. Huang and T.-S. P. Chow, *GaN MOS capacitors and FETs on plasma-etched GaN surfaces,* 2009.

[167] B. Yang, P. Ye, J. Kwo, M. R. Frei, H. J. L. Gossmann, J. Mannaerts, M. Sergent, M. Hong, K. Ng and J. Bude, *Impact of metal/oxide interface on DC and RF performance of depletion-mode GaAs MOSFET employing MBE grown Ga2O3(Gd2O3) as gate dielectric,* Elsevier, 2003.

[168] D. Crecraft and S. Gergel, *Analog Electronics: Circuits, Systems and Signal Processing,* Butterworth-Heinemann, 2002.

[169] F. Fathi and H. Liao, *Reliability study on high-k bi-layer dielectrics,* Research Gate, 2017.

[170] N. Langenberg, S. Kimpeler and A. Moser, *Interconnecting Power-Electronic Buck Converter Modules in a Novel High-Power Test Bench for MVDC Circuit Breakers,* Energies, 2022.

[171] M. Scholz, *ESD protection design in a-IGZO TFT technologies,* Anaheim: EOS/ESD Symposium, 2016.

[172] M.Bain, *SiGe HBTs on bonded SOI incorporating buried silicide layers,* IEEE, 2005.

[173] ITW Performance Polymers, *Adhesives - Electric Vehicles,* ITW Performance Polymers, 2024.

[174] T. Cachelin, *Breaking Down Electric Motors, From Basics to Advanced Systems!,* EV Builders Guide, 2024.